Superconducting Accelerator Magnets

Soren Prestemon
Division Deputy for Technology
Accelerator Technology & Applied Physics Division
October, 2016

Outline

I. Motivation for superconducting accelerator magnets
II. Introduction to superconducting materials
III. Magnetic designs for superconducting accelerator magnets
IV. Mechanical considerations
V. Quench behavior and magnet protection
VI. Other applications

Acknowledgements

- This presentation is meant to be a tutorial – i.e. provide an overview of what goes into the design, fabrication and test of superconducting accelerator magnets

- Much of the presentation comes from USPAS course notes on Superconducting Accelerator Magnets that my colleagues Paolo Ferracin, Ezio Todesco, Helene Felice, and I have made over multiple years

- Thanks to Lance Cooley for information from his USPAS course notes on Superconducting Materials

- Finally, thanks to many colleagues from around the world whose work I have used in here – although I try to provide references throughout, I realize I may have missed some and hope those colleagues will forgive me!

Section I: Motivation for superconducting accelerator magnets

Motivation for superconducting accelerator magnets

- Start with the basics: F=ma
  - For a relativistic charged particle the momentum is $p=mv=m_0\gamma v$
  - Implies that particle momentum, magnetic field and ring radius scale as $p=eB\rho/c$
- High energy rings need high field and/or large radius

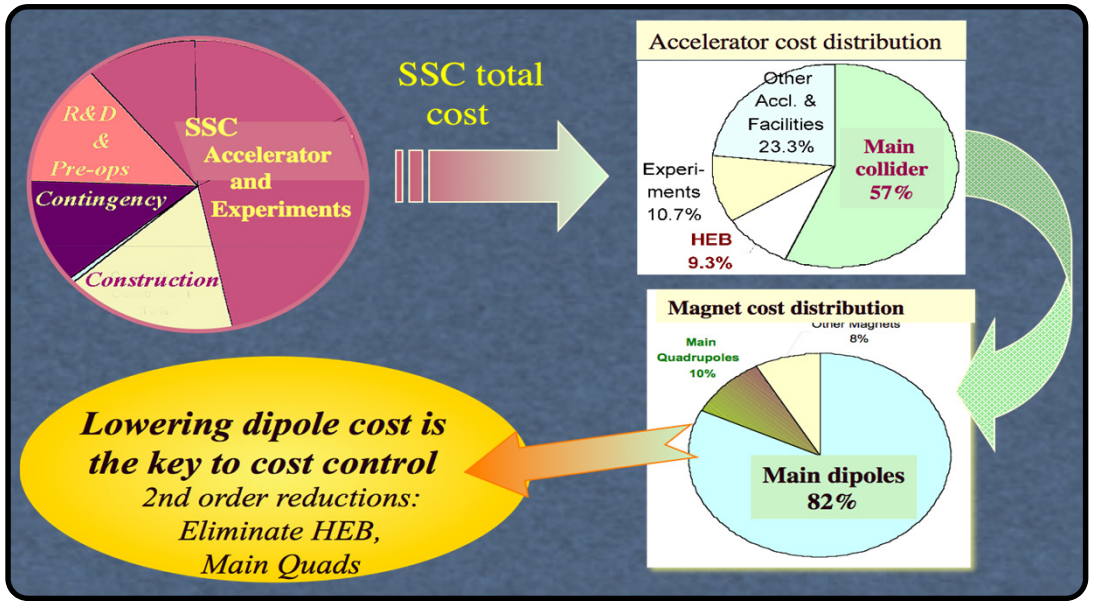

Barletta

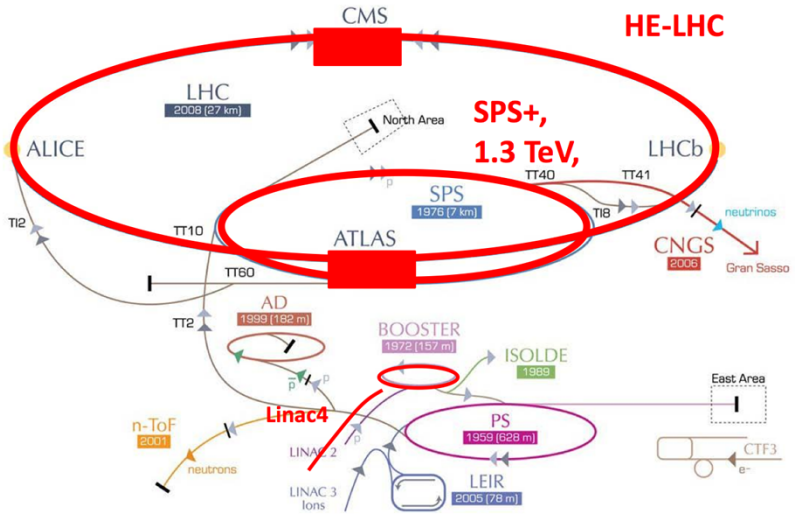

Accelerators have numerous magnet configurations

- Dipoles “steer” the beam: maintain trajectory on a ring
- Quadrupoles serve as focusing optics for charged particles
  - Due to Maxwells equations, focusing in one plane results in defocus in the other plane => consecutive focus-defocus (“FODO”) provides global focusing
- Sextupoles serve to correct chromatic aberrations
  - Real beams have energy spread dp/p

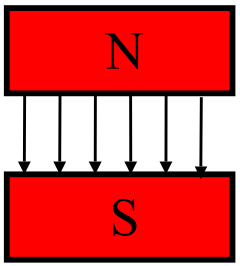

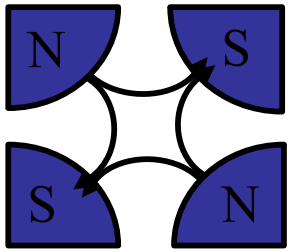

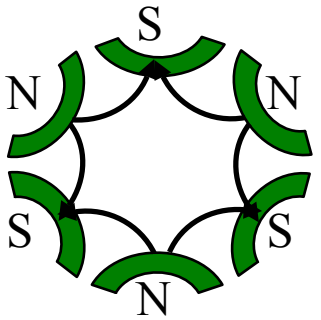

$$\vec{F} = q(\vec{E} + \vec{v} \times \vec{B})$$

Basics of electromagnetism for accelerators

Magnetic field described in terms of potentials:

In free-space, the magnetic field can be determined from a scalar potential V:

$$\vec{B} = -\nabla V \quad \left(\text{results from } \nabla \times \vec{B} = 0 \text{ and identity } \nabla \times (\nabla V) = 0,\ \forall V\right)$$

and from a vector potential A:

$$\vec{B} = \nabla \times \vec{A} \quad \left(\text{results from } \nabla \cdot \vec{B} = 0 \text{ and identity } \nabla \cdot (\nabla \times \vec{A}) = 0,\ \forall \vec{A}\right)$$

In two dimensions, A is a scalar and we can use complex notation:

$$B_x - iB_y = B^* = i\frac{dF}{dz} = i\frac{d}{dz}(A + iV)$$

$$z = x + iy$$

$$\frac{df}{dz} = \frac{\partial f}{\partial x} = -i\frac{\partial f}{\partial y}$$

$$\left.\begin{aligned} \frac{\partial u}{\partial x} &= \frac{\partial v}{\partial y} \\ \frac{\partial u}{\partial y} &= -\frac{\partial v}{\partial x} \end{aligned}\right\} \text{Cauchy Riemann}$$

F is an analytic function in a good-field region, and can be expanded as a Taylors series for $|z|<|z_0|=r_0$:

$$F(z) = F(x+iy) = F\left(re^{i\theta}\right) = \sum_{n\geq 0} c_n z^n \quad \Rightarrow B^*(z) = i\sum_{n\geq 1} n c_n (z)^{n-1}$$

$$\left.\begin{aligned} c_n &= \lambda_n + i\mu_n \\ a_n &= \frac{n\mu_n}{B_0} r_0^{n-1} \\ b_n &= -\frac{n\lambda_n}{B_0} r_0^{n-1} \end{aligned}\right\} \quad \Rightarrow B^*(z) = -B_0 \sum_{n\geq 1} (a_n + ib_n)\left(\frac{z}{r_0}\right)^{n-1}$$

Note: the coefficients are a function of the reference radius and the characteristic field. By tradition:
a_n: "skew" coefficients
b_n: "normal" coefficients

Multipole expansion of the complex potential provides direct access to the charged particle optics

Magnetic field described in terms of multipoles:

$$F(x,y) = A(x,y) + iV(x,y) = \sum_{n\geq 0} (\lambda + i\mu_n)(x+iy)^n$$

$$\Rightarrow A(x,y) = -B_0 \left[b_1 x + a_1 y + \frac{b_2}{2r_0}(x^2 - y^2) + \frac{a_2}{r_0} xy + \ldots \right]$$

$$\Rightarrow V(x,y) = B_0 \left[a_1 x - b_1 y + \frac{a_2}{2r_0}(x^2 - y^2) + \frac{b_2}{r_0} xy + \ldots \right]$$

Example: *V* describes geometry of magnetized surfaces to yield a multipole field;
for a pure normal dipole:
- only b_1 non-zero
- $b_1 y = +/- V_0$

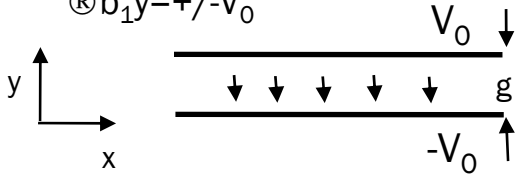

$$B_y = \frac{2V_0}{g}$$

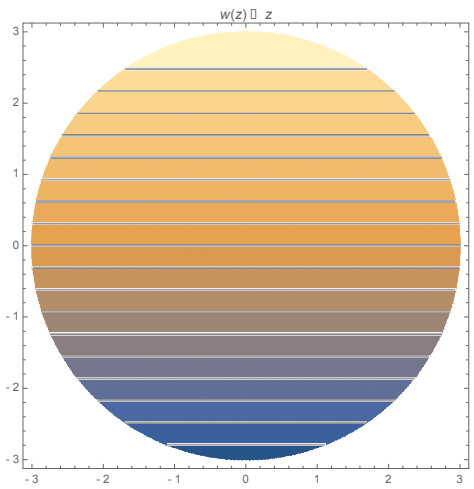

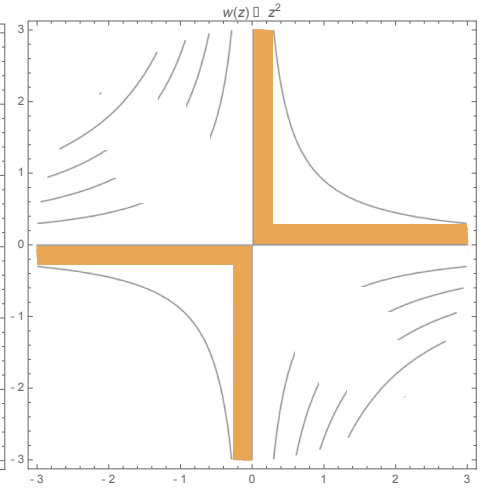

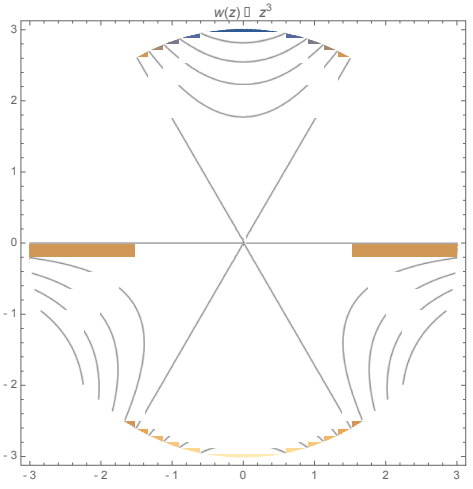

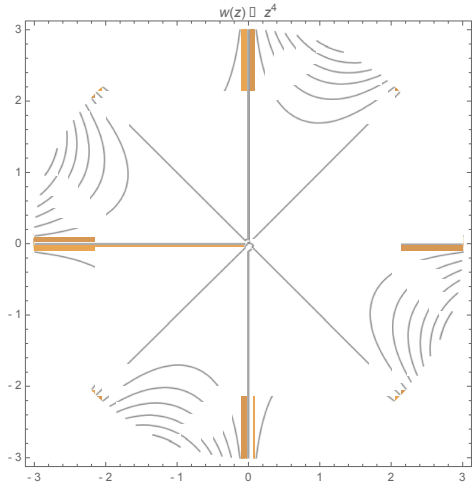

Section II: Introduction to superconductors

But first, a bit of history…

Superconductivity had its start in the 20th century

- 1911: Kamerlingh Onnes discovery of mercury superconductivity: "Perfect conductors"
  - A few years earlier he had succeeded in liquefying Helium, a critical technological feat needed for the discovery
- 1933: Meissner and Ochsenfeld discover perfect ***diamagnetic*** characteristic of superconductivity

Kamerlingh Onnes, Nobel Prize 1913

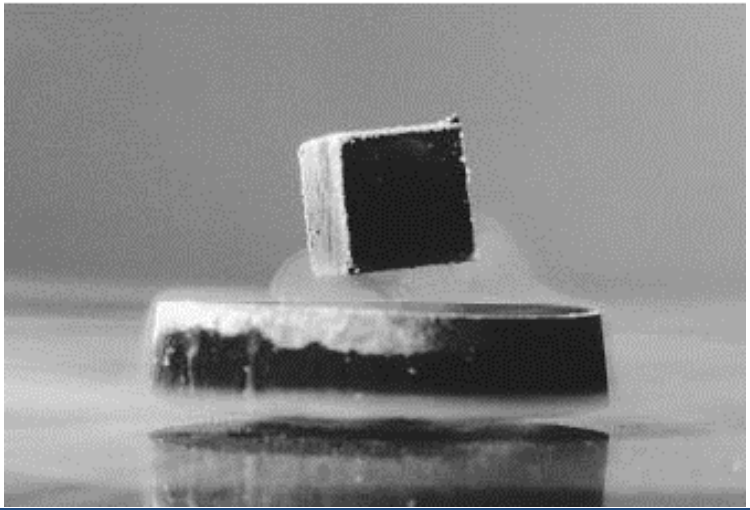

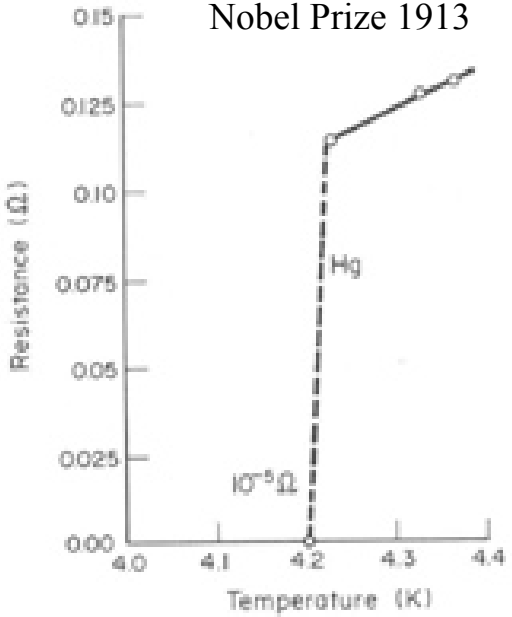

The theory of superconductivity evolved in the first half of the century

- A theory of superconductivity took time to evolve:
  - 1935: London brothers propose two equations for E and H
    - results in concept of penetration depth λ
  - 1950:Ginzburg and Landau propose a macroscopic theory (GL) for superconductivity, based on Landau's theory of second-order phase transitions
    - Results in concept of coherence length ℓ

Heinz and Fritz London

Ginzburg and Landau (circa 1947)
Nobel Prize 2003: Ginzburg, Abrikosov, Leggett

The theory behind type II superconductivity was a major breakthrough for the field

- **1957: Abrikosov considered GL theory for case $\lambda/\xi >> 1$**
  - Introduced concept of Type II superconductor
  - Predicted flux penetrates in fixed quanta, in the form of a vortex array

Nobel Prize 2003: Ginzburg, Abrikosov, Leggett (the GLAG members)

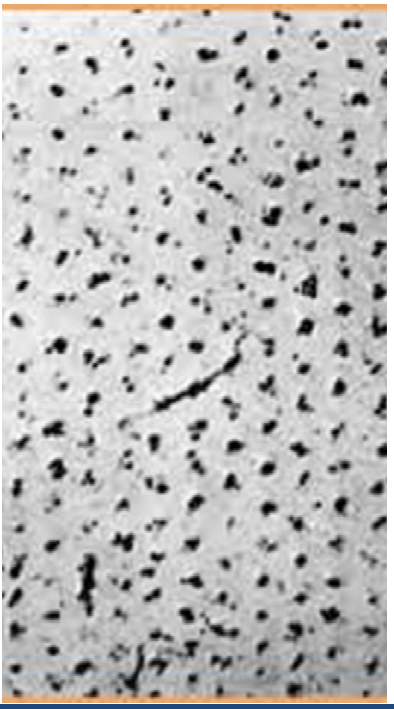

Abrikosov with Princess Madeleine

The now well-established description of low temperature superconductivity is the "BCS" theory

- 1957: Bardeen, Cooper, and Schrieffer publish microscopic theory (BCS) of Cooper-pair formation that continues to be held as the standard for low-temperature superconductors

Bardeen, Cooper and Schrieffer
Nobel Prize 1972

History – High temperature superconductors

- 1986: Bednorz and Muller discover superconductivity at high temperatures in layered materials comprising copper oxide planes

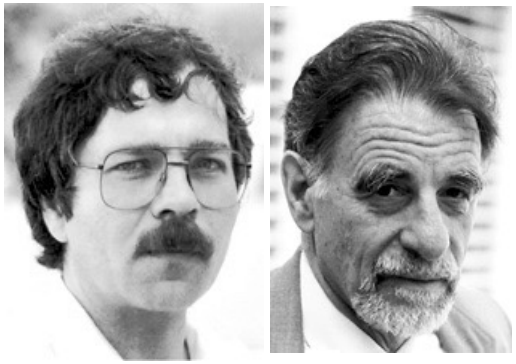

George Bednorz and Alexander Muller
Nobel prize for Physics (1987)

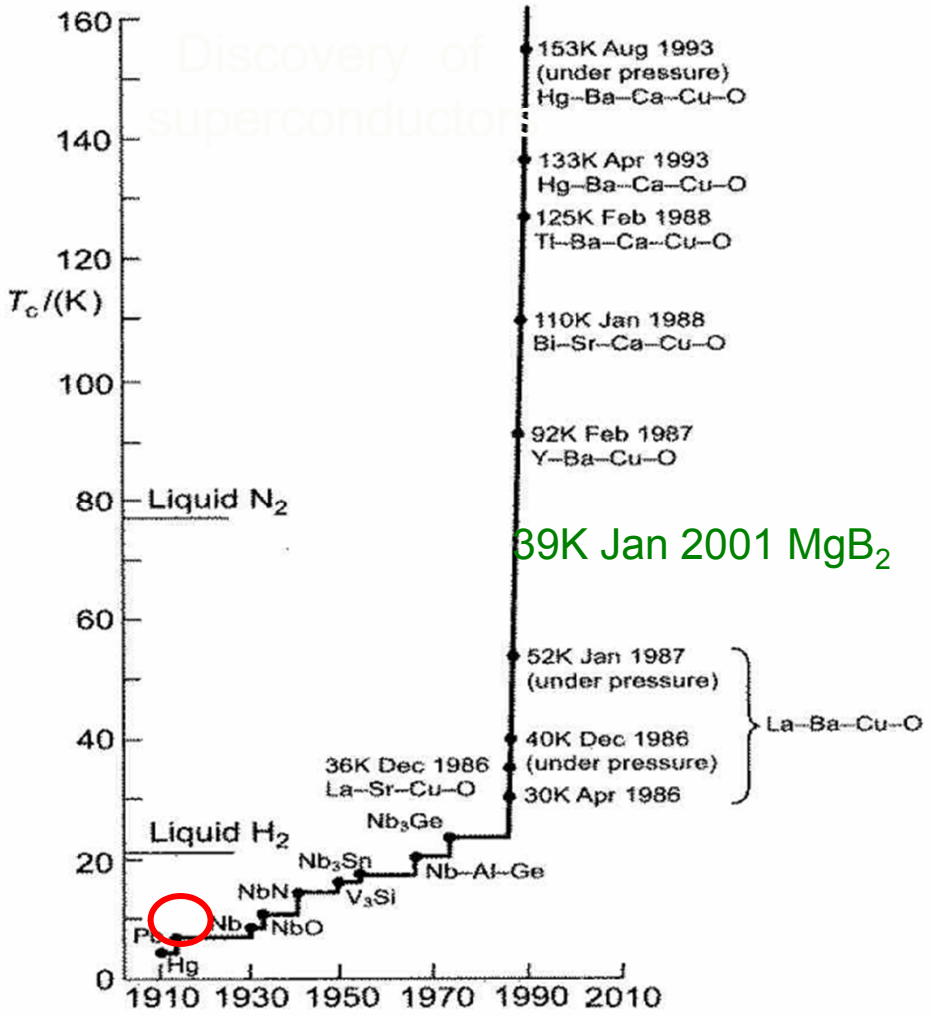

Diamagnetic behavior of superconductors

- **What differentiates a "perfect" conductor from a diamagnetic material?**

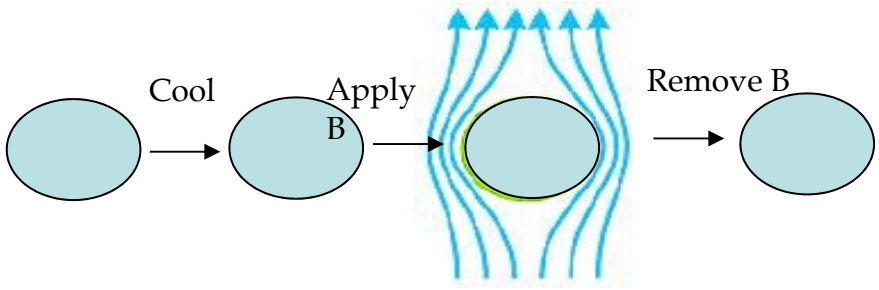

A perfect conductor apposes any change to the existing magnetic state

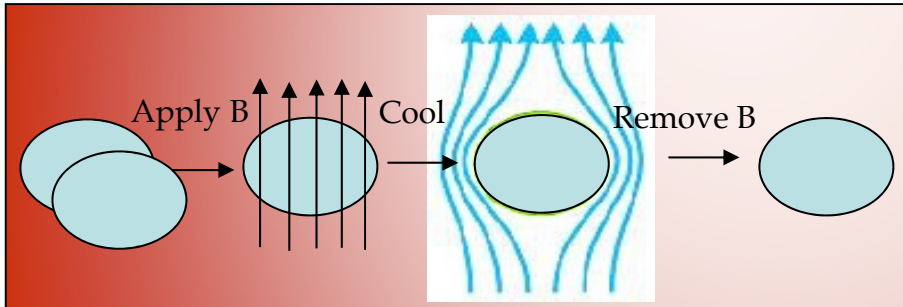

Superconductors exhibit diamagnetic behavior: flux is always expulsed - Meissner effect

Type I and II superconductors

- Type I superconductors are characterized by the Meissner effect, i.e. flux is fully expulsed through the existence of supercurrents over a distance λ, the "penetration depth".
- Type II superconductors find it energetically favorable to allow flux to enter via normal zones of fixed flux quanta: "fluxoids" or vortices.
  - The fluxoids or flux lines are vortices of normal material of size ~$\pi\xi^2$ "surrounded" by supercurrents shielding the superconducting material.

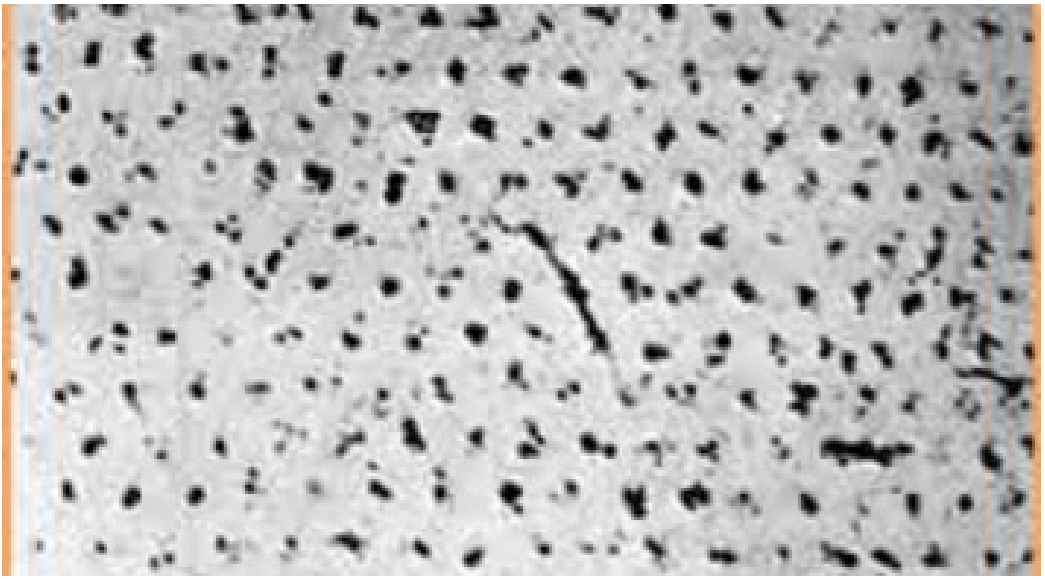

First photograph of vortex lattice,
U. Essmann and H. Trauble
Max-Planck Institute, Stuttgart
Physics Letters 24A, 526 (1967)

Concept of coherence length

- The superelectron density decreases to zero near a superconducting /normal interface, with a characteristic length ξ (coherence length, first introduced by Pippard in 1953). The two length scales ξ and λ define much of the superconductors behavior.
  - The coherence length is proportional to the mean free path of conduction electrons; e.g. for pure metals it is quite large, but for alloys (and ceramics…) it is often very small. Their ratio, the GL parameter, determines flux penetration:

$$\kappa = \lambda_L / \xi$$

- From "GLAG" theory, if:

$\kappa < 1/\sqrt{2}$ Type I superconductor

$\kappa > 1/\sqrt{2}$ Type II superconductor

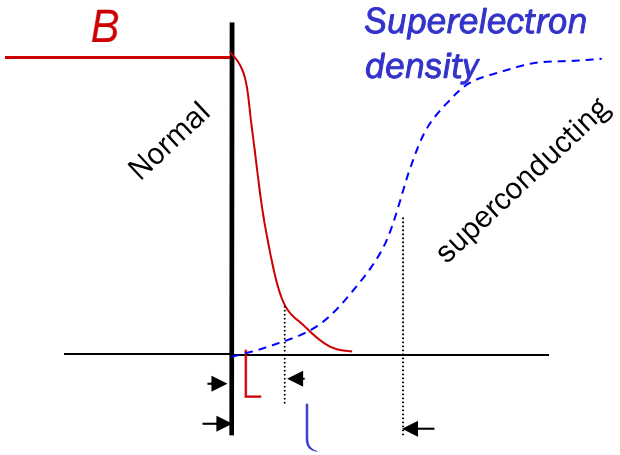

Note: in reality ξ and λ *are functions of temperature*

Fluxoids

- Fluxoids, or flux lines, are continuous thin tubes characterized by a normal core and shielding supercurrents.
- The flux contained in a fluxoid is quantized:

$$\phi_0 = h/(2e)$$

$$h = \text{Planck's constant} = 6.62607 \times 10^{-34}\ \text{Js}$$

$$e = \text{electron charge} = 1.6022 \times 10^{-19}\ \text{C}$$

  - The fluxoids in an idealized material are uniformly distributed in a triangular lattice so as to minimize the energy state
  - Fluxoids in the presence of current flow (e.g. transport current) are subjected to Lorentz force:

$$\vec{F}_L = \vec{J} \times \vec{B}$$

$\Rightarrow$ Concept of flux-flow and associated heating

Solution for real conductors: provide mechanism to ***pin*** the fluxoids

Flux pinning

- Fluxoids can be pinned by a wide variety of material defects
  - Inclusions
  - Lattice dislocations / grain boundaries
  - Precipitation of other material phases

Fig. 1: Microstructure of a NbTi filament (Courtesy of P.J. Lee, University of Wisconsin at Madison).

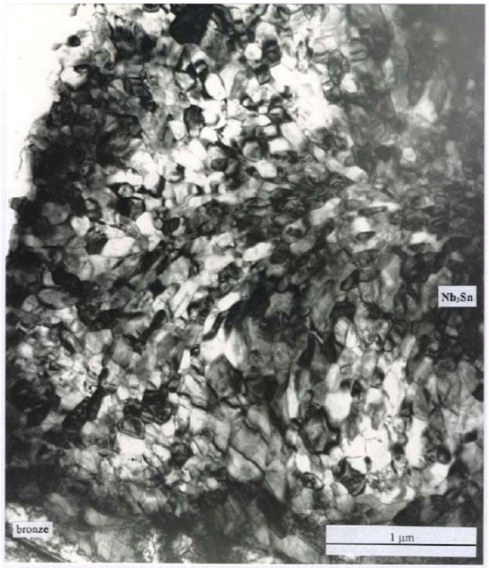

Fig. 6: Microstructure of a Nb_3Sn filament (Courtesy of C. Verwaerde, Alstom/MSA).

Energy perspective

- Fluxoids can be pinned by a wide variety of material defects
  - Inclusions
  - Lattice dislocations / grain boundaries
  - Precipitation of other material phases
- Pinning sites effectively reduce the energy state of the system; transport current has the effect of reducing the depth of the potential well
- Pinning a fluxoid "saves" a fraction of the vortex core energy:

$$\varepsilon_0 = \frac{1}{2}\pi\mu_0\xi^2 H_c^2$$

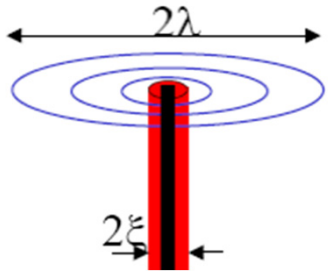

From Dhalle, IOP Handbook of Superconducting Materials

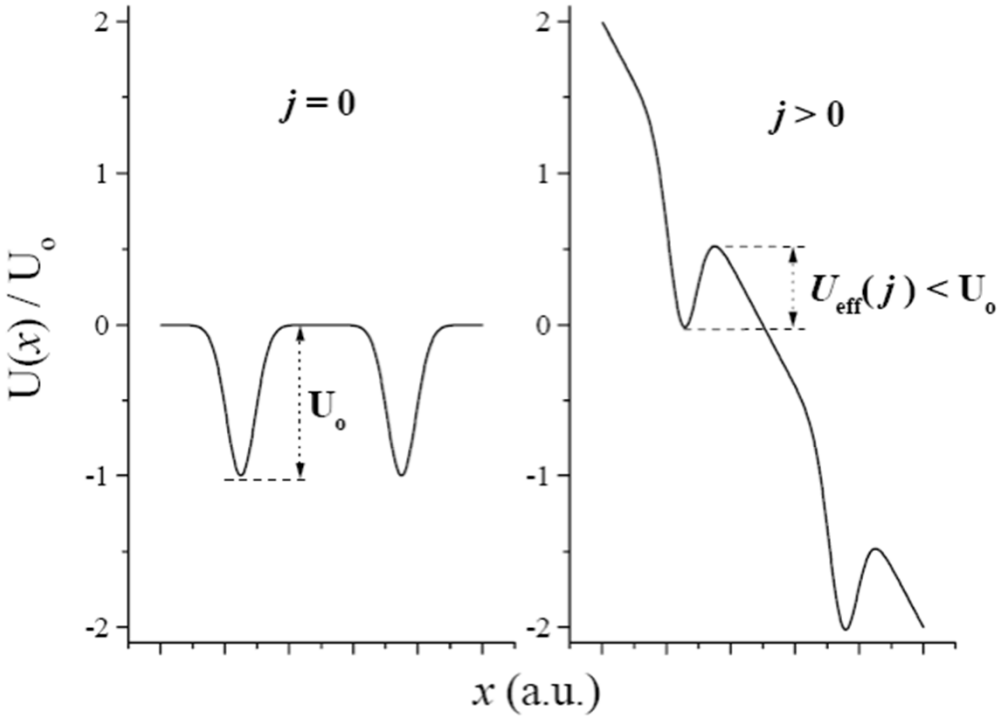

Figure 26 : schematic description of Anderson-Kim flux creep. The left panel shows the undisturbed pinning-potential landscape, to which in the right panel the free energy contribution of the 'Lorentz' force exerted by a current density is added. The effect of the current density is to lower the energy barrier for thermally activated hopping of flux lines (or flux bundles) from one pinning site to the next.

Examples of Superconductors

- Many elements are superconducting at sufficiently low temperatures
- None of the pure elements are useful for applications involving transport current, i.e. they do not allow flux penetration
- Superconductors for transport applications are characterized by alloy/composite materials with $\kappa >> 1$

Material	T_c (K)	$\lambda(0)$, nm	$\xi(0)$, nm	H_{c2} (T)
Nb-Ti	9.5	240	4	13
Nb-N	16	200	5	15
Nb_3Sn	18	65	3	30
MgB_2 (dirty)	32-39	140	6	35
$YBa_2Cu_3O_7$	92	150	1.5	>100
Bi-2223	108	200	1.5	>100

Table 2.9. Critical Temperature and Critical Field of Type I Superconductors

Material	T_c (K)	$\mu_0 H_0$ (mT)
Aluminum	1.2	9.9
Cadmium	0.52	3.0
Gallium	1.1	5.1
Indium	3.4	27.6
Iridium	0.11	1.6
Lanthanum α	4.8	
β	4.9	
Lead	7.2	80.3
Lutecium	0.1	35.0
Mercury α	4.2	41.3
β	4.0	34.0
Molybdenum	0.9	
Osmium	0.7	~6.3
Rhenium	1.7	20.1
Rhodium	0.0003	4.9
Ruthenium	0.5	6.6
Tantalum	4.5	83.0
Thalium	2.4	17.1
Thorium	1.4	16.2
Tin	3.7	30.6
Titanium	0.4	
Tungsten	0.016	0.12
Uranium α	0.6	
β	1.8	
Zinc	0.9	5.3
Zirconium	0.8	4.7

A variety of practical, commercially available superconductors now exist for magnet applications

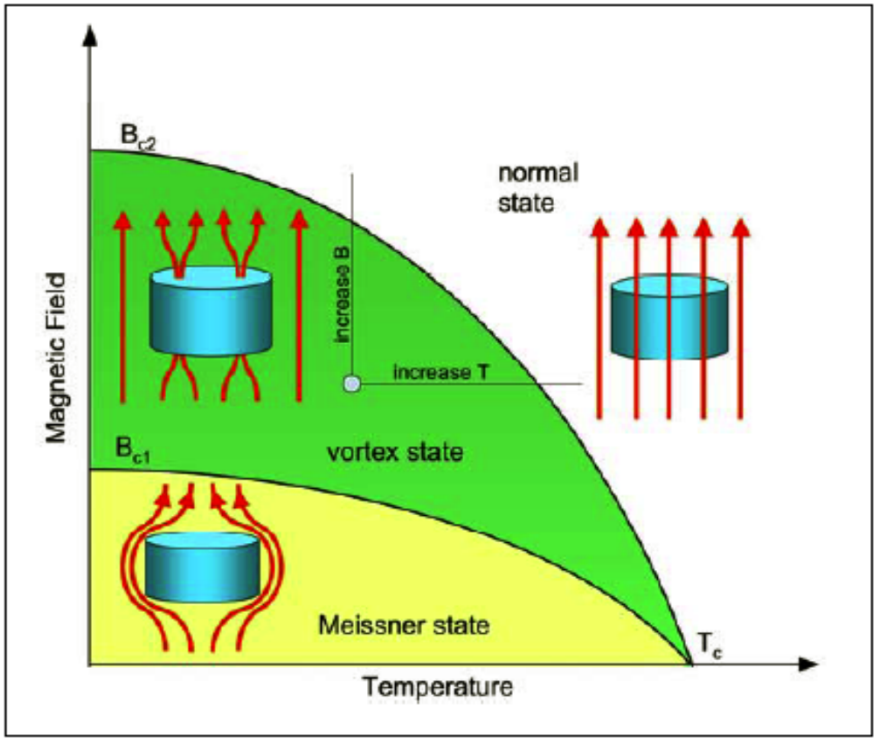

A variety of practical, commercially available superconductors now exist for magnet applications

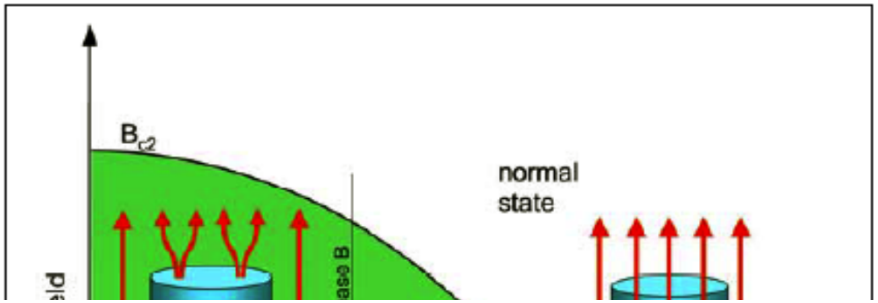

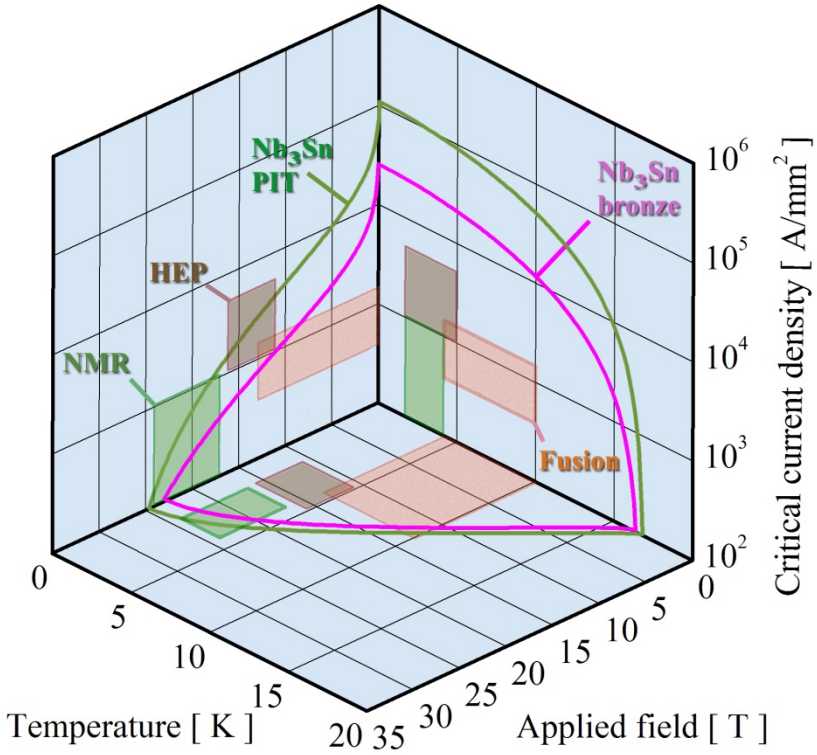

A variety of practical, commercially available superconductors now exist for magnet applications

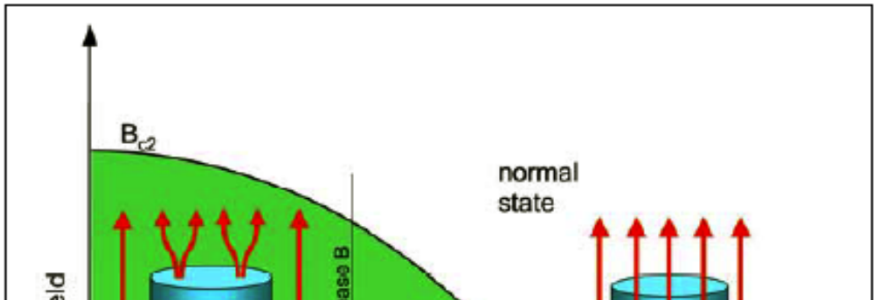

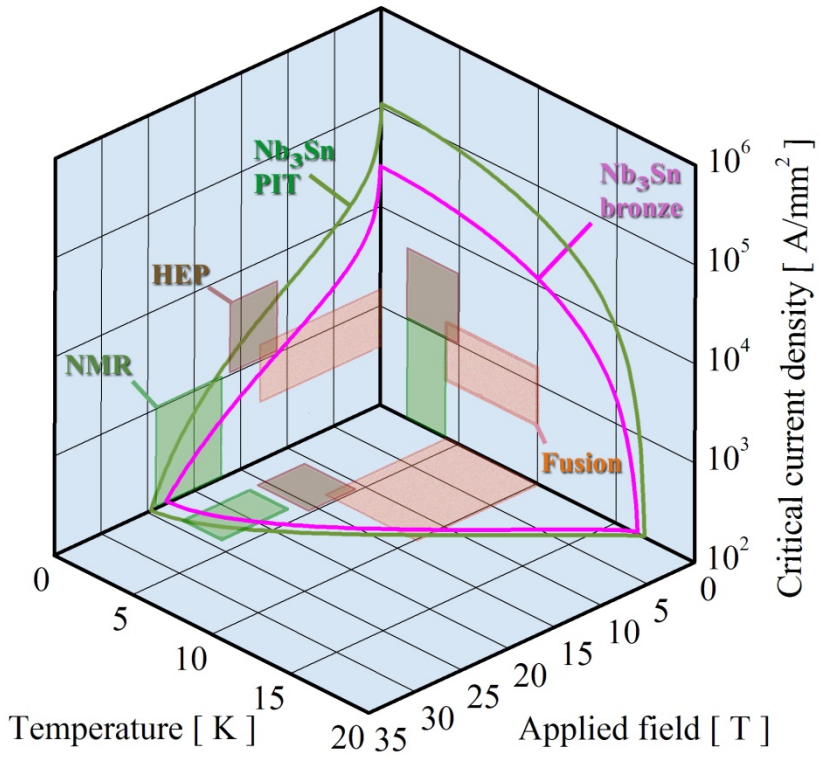

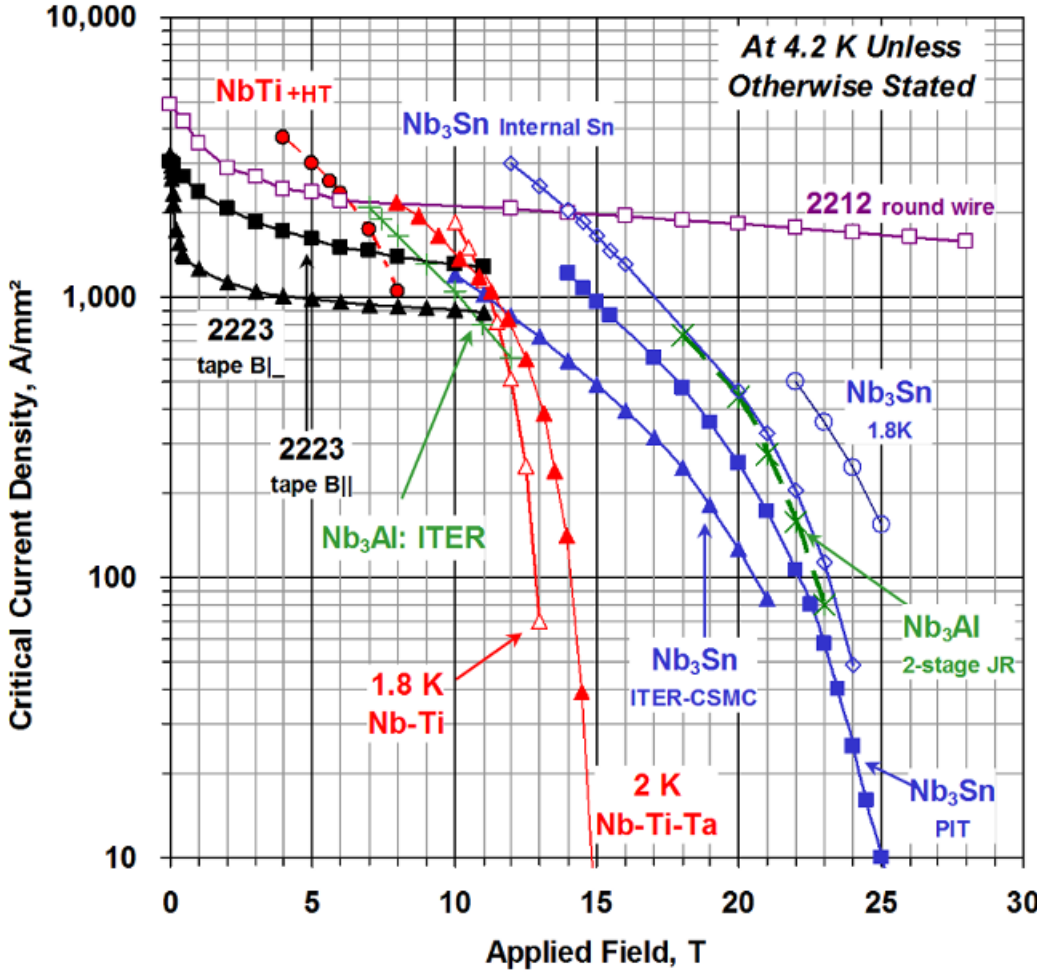

Concept of Critical Surface and the Field-Temperature Phase Boundary

- The critical surface defines the boundaries between superconducting state and normal conducting state in the space defined by temperature, magnetic field, and current densities.
- The surface, determined experimentally, can be fitted with parameterization curves.

M.N. Wilson, [4], p. 2.

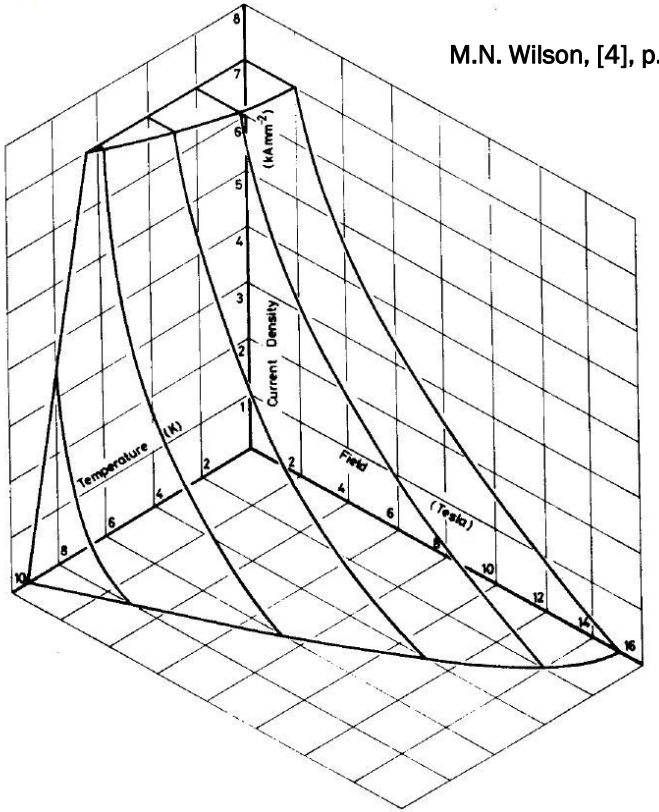

A. Godeke, [2], p. 43.

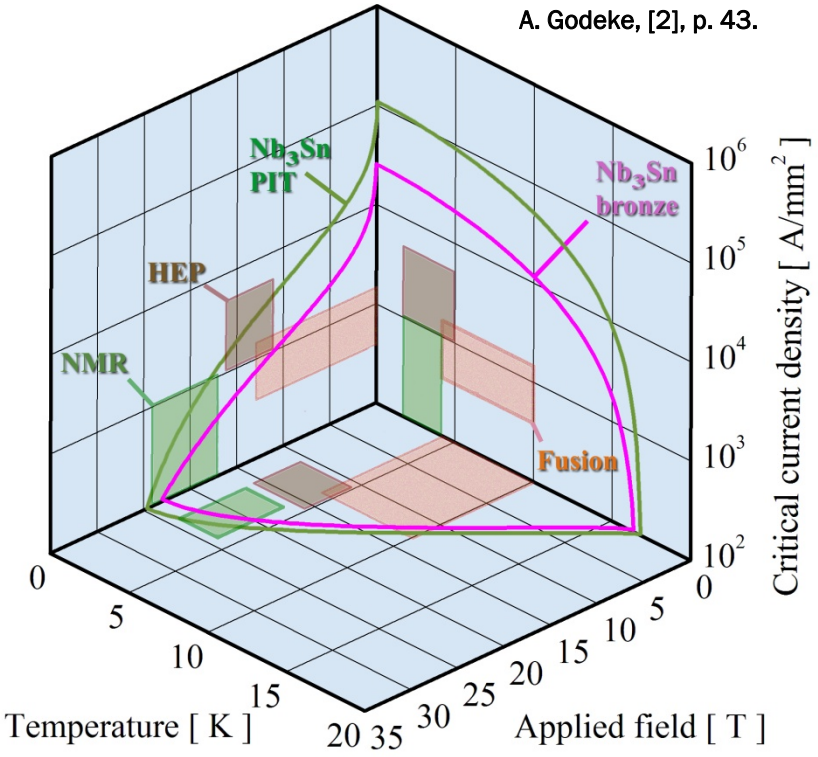

Energy deposition from point disturbances – basic concept of conductor stability

- The length *l* defines the Minimum Propagation Zone (MPZ).
  - A normal zone longer that *l* will keep growing (quench). A normal zone shorter than *l* will collapse.

$$\frac{2kA(\theta_c - \theta_0)}{l} = J_c^2 \rho A l \quad \Rightarrow \quad l = \sqrt{\frac{2k(\theta_c - \theta_0)}{J_c^2 \rho}}$$

- An example:
  - A typical NbTi 6 T magnet has the following properties
    - $J_c = 2 \cdot 10^9$ A m^{-2}
    - $\rho = 6.5 \cdot 10^{-7}$ Ω m
    - $k = 0.1$ W m^{-1} K^{-1}
    - $\theta_c = 6.5$ K
    - $\theta_0 = 4.2$ K

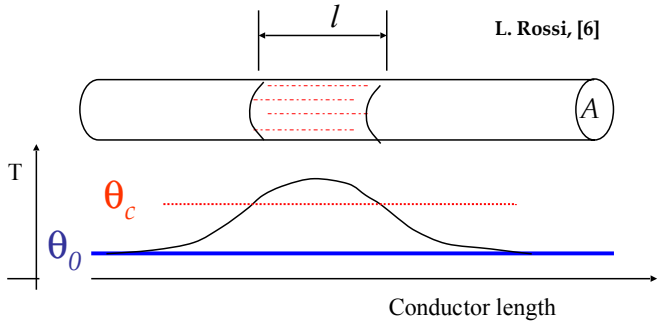

  - In this case, *l* = 0.5 mm and, assuming a 0.3 mm diameter strand, the required energy to bring to θ_c is 10^{-9} J.

- *A wire made purely of superconductor, without any stabilizer (e.g. copper) around, would quench with nJ of energy.*
  - *In order to increase l, since we do not want to reduce J_c, we have to increase k/ρ : we need a* ***composite conductor****!*

Composite conductors provide stability – a key breakthrough for the development of superconducting magnets

- We now consider the situation where the superconductor is surrounded by material with low resistivity and high conductivity.
- Copper properties at 4.2 K
  - resistivity $\rangle = 3 \cdot 10^{-10} \wedge$ m (instead of $6.5 \cdot 10^{-7} \wedge$ m for NbTi)
  - k = 350 W m^{-1} K^{-1} (instead of 0.1 W m^{-1} K^{-1} for NbTi).

- We can therefore increase $k/\rangle$ by almost a factor 10^7.

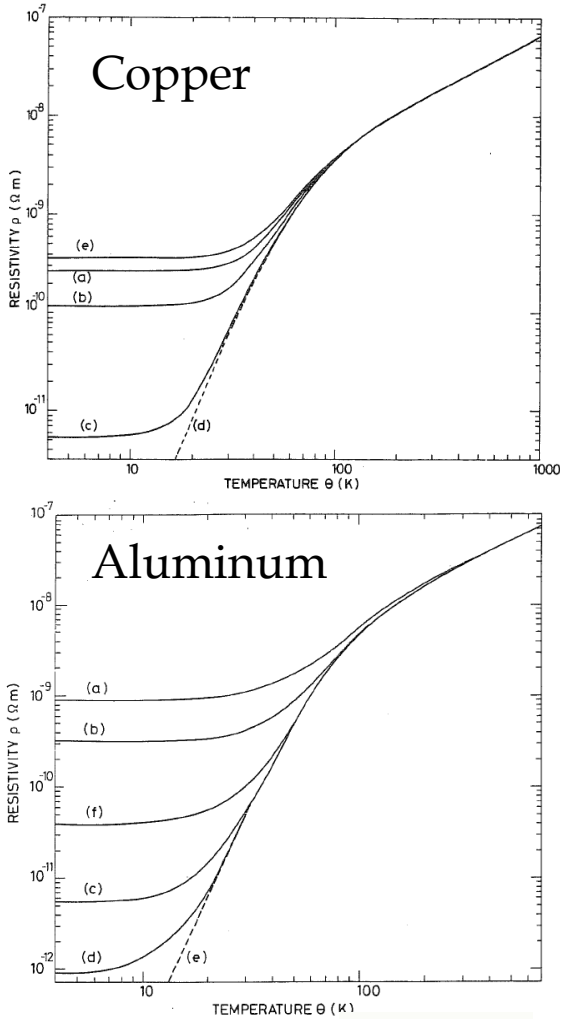

M. Wilson, [2]

The essential dynamic processes involved in conductor stability or not (quench)

- The concept of stability concerns the interplay between the following elements:
  - The addition of a (small) thermal fluctuation local in time and space
  - The heat capacities of the neighboring materials, determining the local temperature rise
  - The thermal conductivity of the materials, dictating the effective thermal response of the system
  - The critical current dependence on temperature, impacting the current flow path
  - The current path taken by the current and any additional resistive heating sources stemming from the initial disturbance

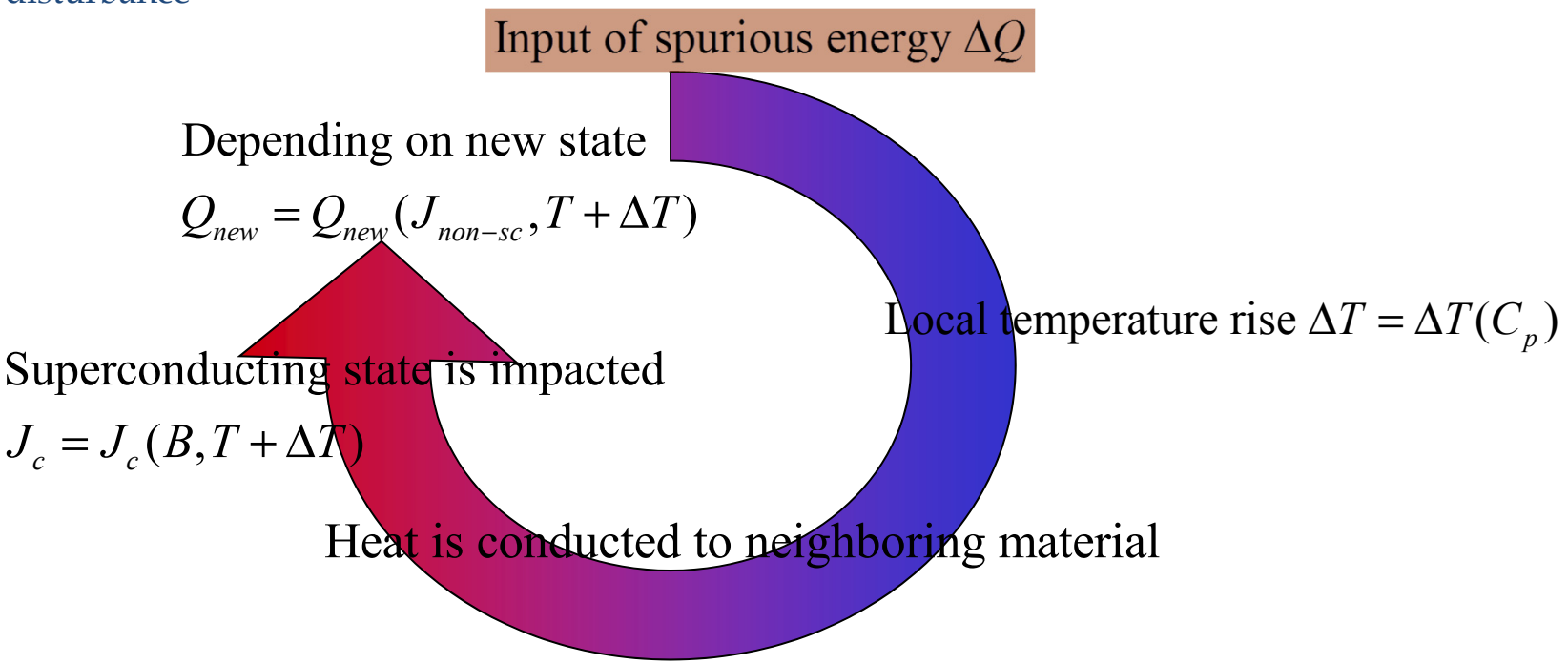

Calculation of the bifurcation point for superconductor instabilities

Thanks to Matteo Allesandrini, Texas Center for Superconductivity, for these calculations and slides

Heat Balance Equation in 1D, without coolant: *[W/m³]*

$$\frac{d}{dx}\left(k(T)\cdot\frac{dT}{dx}\right)+\rho(T)\cdot J^2+Q_{initial\_pulse}-C(T)_{volume}\cdot\frac{dT}{dt}=0$$

Heat conduction | Joule effect | Quench trigger | Heat stored in the material

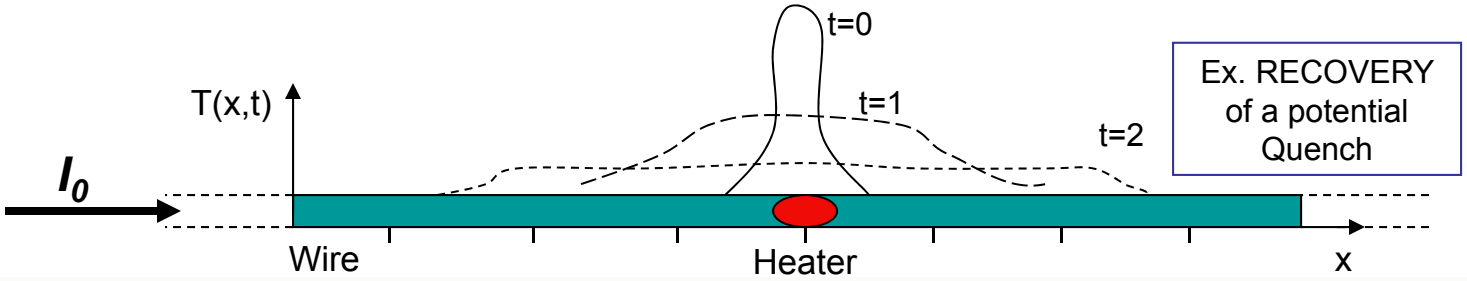

Assumption on $\rho(T)\cdot J^2$:

CASE 1. $T < T_{sc\_crit}$

- 1.a) $T < T_{current\ sharing}$ — $I_{sc}=I_o$, $I_{metal}=0$
- 1.b) $T > T_{current\ sharing}$ — $I_{sc}=I_{crit(T)}$, $I_{metal}=I_0-I_{sc}$

CASE 2. $T > T_{sc\_crit}$ -- $I_{sc}=0$, $I_{metal}=I_0$

Temperature profile

With T_{cr} = **39 K**

EXAMPLE: (note material properties are not realistic here)

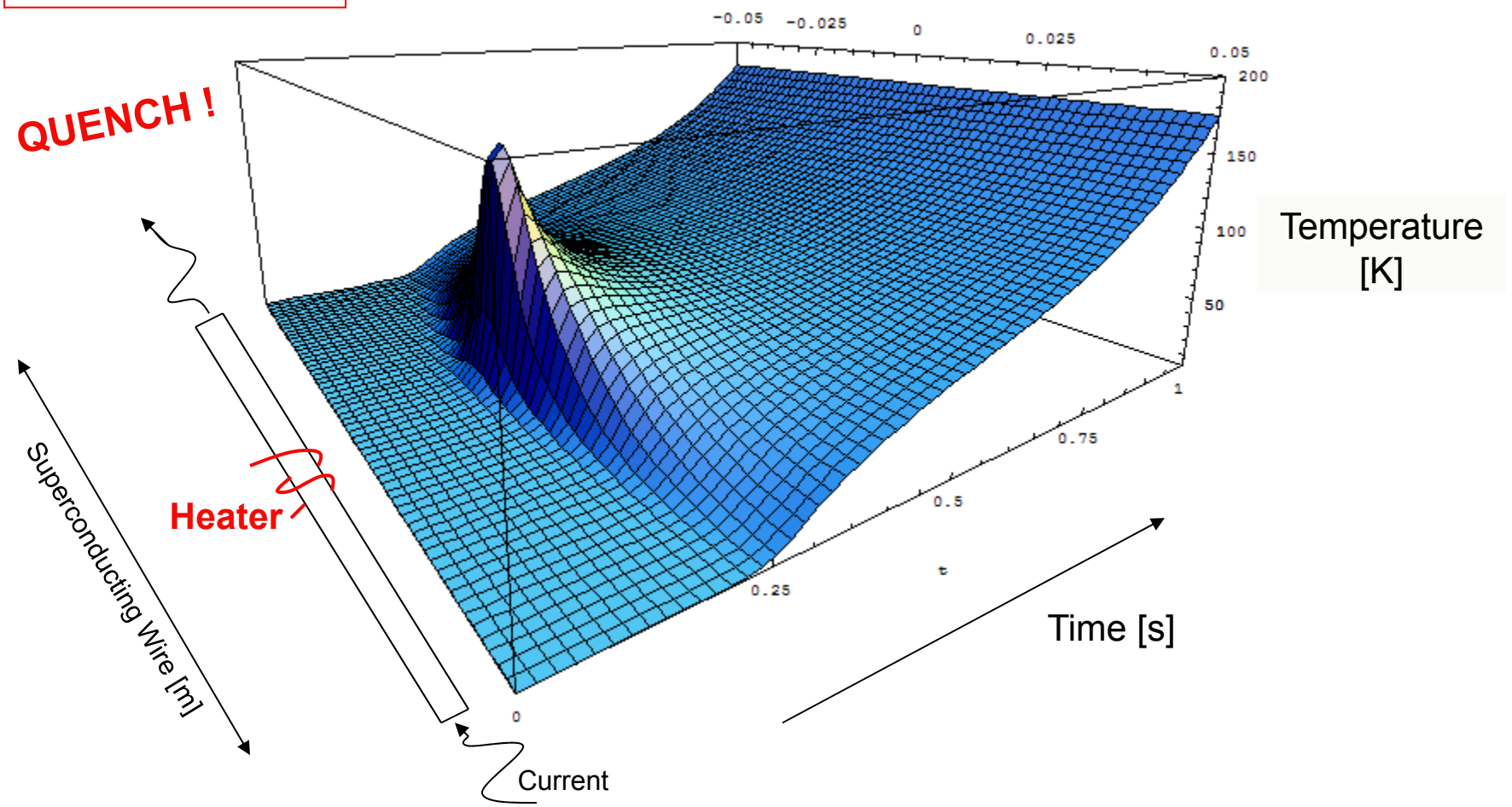

Example simulation of a Nb_3Sn development magnet

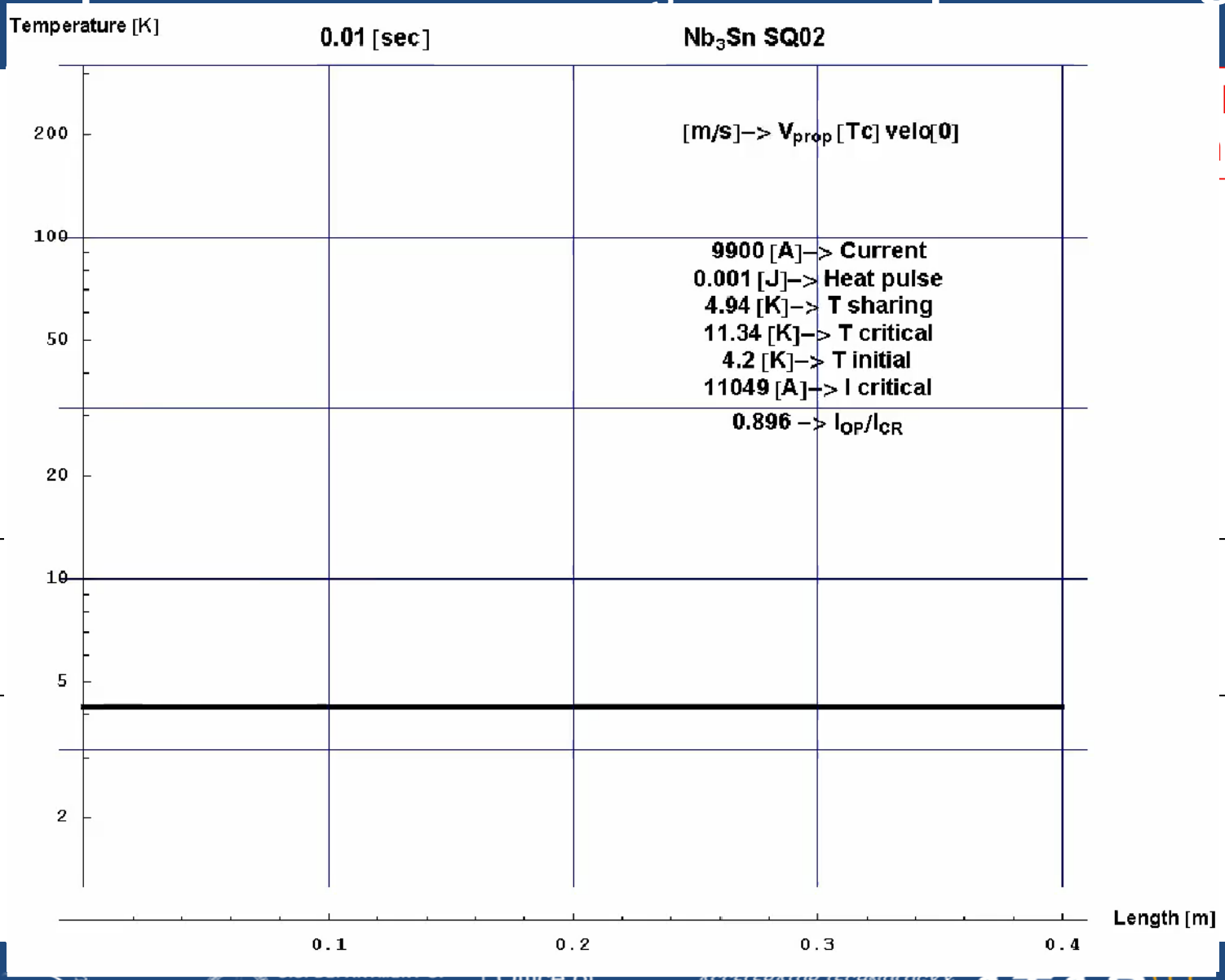

ENCH
1 [mJ]

-- $T_{critical}$

-- $T_{sharing}$

HTS specific stability issues

- Whereas flux flow usually results in a flux jump condition in LTS materials, the far higher critical temperature of HTS materials provides significant heat capacity to mitigate the avalanche scenario
- The superconducting parameters for HTS materials and the (typically) higher operating temperature tend to increase the possibility of thermally induced flux motions: "melting" of the fluxoid lattice

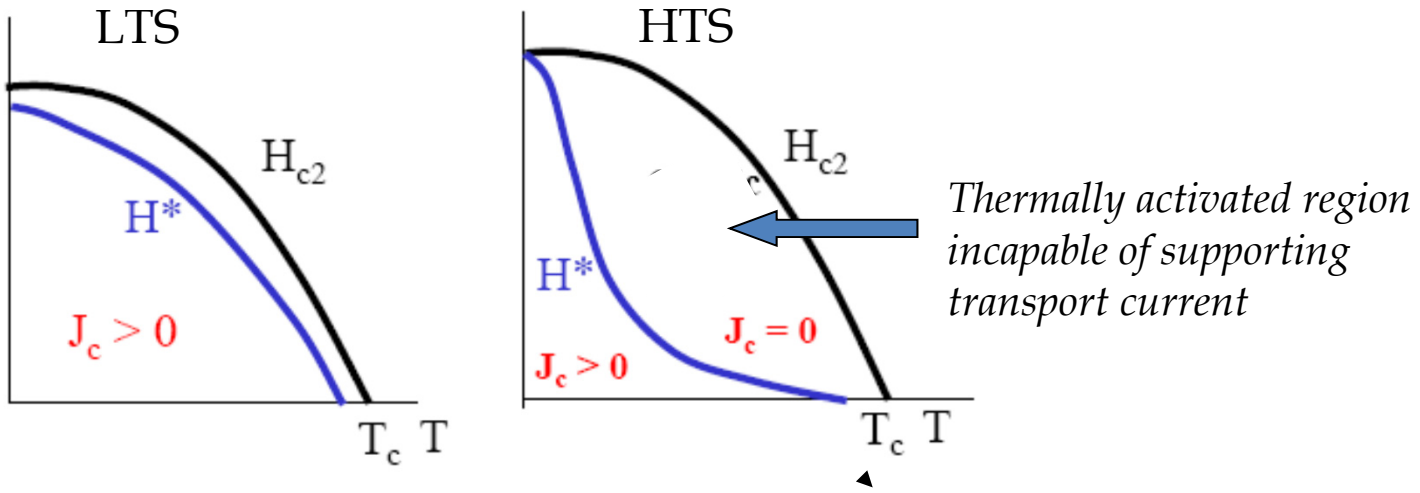

Example: Quench propagation in Bi2212

- Quench initiation in HTS requires larger (10-100) amplitude thermal sources (i.e. higher stability)
- BUT: high temperature margin results in slow quench propagation – risk of high hot-spot temperature before quench is detected

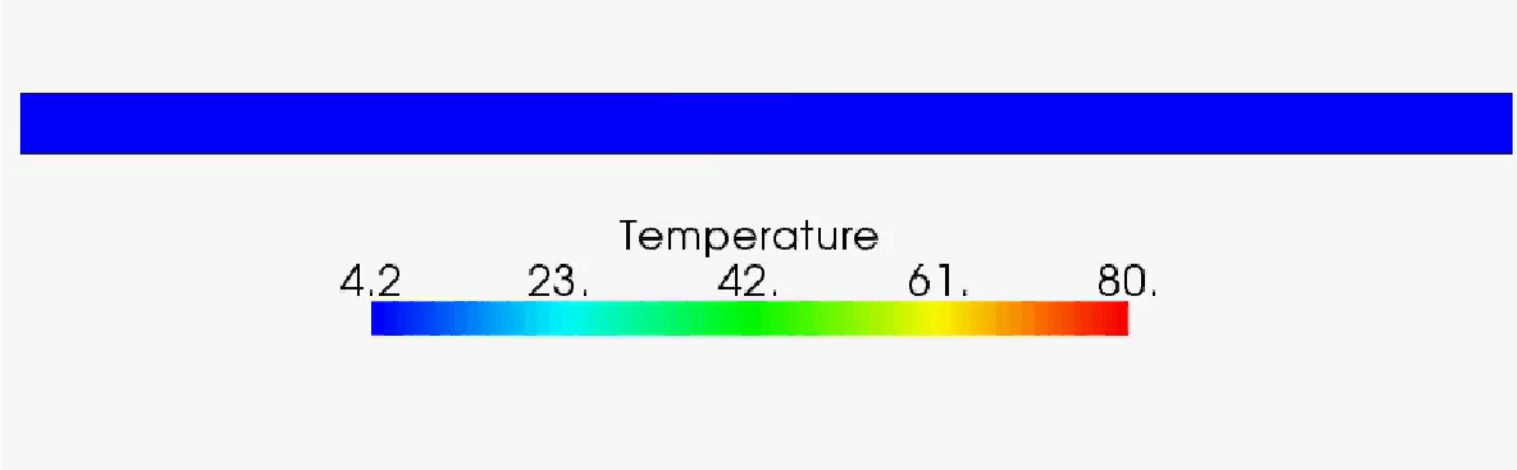

The low temperature superconductors for accelerator applications

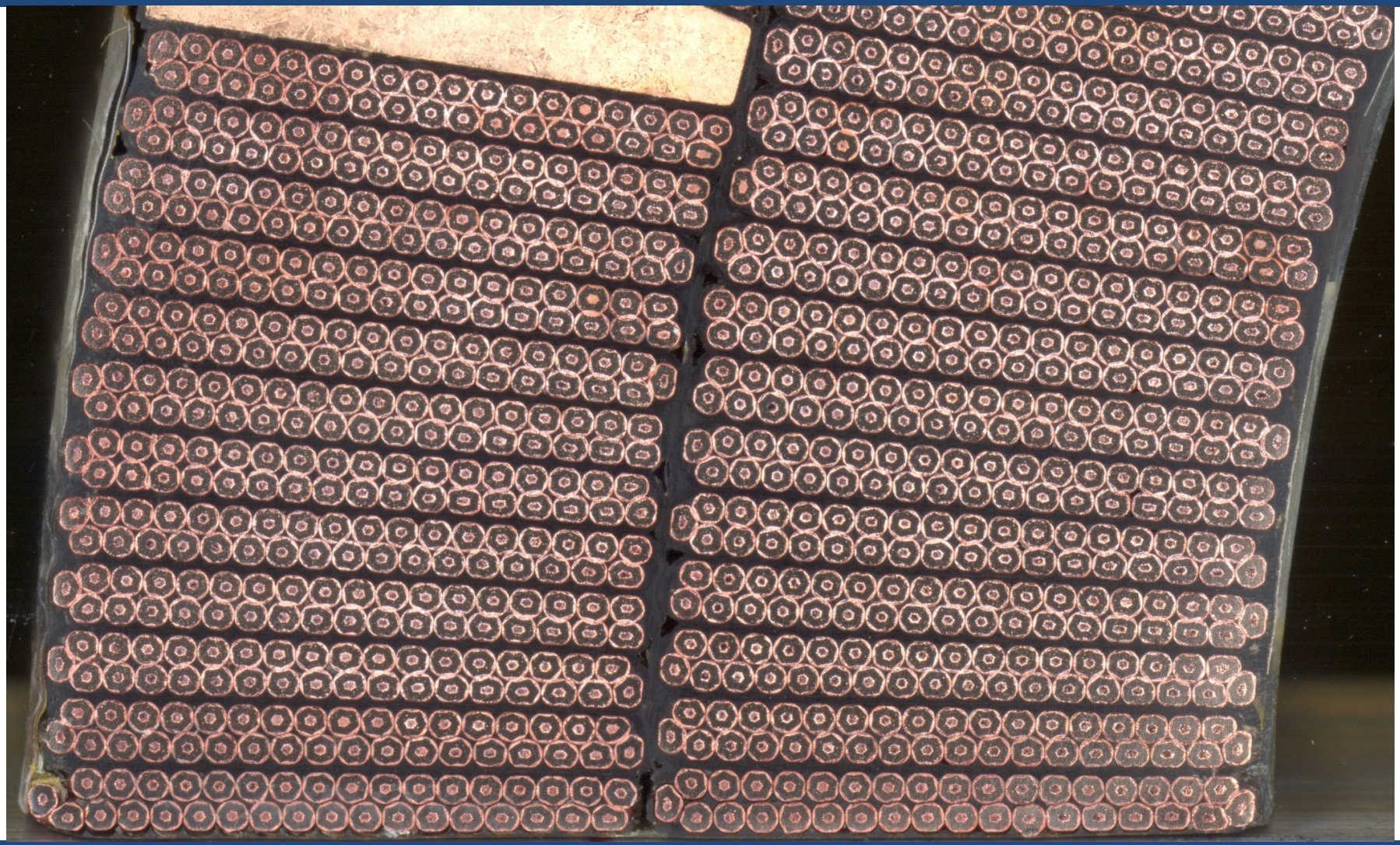

Practical superconductors are more complicated than just "superconductor and stabilizer"

- The superconducting materials used in accelerator magnets are
  - subdivided in filaments of small diameters
    - to reduce magnetic instabilities called flux jumps
    - to minimize field distortions due to superconductor magnetization
  - twisted together
    - to reduce interfilament coupling and AC losses
  - embedded in a copper matrix
    - to provide stability against thermal disturbances
    - to protect the superconductor after a quench

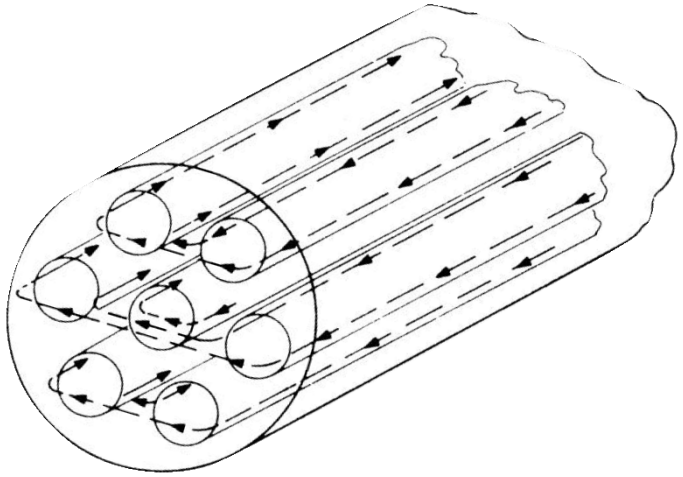

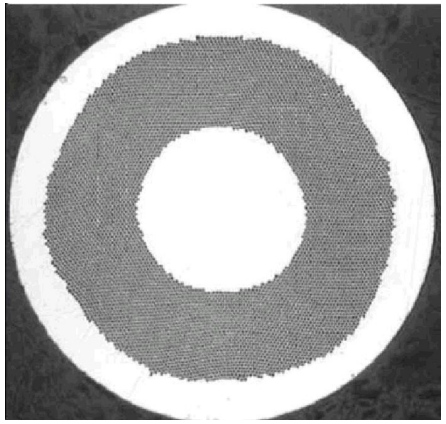

NbTi LHC wire (A. Devred, [1])

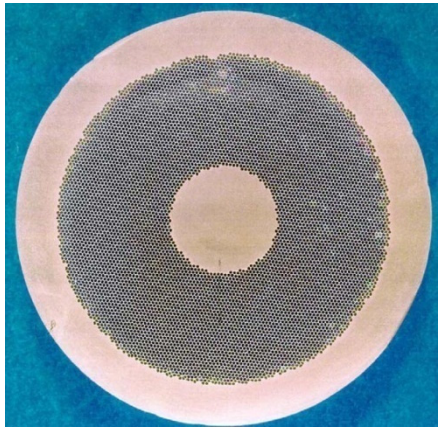

NbTi SSC wire (A. Devred, [1])

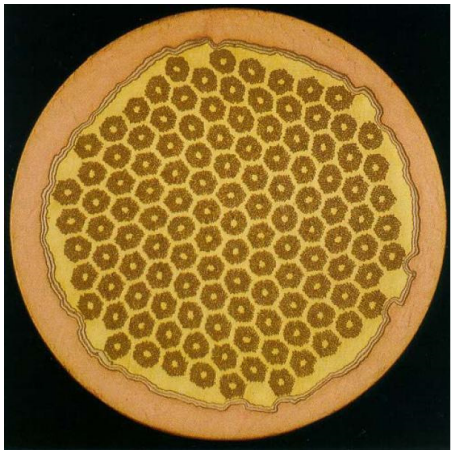

Nb_3Sn bronze-process wire (A. Devred, [1])

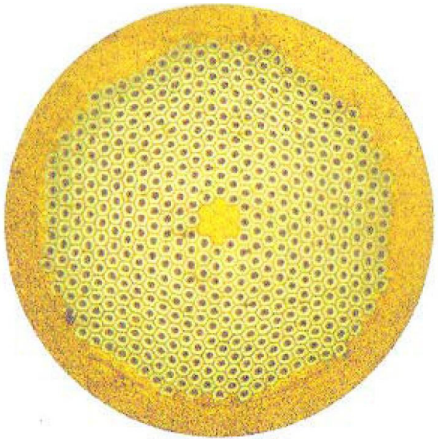

Nb_3Sn PIT process wire (A. Devred, [1])

Fabrication of NbTi multifilament wires is a complex but well-established process

- Monofilament rods are stacked to form a multifilament billet, which is then extruded and drawn down.
- Heat treatments are applied to produce pinning centers (α-Ti precipitates).
- When the number of filaments is very large, multifilament rods can be re-stacked (double stacking process).

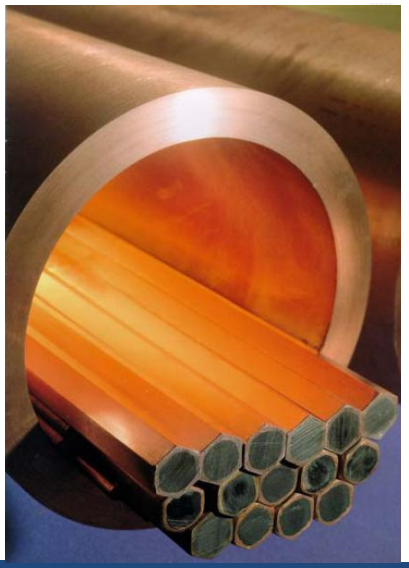

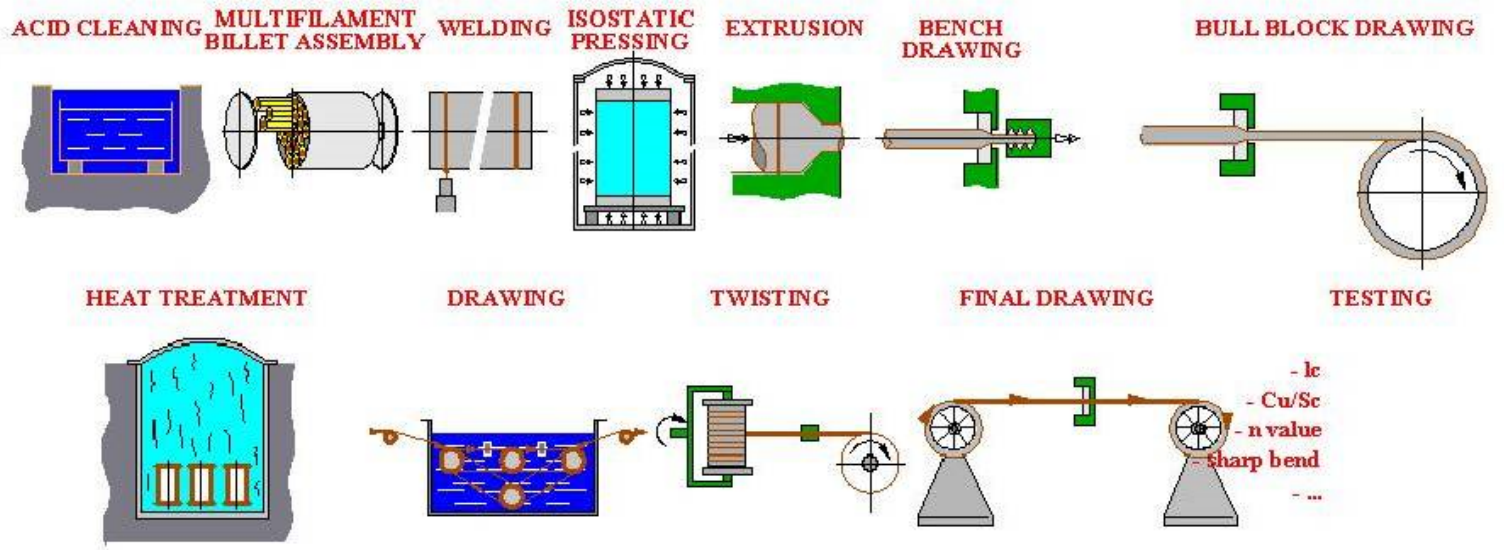

A. Devred, [1]

Multiple routes to the fabrication of Nb_3Sn multifilament wires exist – the Bronze process yields small filaments

- Bronze process
  - Pro: small filament size
  - Con: limited amount of Sn in bronze and annealing steps during wire fabrication to maintain bronze ductility.
  - Non-Cu J_C up to 1000 A/mm^2 at 4.2 K and 12 T.

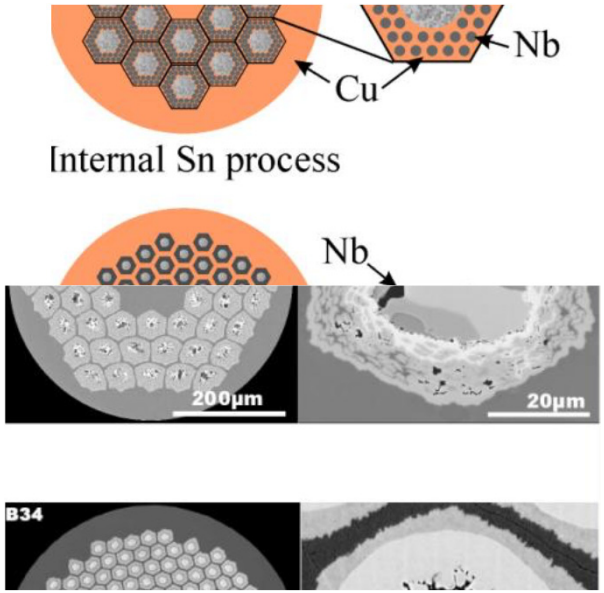

- Internal tin process
  - Pro: no annealing steps and not limited amount of Sn
  - Con: small filament spacing => large effective filament size (100 µm)
  - Non-Cu JC up to 3000 A/mm2 at 4.2 K and 12 T.

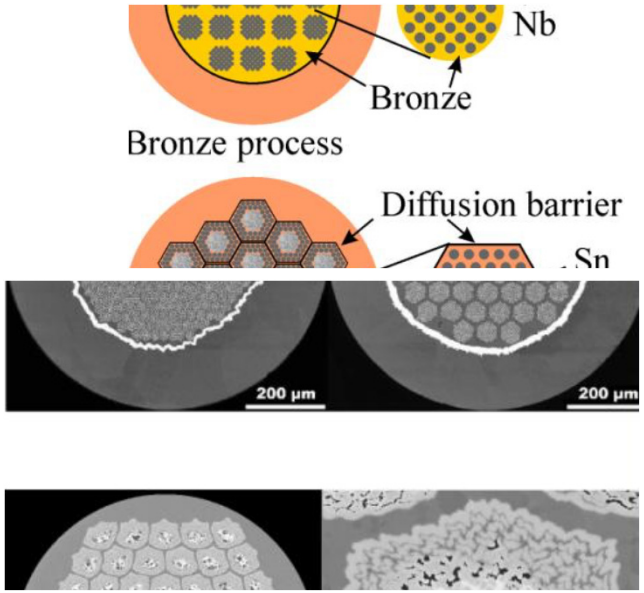

- Powder in tube (PIT) process
  - Pro: small filament size (30 µm) and short heat treatment (proximity of tin to Nb).
  - Con: fabrication cost.
  - Non-Cu JC up to 2300 A/mm2 at 4.2 K and 12 T.

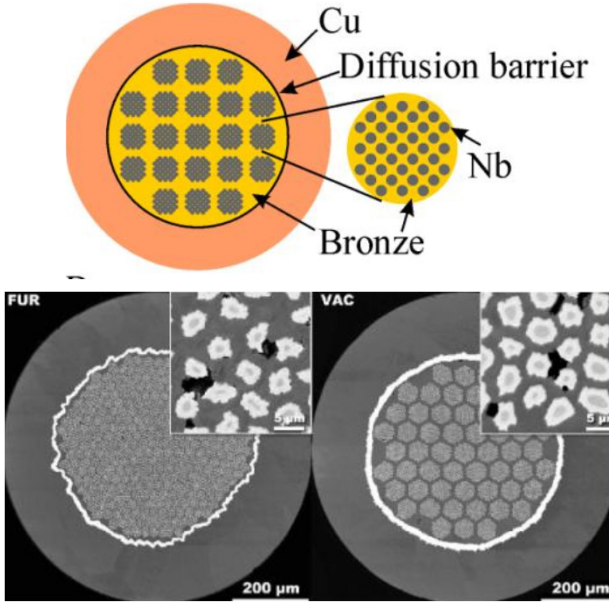

Motivation for superconducting cables, and the workhorse for accelerator magnets, the Rutherford cable

- Most of the superconducting coils for particle accelerators are wound from a multi-strand cable:
  - reduction of the strand piece length;
  - reduction of number of turns
    - easy winding;
    - smaller coil inductance
      - less voltage required for power supply during ramp-up;
      - after a quench, faster current discharge and less coil voltage.
  - current redistribution in case of a defect or a quench in one strand.
- The strands are twisted to
  - reduce interstrand coupling currents Losses and field distortions
  - provide more mechanical stability
- The most commonly used multi-strand cable for accelerators is the Rutherford cable

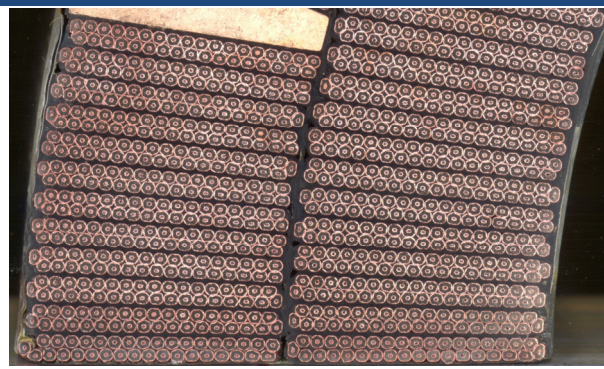

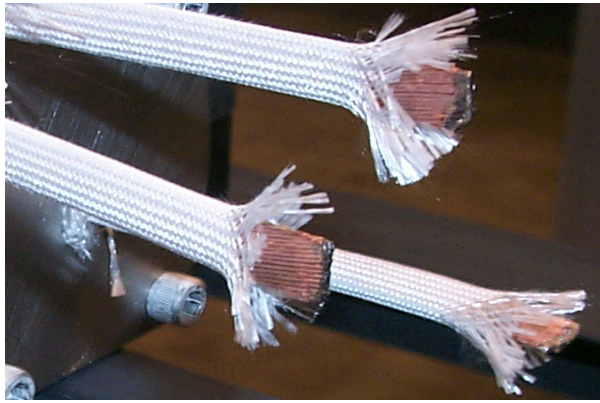

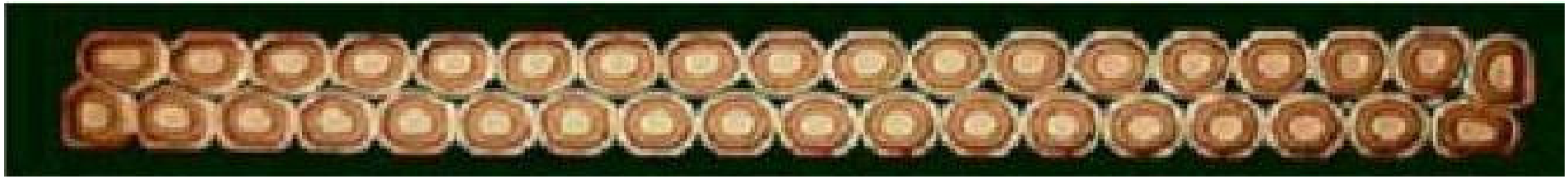

4. Superconducting cables
Fabrication of Rutherford cable

- Rutherford cables are fabricated by a cabling machine.
  - Strands are wound on spools mounted on a rotating drum.
  - Strands are twisted around a conical mandrel into an assembly of rolls (Turk's head). The rolls compact the cable and provide the final shape.

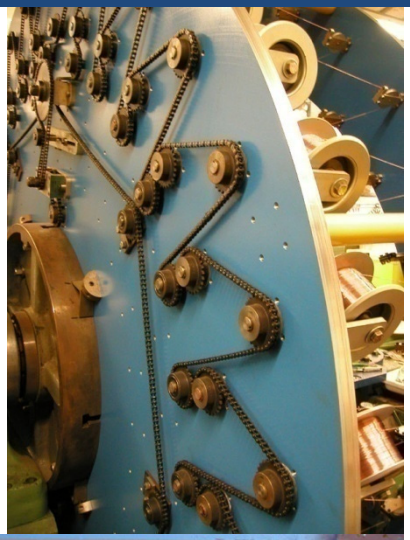

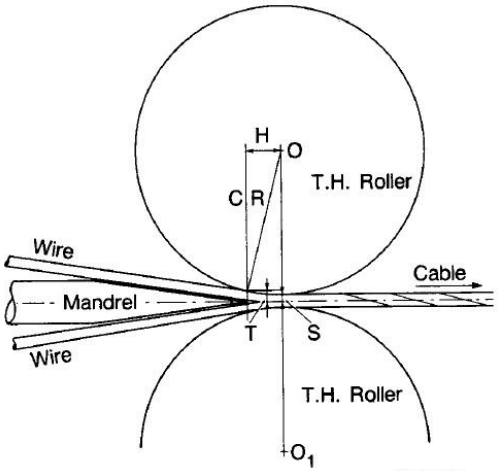

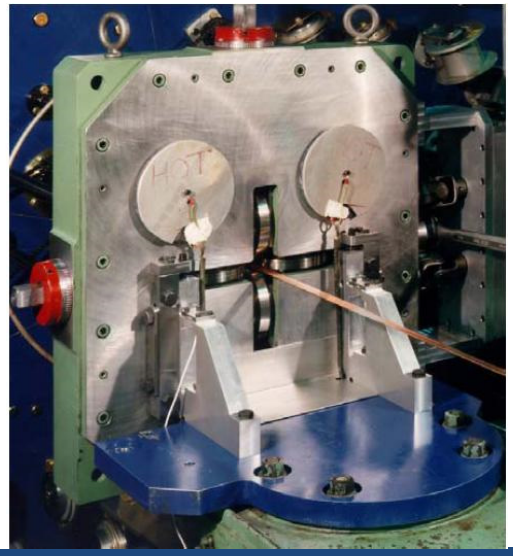

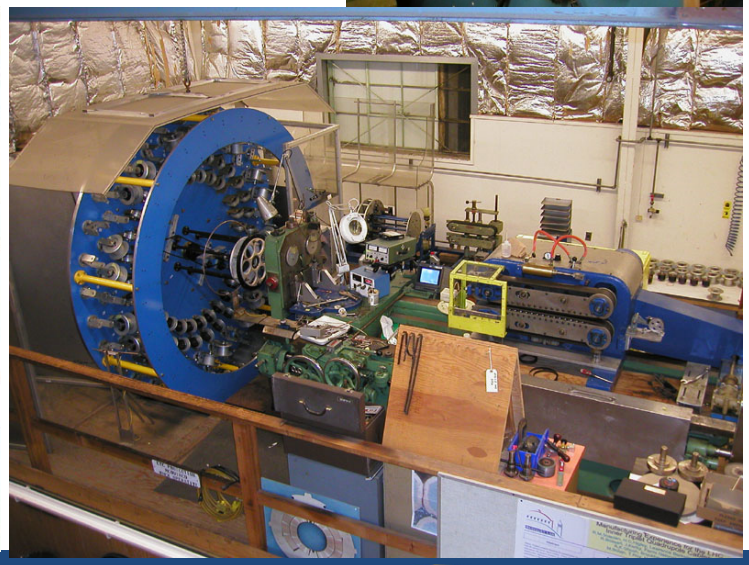

4. Superconducting cables
Fabrication of Rutherford cable

Understanding AC losses via magnetization

- Screening currents are bound currents that correspond to sample magnetization.
  - Integration of the hysteresis loop quantifies the energy loss per cycle

=> Will result in the same loss as calculated using EJ_c

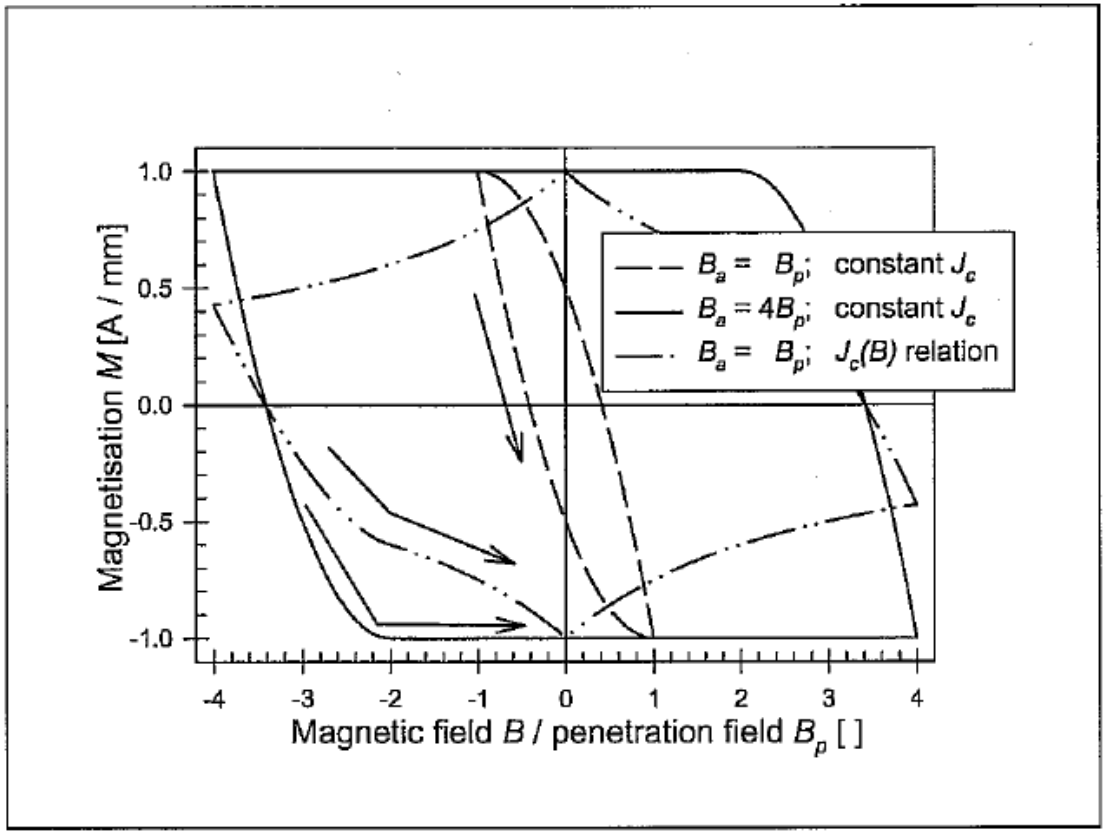

Figure 2.3 Magnetisation loops calculated for an infinite slab parallel to the magnetic field.

Coupling losses are losses in the stabilizer due to current flow from one filament to another

- A multifilamentary wire subjected to a transverse varying field will see an electric field generated between filaments of amplitude:

$$E = \frac{\dot{B}L}{2\pi}$$; L is the twist-pitch of the filaments

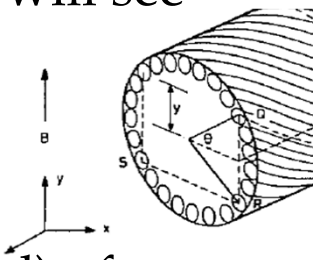

- The metal matrix then sees a current (parallel to the applied field) of amplitude:

$$J = \frac{\dot{B}L}{2\pi\rho_t}$$

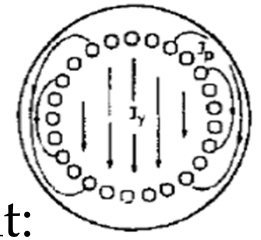

- Similarly, the filaments couple via the periphery to yield a current:

$$J_p(\theta) = \frac{\dot{B}L\cos(\theta)}{2\pi\rho_m}$$

- There are also eddy currents of amplitude:

$$J_e(\theta) = \frac{\dot{B}a\cos(\theta)}{\rho_m}$$

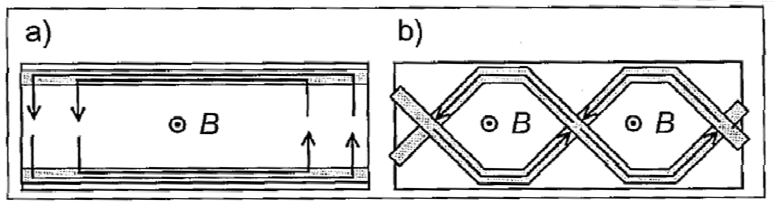

Figure 2.4 Schematic of coupling currents between two filaments in a wire or tape.

Coupling losses – Rutherford cables

- Coupling currents also form between strands in cables

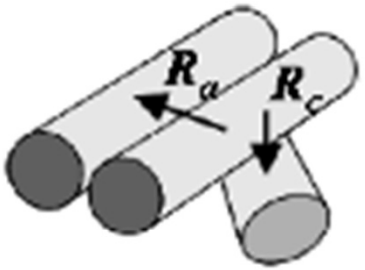

Fig. 18. Crossover resistance R_c and adjacent resistance R_a.

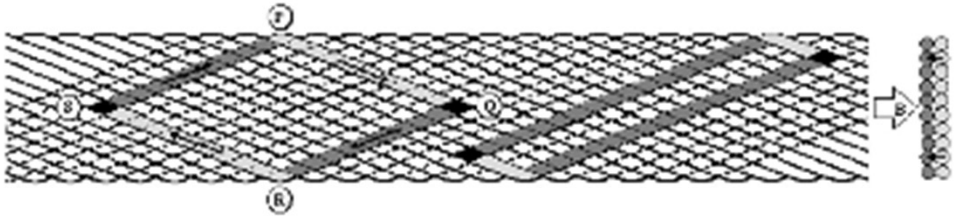

Fig. 19. Coupling currents flowing via crossover resistance R_c in transverse field (upper wires shown light grey).

$$\frac{\dot{Q}_{tc}}{\dot{Q}_{ta}} = \frac{R_a}{R_c}\frac{N(N-1)}{20}$$

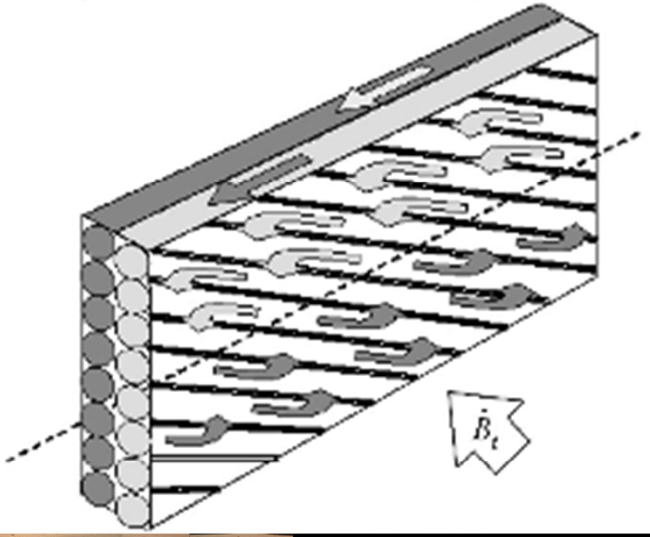

*Add **core** to dramatically reduce transverse coupling R_c, while maintaining decent R_a for current sharing*

AC losses can impact performance in colliders

- **Boundary induced coupling currents (BICCs)**
  - Current imbalances induced by ramping fields
  - Sextupole value at a given field can depend on the history; makes beam dynamics difficult

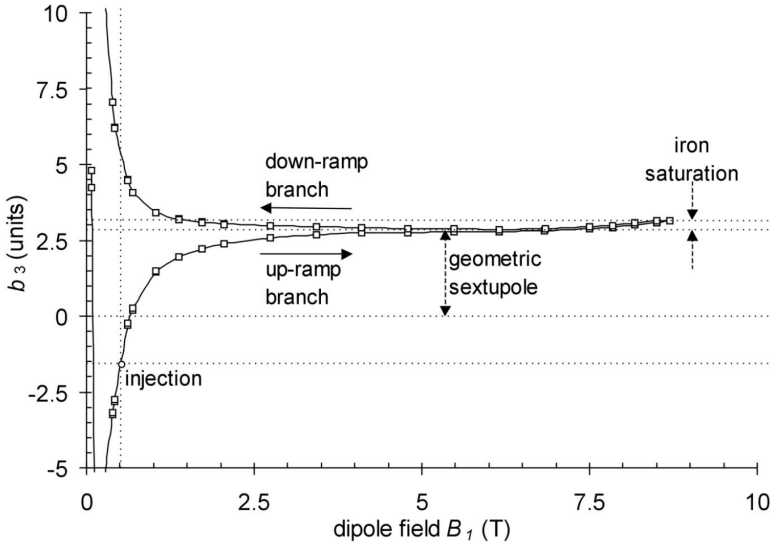

Markus Haverkamp
Decay and Snapback in Superconducting Accelerator Magnets
Ph.D. thesis University of Twente

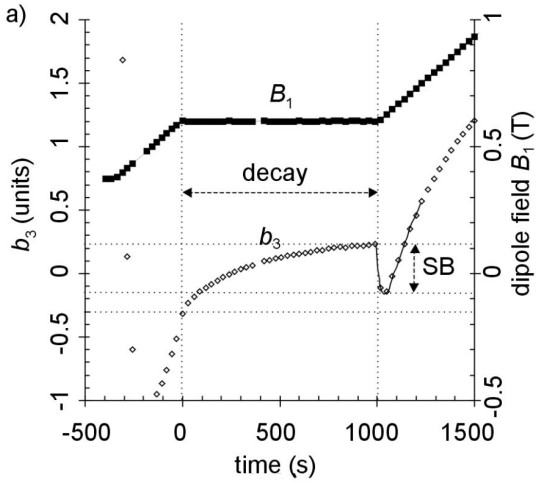

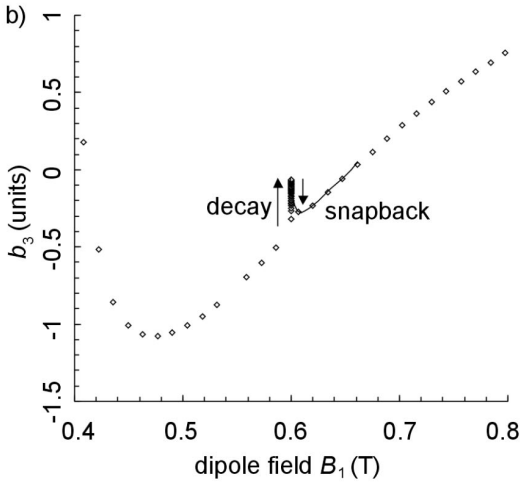

Magnetic designs for superconducting accelerator magnets

For high field accelerator magnets, the stored energy and magnetic forces are the dominant technical issue

- The magnetic field possesses an energy density [J/m^3] $U = \frac{B_0^2}{2\mu_0}$
- The total energy [J] is given by $E = \int_{all\_space} \frac{B_0^2}{2\mu_0} dV$
- Or, considering only the coil volume, by $E = \frac{1}{2}\int_V \vec{A}\cdot\vec{j}\,dV$
- Knowing the inductance L, it can also be expresses as $E = \frac{1}{2}LI^2$
- The total energy stored is strongly related to mechanical and protection issues.

Overview of accelerator dipole magnets

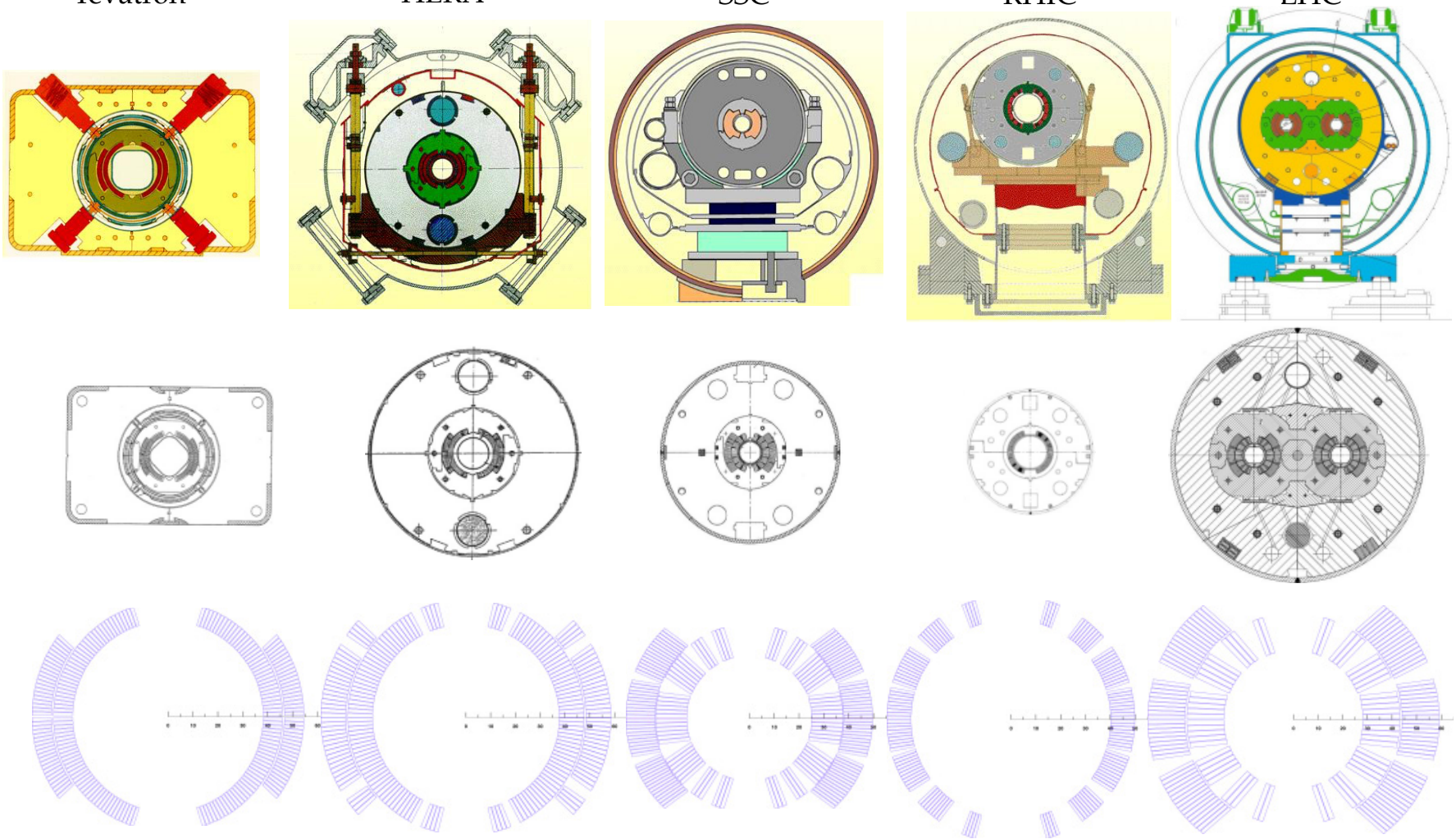

For high-field dipoles a number of concepts have been, and are being, investigated

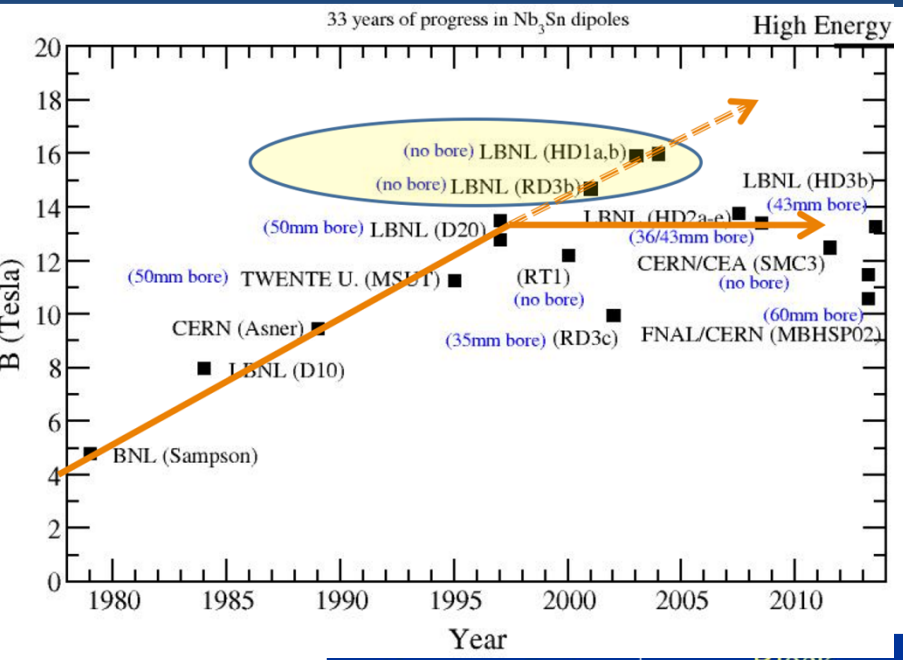

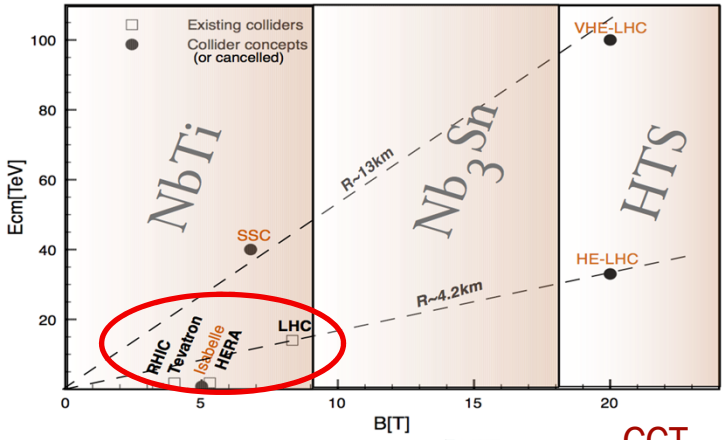

CCT

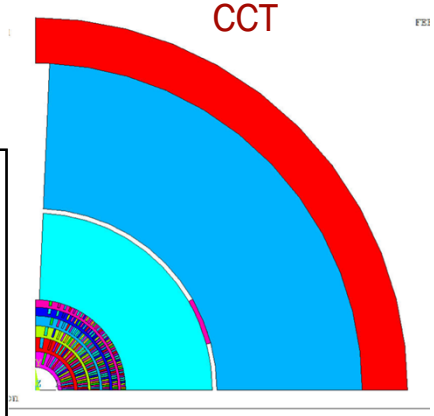

TAMU

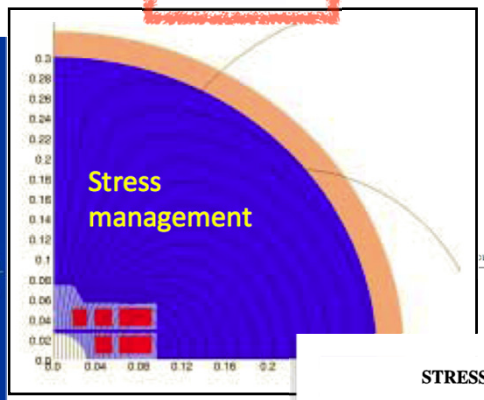

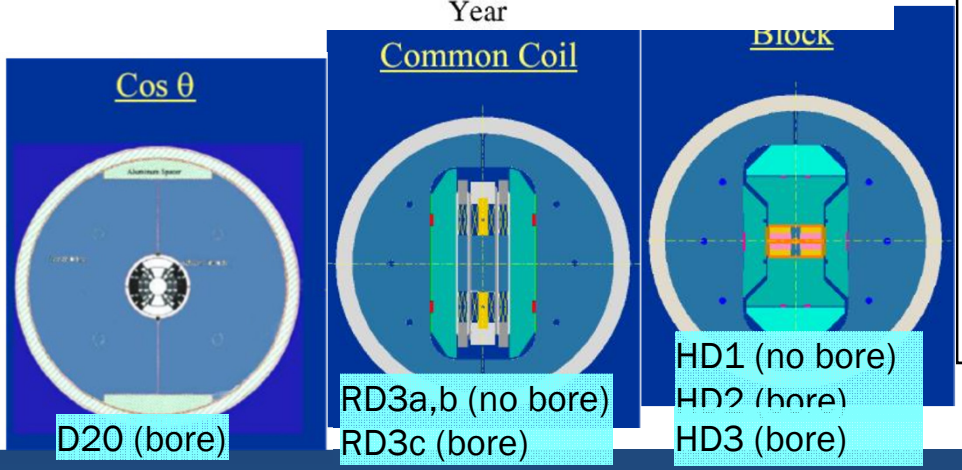

STRESS MANAGEMENT IN HIGH-FIELD DIPOLES

N. Diaczenko, T. Elliott, A. Jaisle, D. Latypov, P. McIntyre, P. McJunkins, L. Richards, W. Shen, R. Soika, D. Wendt, Dept. of Physics, Texas A&M University, College Station, TX 77843
R. Gaedke, Dept. of Physics, Trinity University, San Antonio, TX 78212

For high-field dipoles a number of concepts have been, and are being, investigated

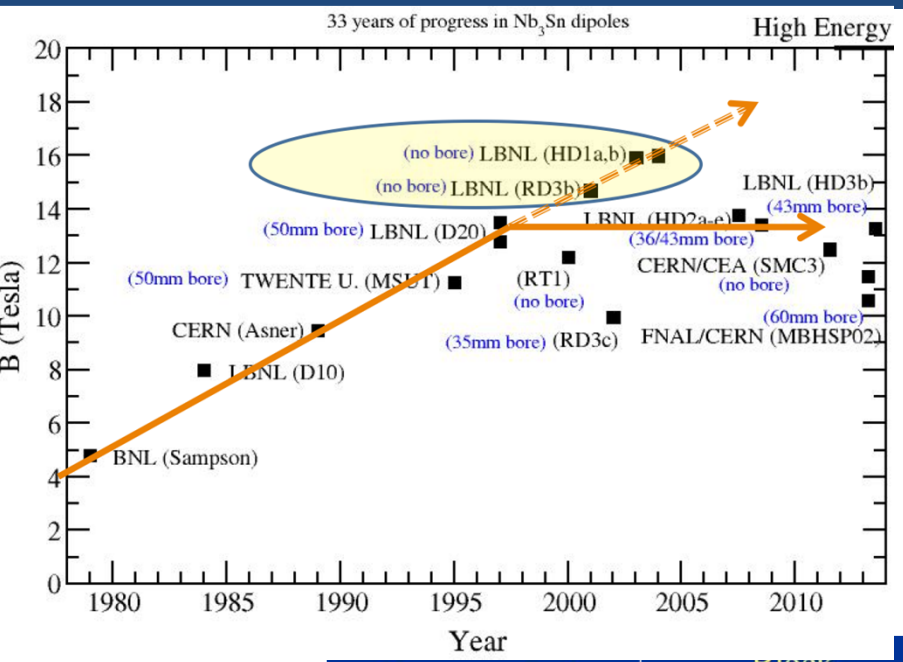

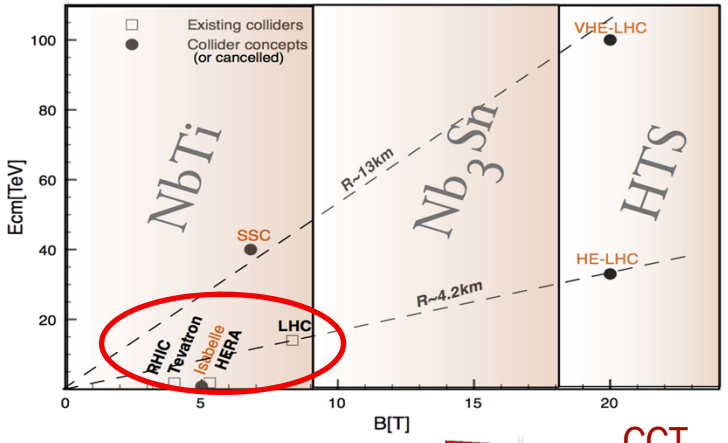

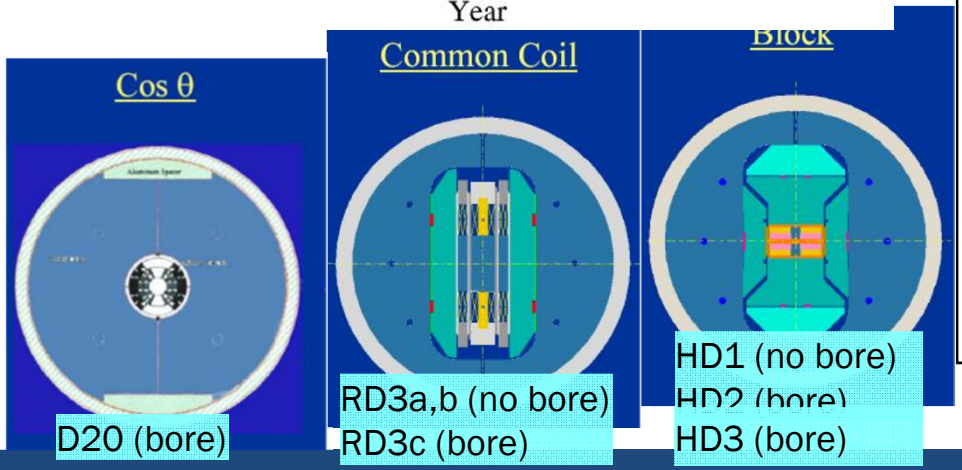

TAMU

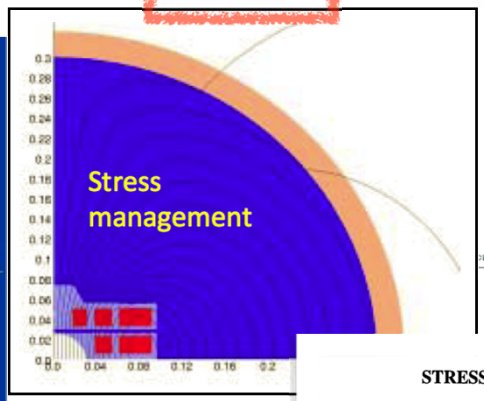

CCT

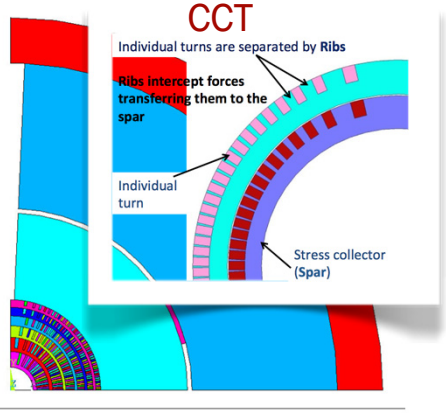

STRESS MANAGEMENT IN HIGH-FIELD DIPOLES

N. Diaczenko, T. Elliott, A. Jaisle, D. Latypov, P. McIntyre, P. McJunkins, L. Richards, W. Shen, R. Soika, D. Wendt, Dept. of Physics, Texas A&M University, College Station, TX 77843
R. Gaedke, Dept. of Physics, Trinity University, San Antonio, TX 78212

Mechanical considerations

The forces acting on the coils tend to separate them from the pole
Example: Tevatron main dipole

- Let's consider the case of the Tevatron main dipole (B_{nom}= 4.4 T).
- In a infinitely rigid structure without pre-stress the pole would move of about -100 μm, with a stress on the mid-plane of -45 MPa.

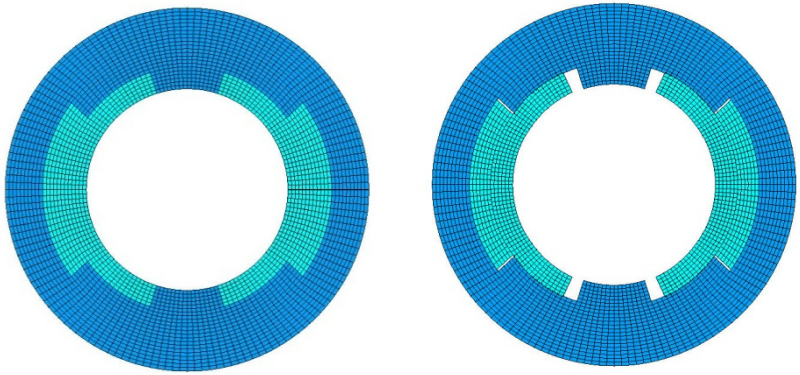

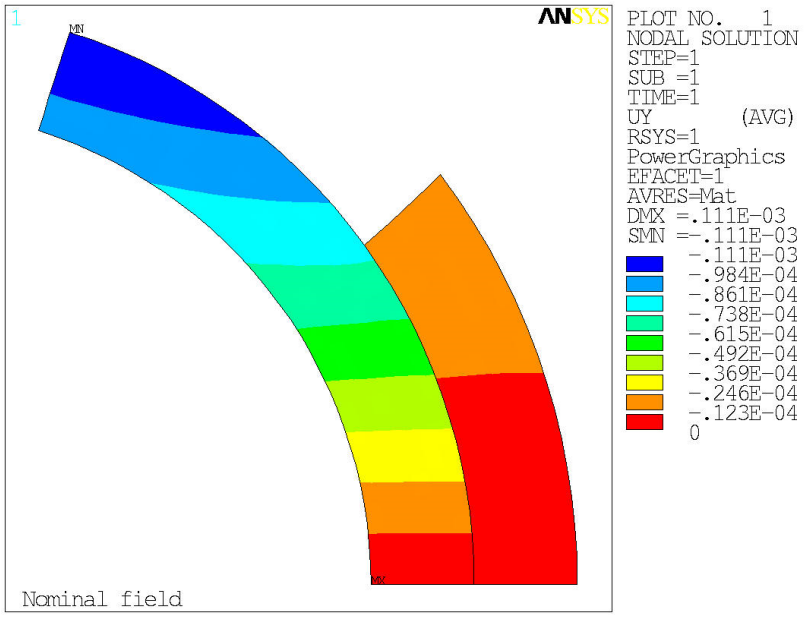

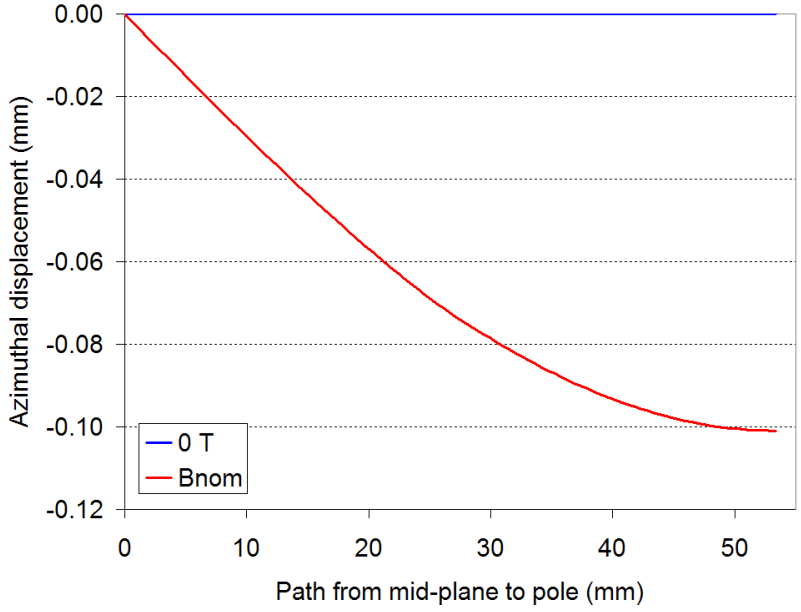

Application of prestress to eliminate separation: Tevatron main dipole

- We now apply to the coil a pre-stress of about -33 MPa, so that no separation occurs at the pole region.
- The displacement at the pole during excitation is now negligible, and, within the coil, the conductors move at most of -20 μm.

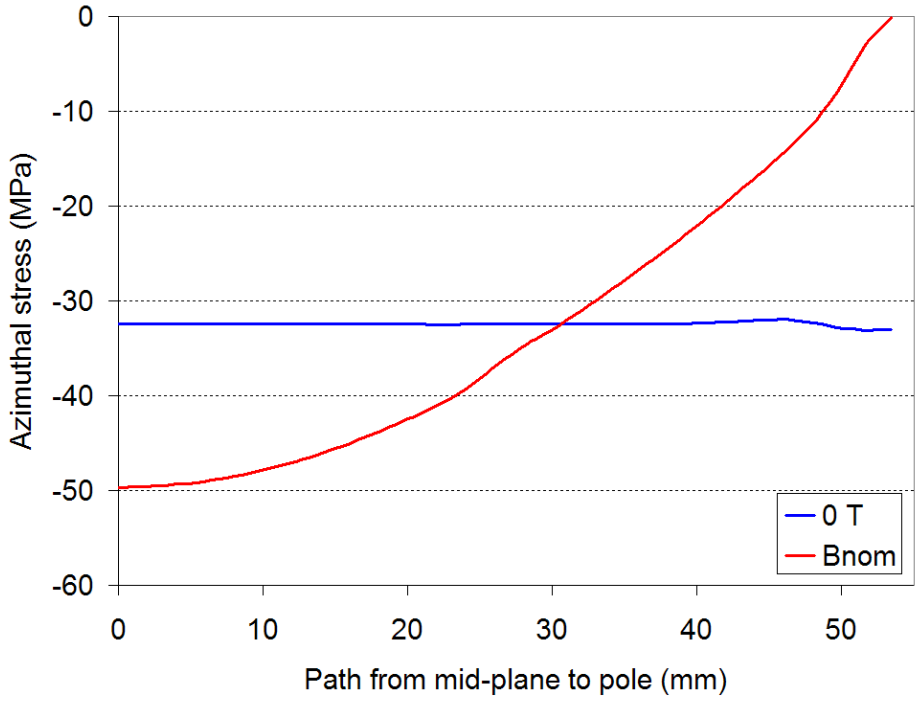

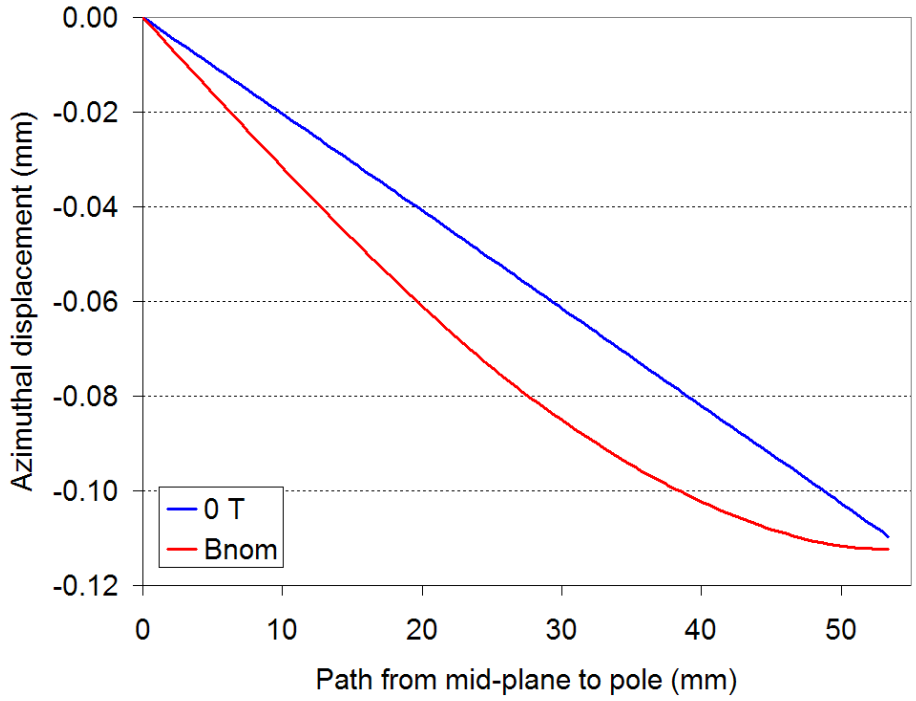

Impact of insufficient prestress on the Tevatron main dipole

- We focus now on the stress and displacement of the pole turn (high field region) in different pre-stress conditions.
- The total displacement of the pole turn is proportional to the pre-stress.
  - A full pre-stress condition minimizes the displacements.

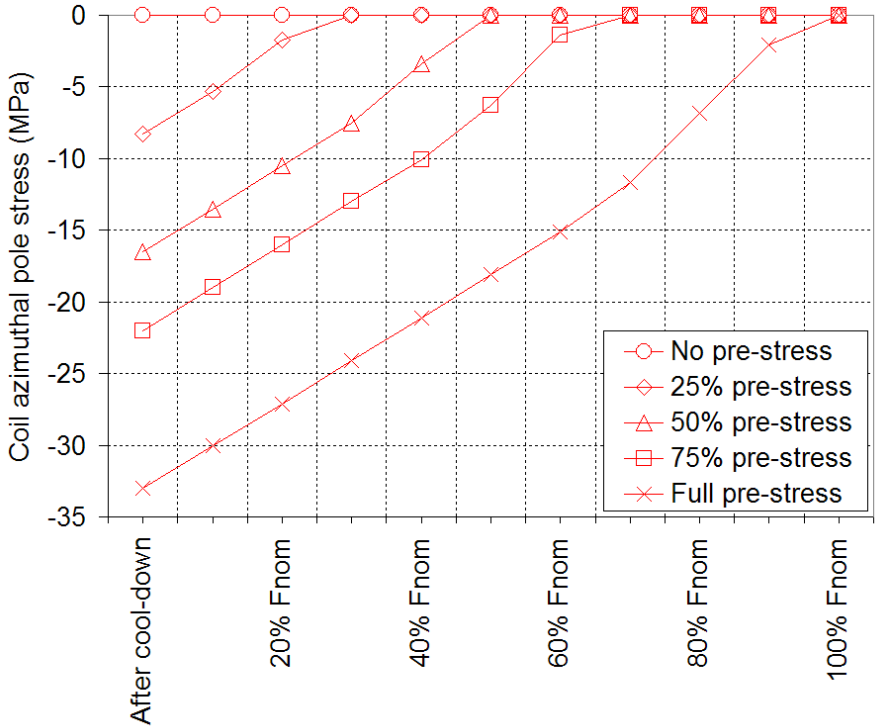

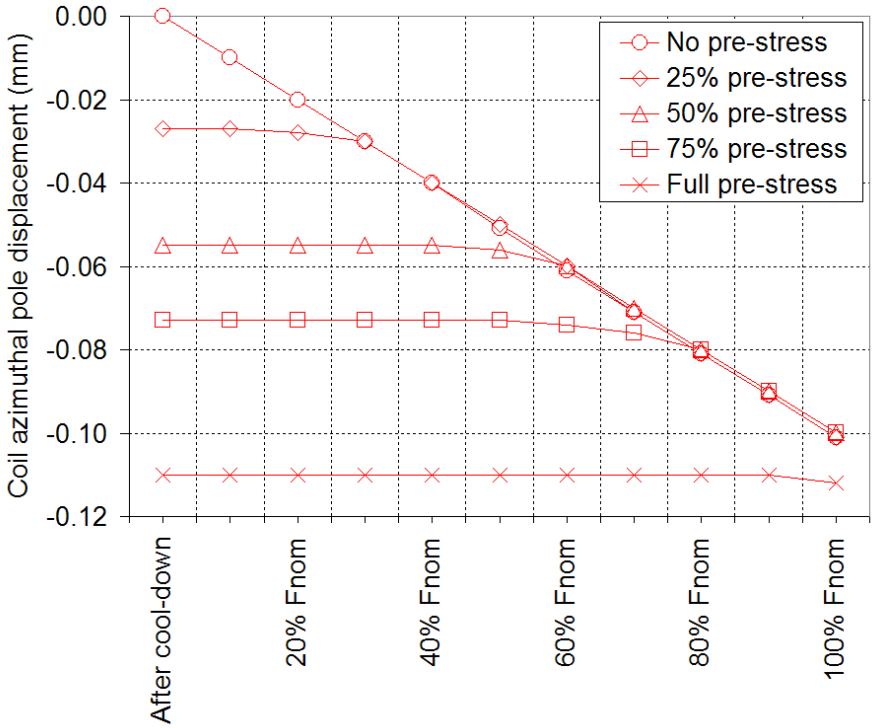

The correlation between coil separation and training is an active area for investigation: Experience in Tevatron

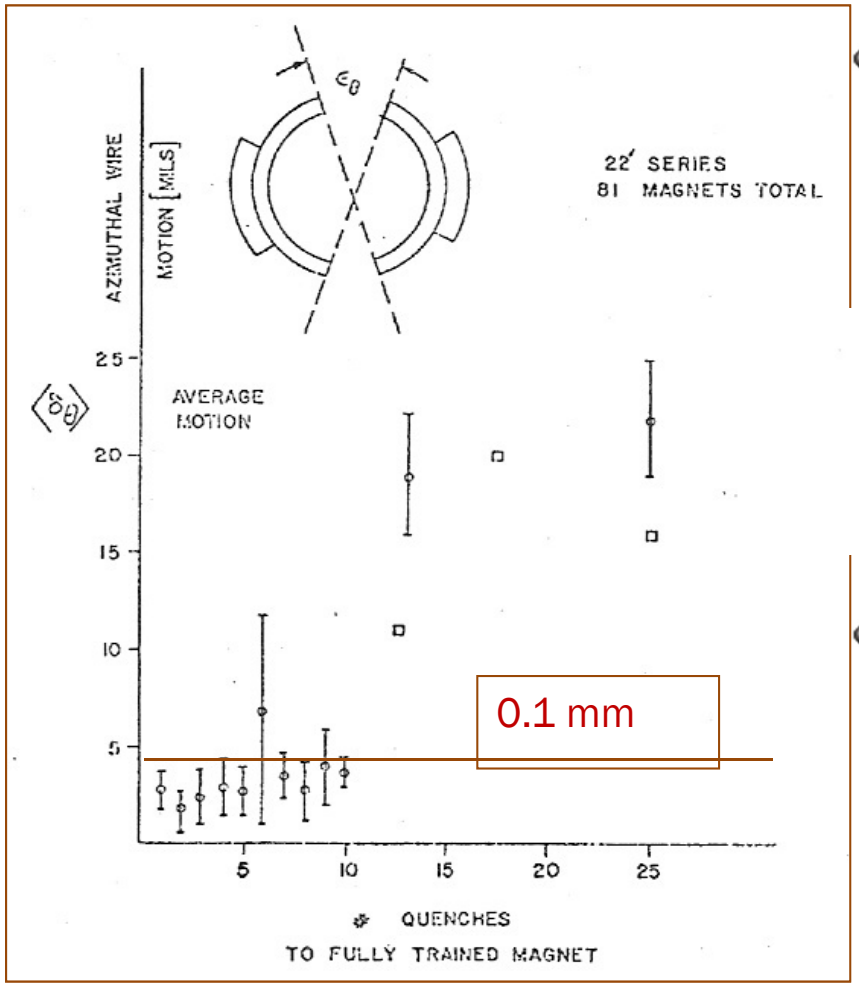

A.V. Tollestrup, [10]

- Above movements of 0.1 mm, there is a correlation between performance and movement: the larger the movement, the longer the training

elastic. It shows very little hysteresis. However, the azimuthal motion has given more trouble. Early in the program, magnets were built such that the elastic forces when cold were less than the magnetic forces, and the conductor at the key moved. Fig. 11 shows data from 81 magnets whose training took from one quench to over 25. Some magnets in this series had preload small

- Conclusion: one has to prestress to avoid movements that can limit performance

error bars are just a square root of the number of magnets at each point. It is seen that this motion does not couple into the training until it is large enough so that the conductor is completely unclamped. Why it takes some magnets one quench and others 10 quenches to train when the conductor remains clamped is a mystery.

Application of prestress to eliminate separation: RHIC main dipole

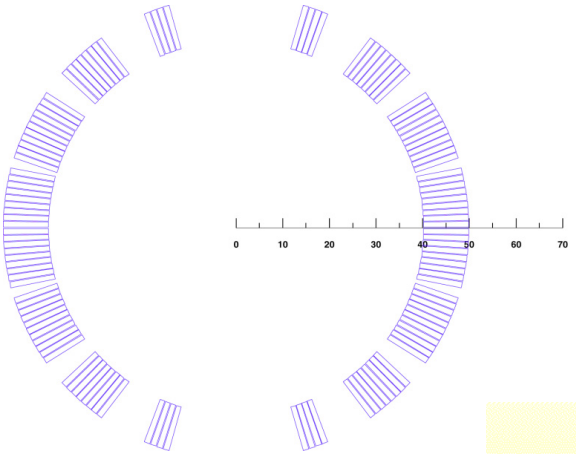

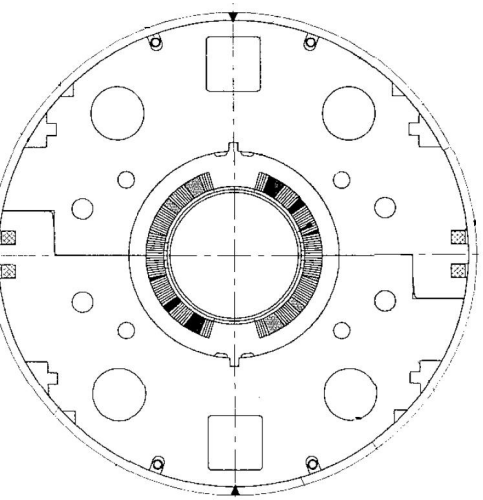

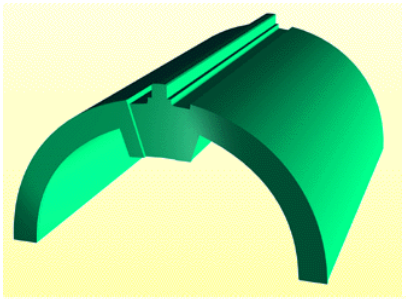

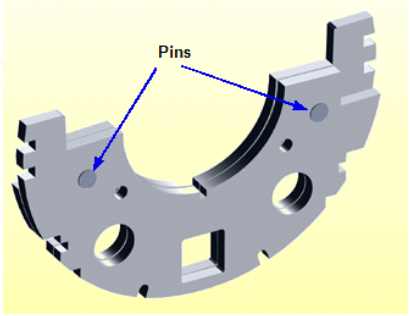

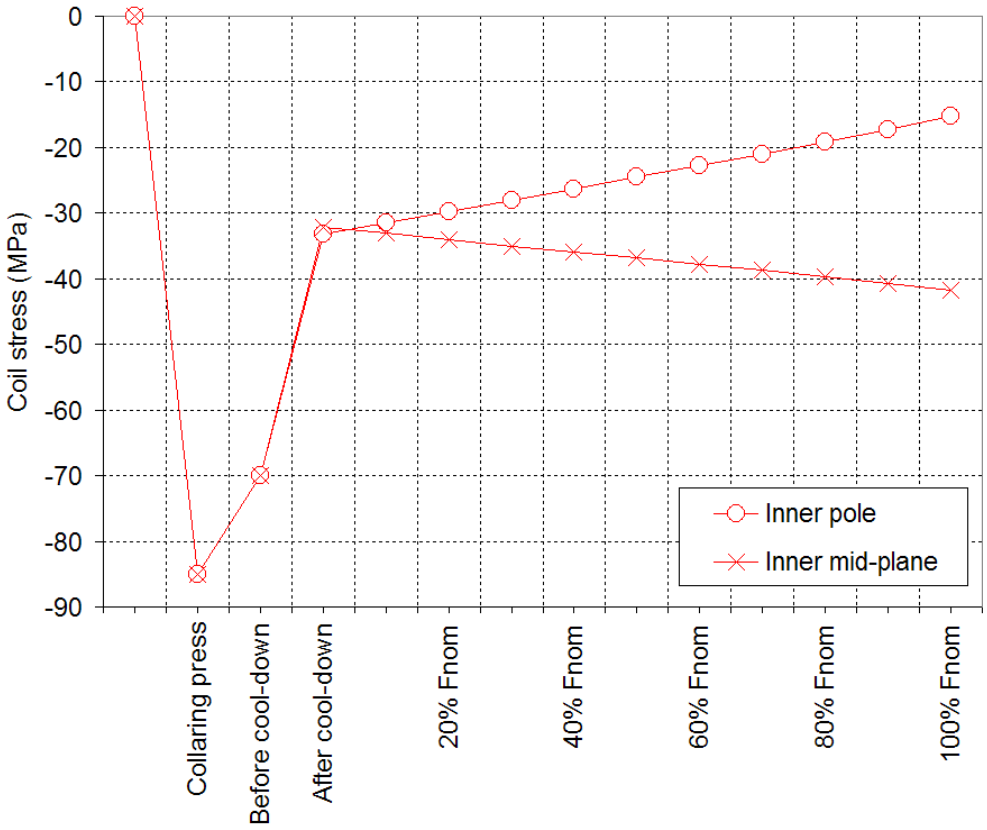

Application of prestress to eliminate separation: LHC main dipole

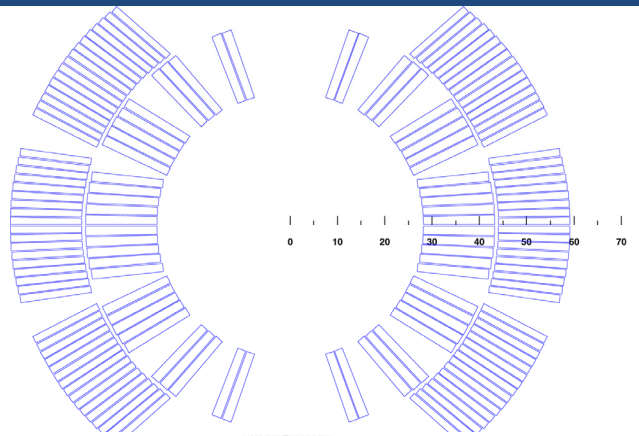

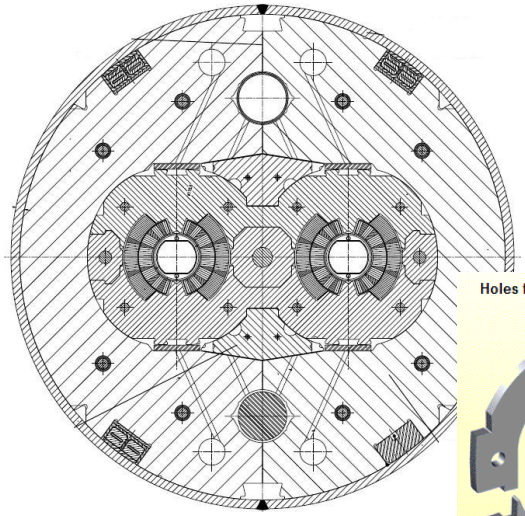

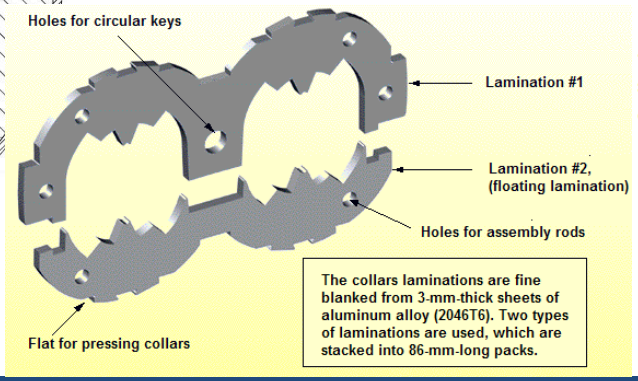

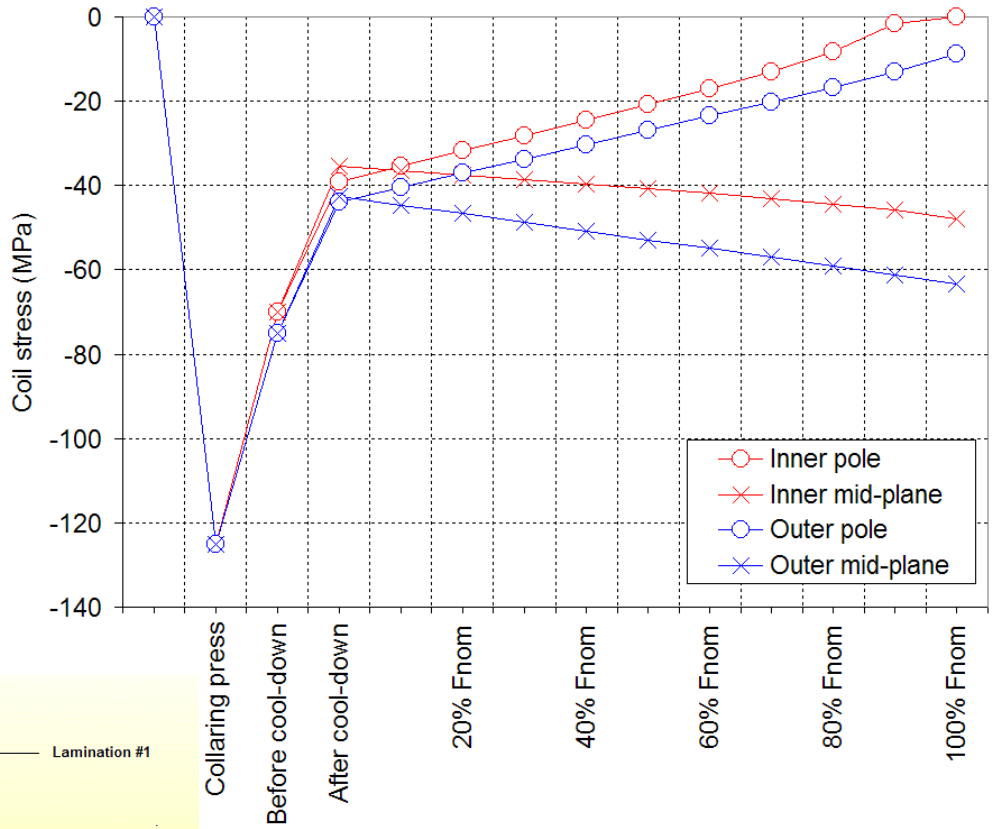

Shell –based support structure concept

- Shell-based support structure often referred as “bladder and keys” structure
  - developed at LBNL for strain sensitive material

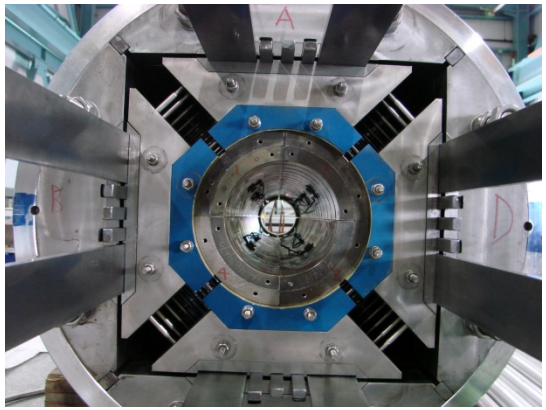

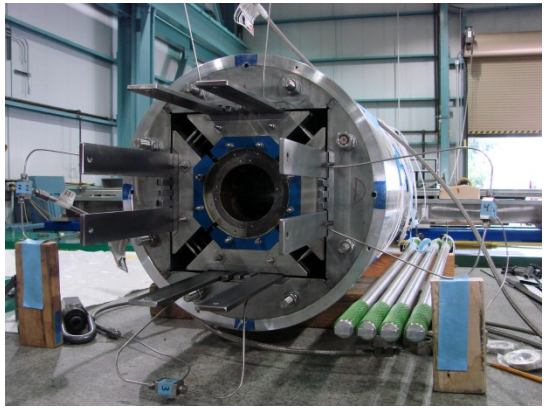

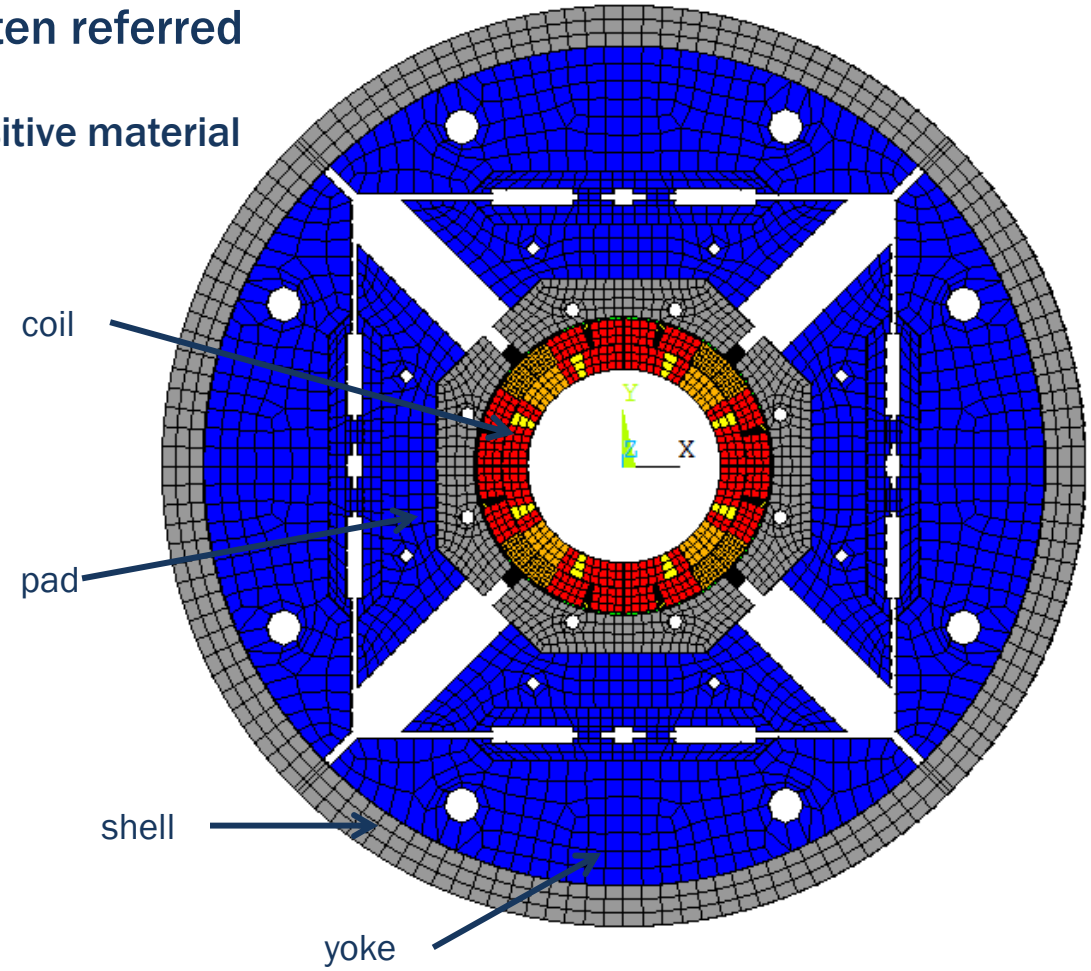

Shell-based support structure Concept

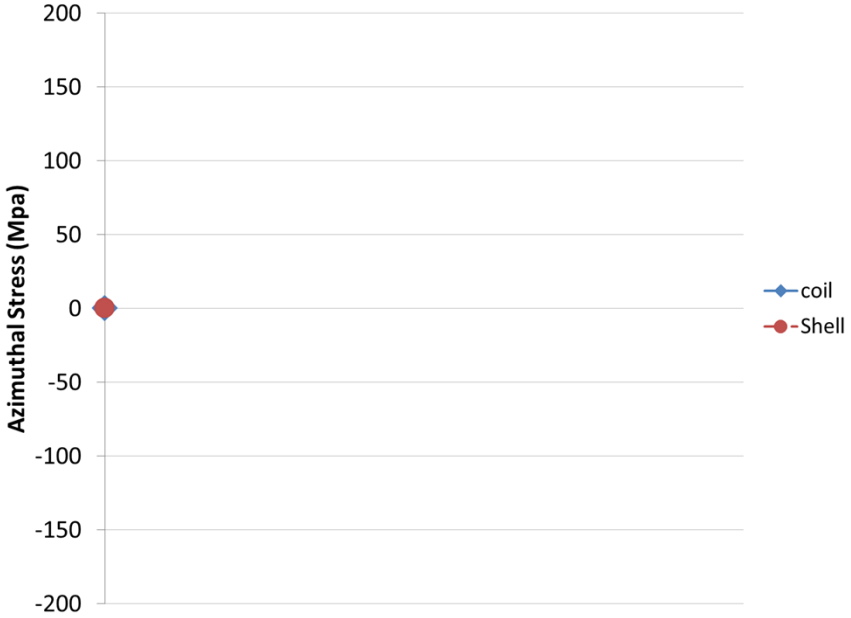

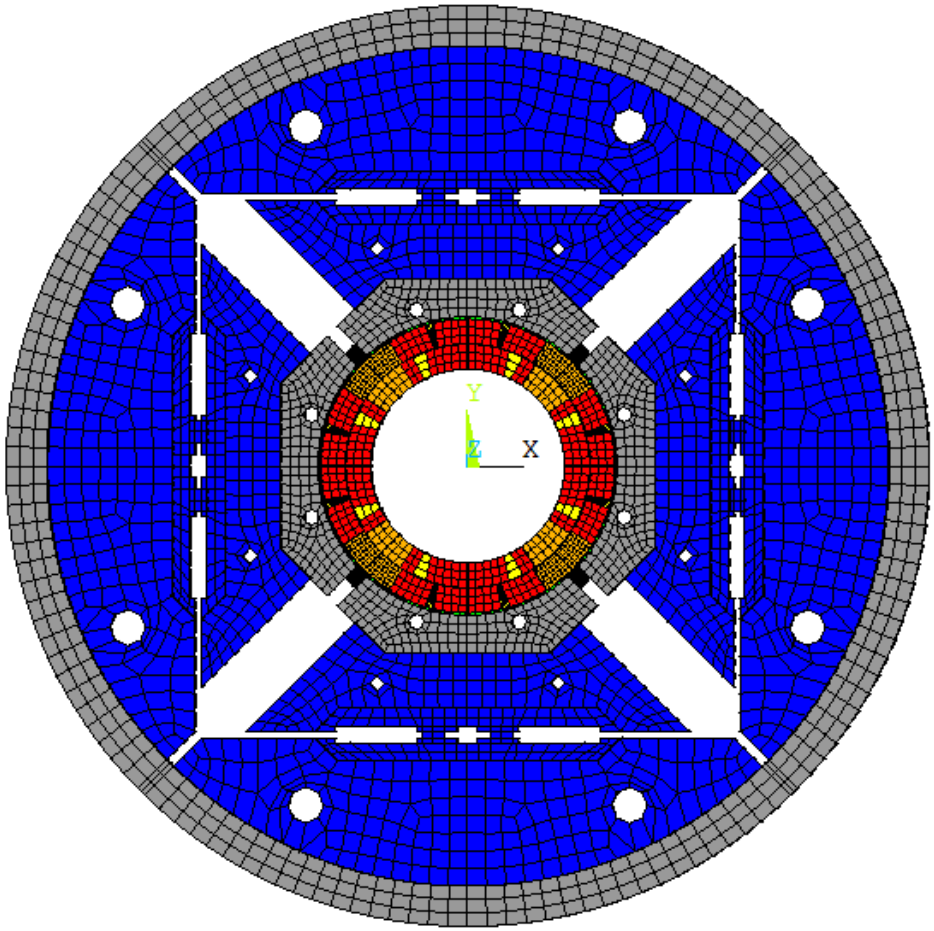

Shell-based support structure Concept

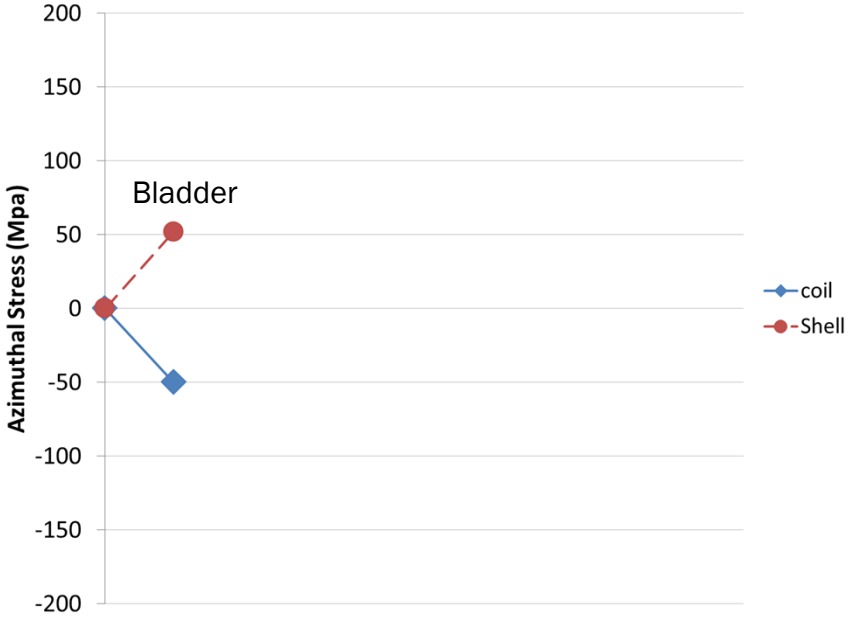

Inflated Bladders

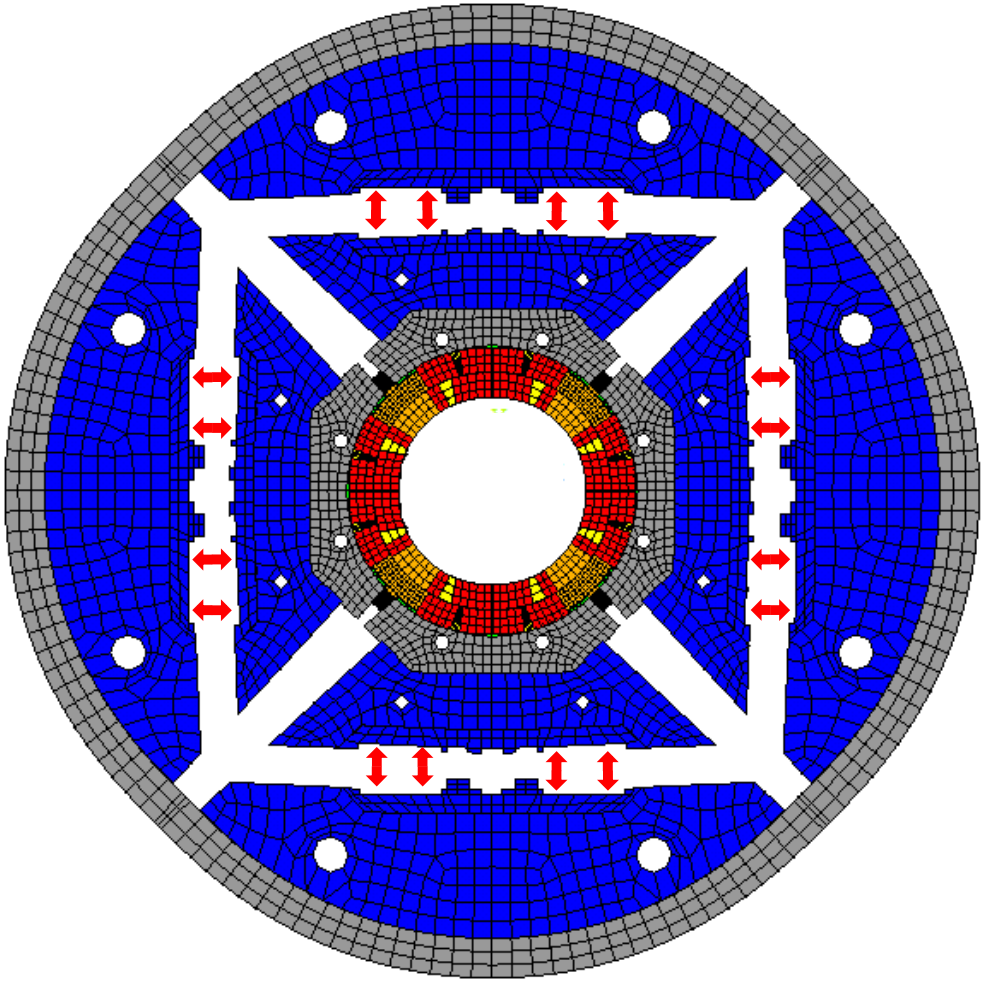

Displacement scaling 30

Shell-based support structure Concept

Shimming of the load leys

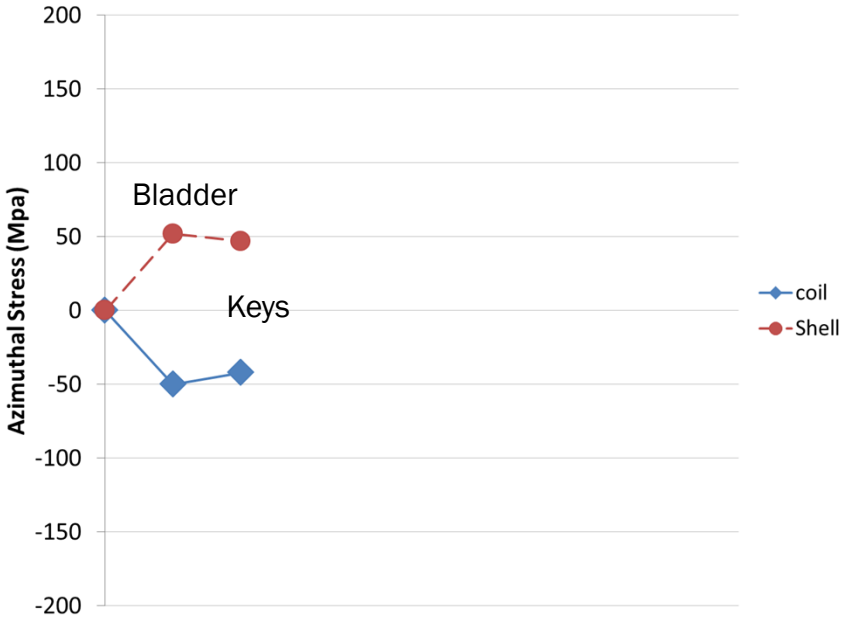

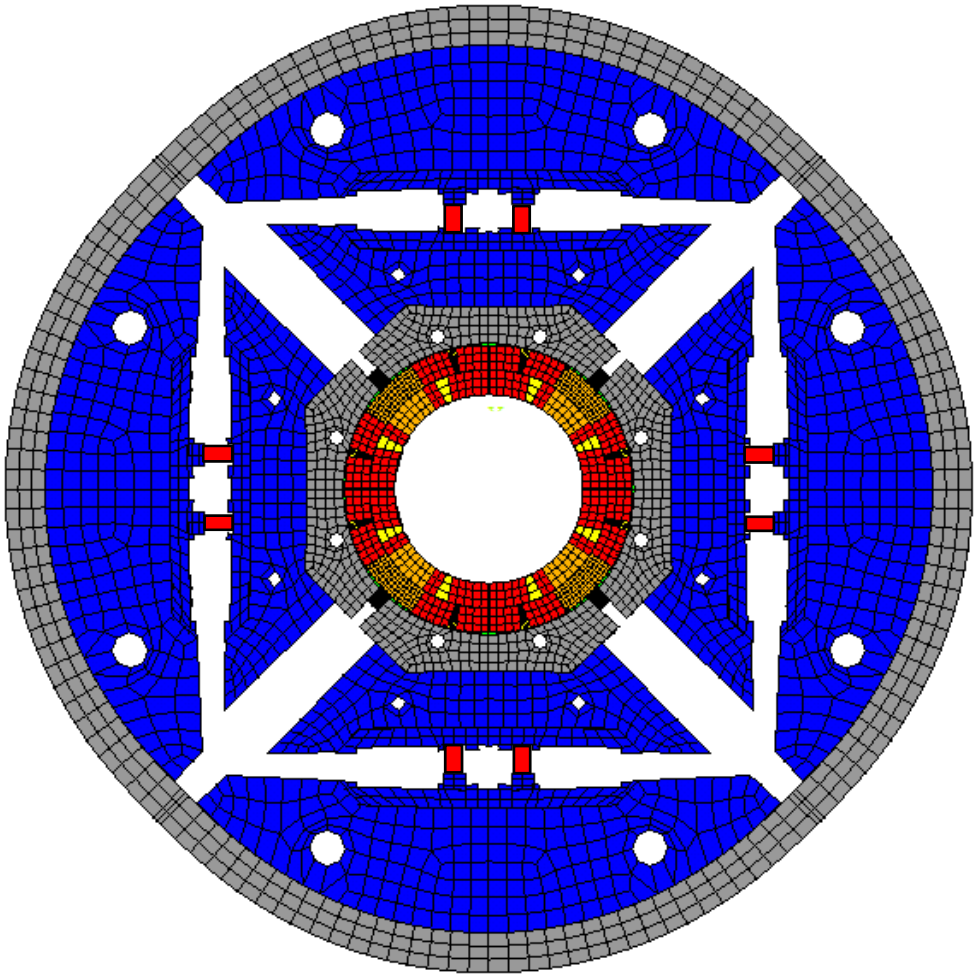

Displacement scaling 30

Shell-based support structure Concept

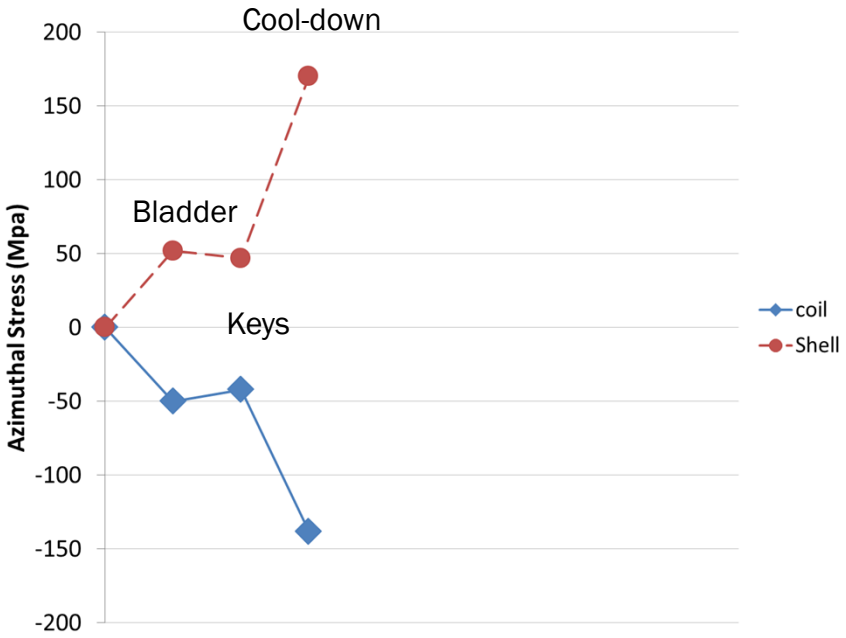

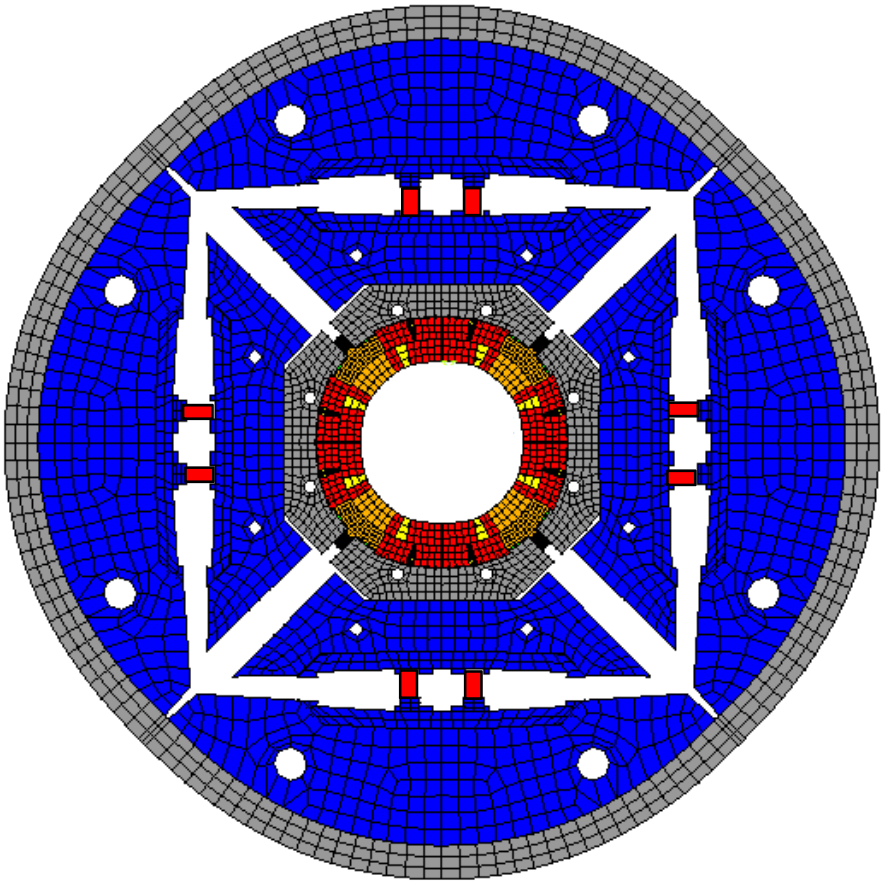

Displacement scaling 30

Shell-based support structure Concept

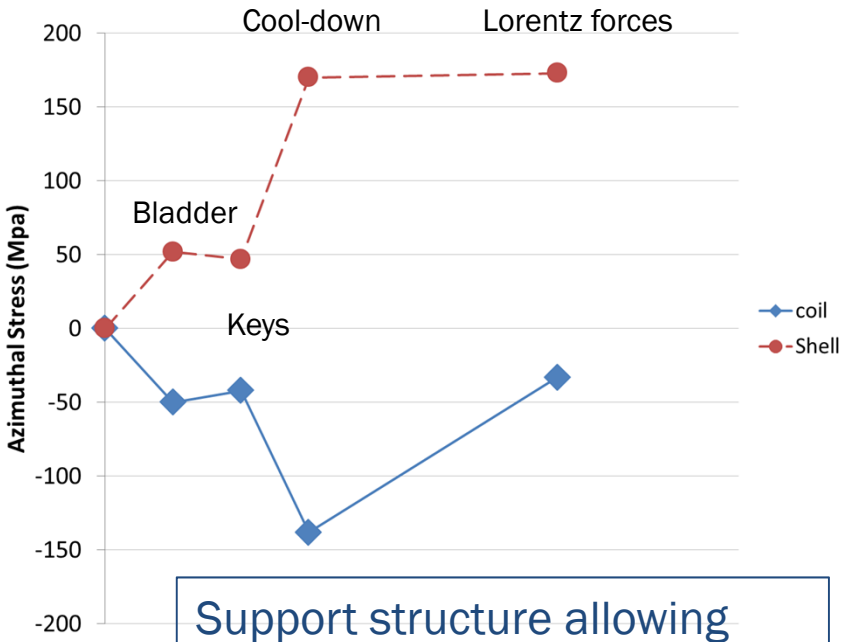

Support structure allowing fine tuning of the pre-stress

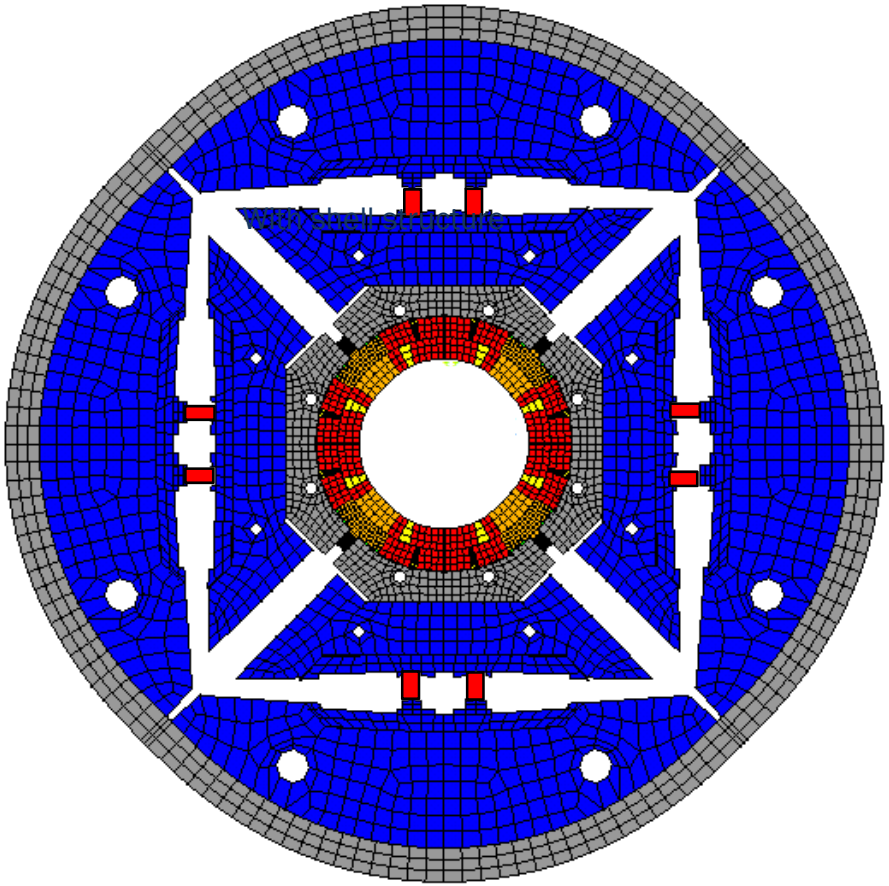

Displacement scaling 30

Application of prestress to eliminate separation: LARP TQ quadrupole

- With low pre-stress, unloading but still good quench performance
- With high pre-stress, stable plateau but small degradation

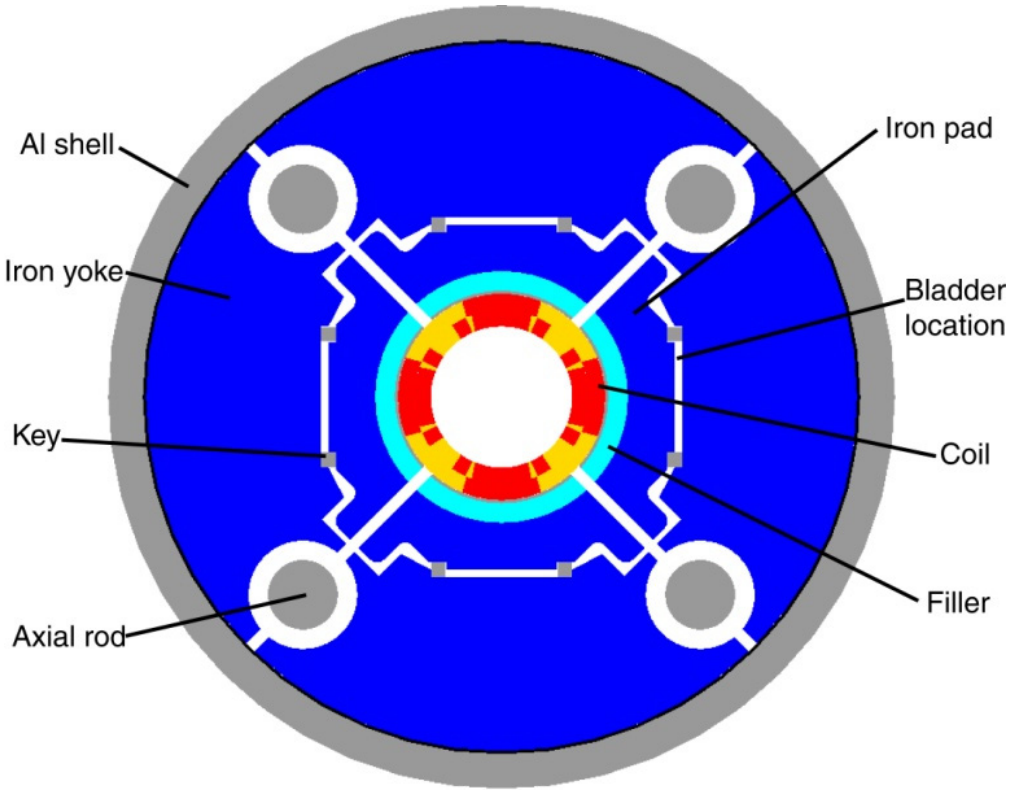

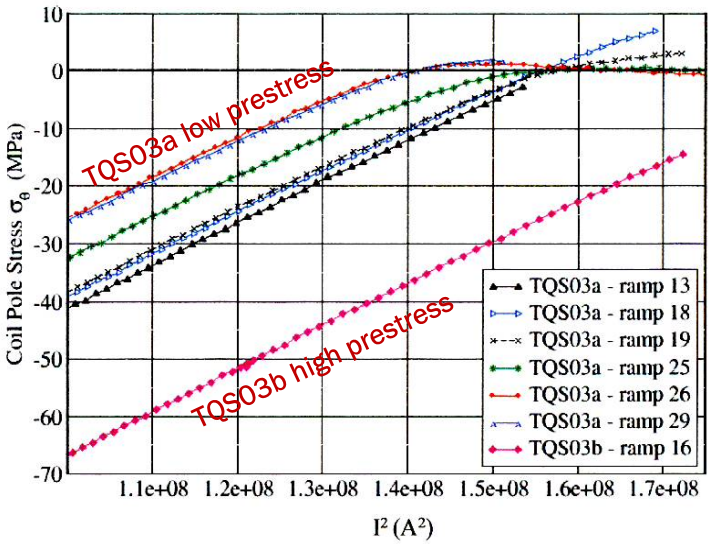

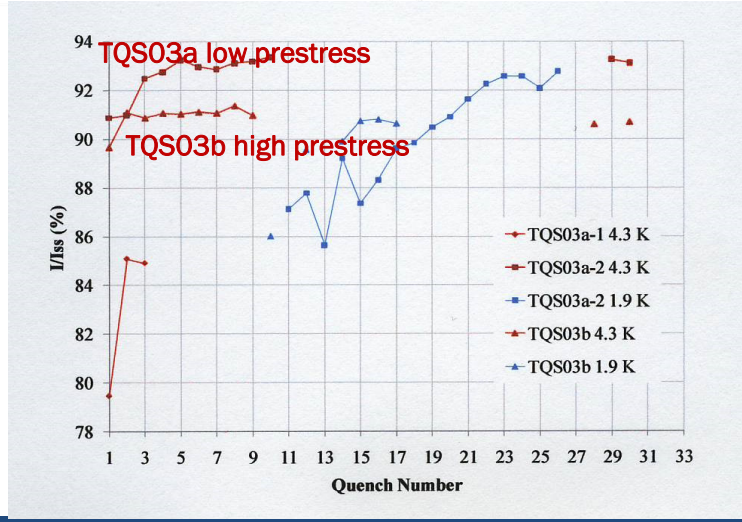

A novel approach to address stress issues in high-field dipoles: CCT Superconducting Magnets

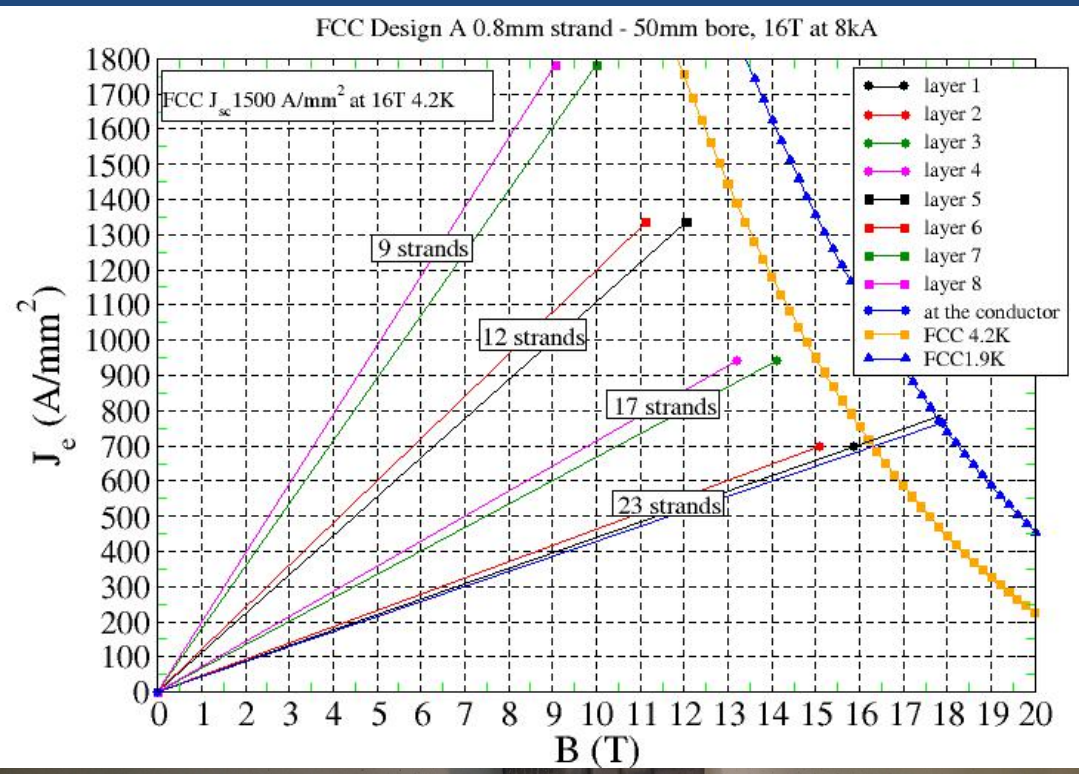

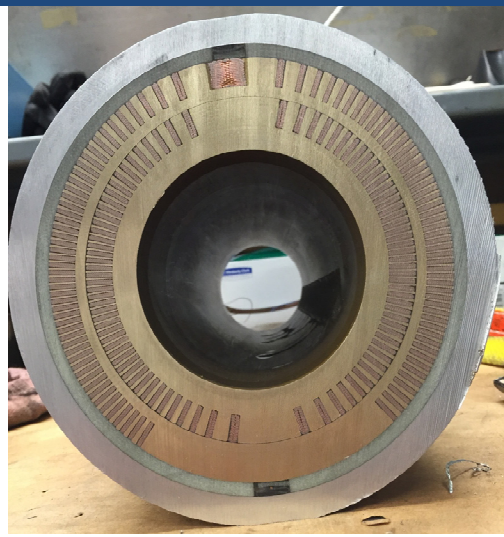

CCT Inner and Outer Layer Mandrels

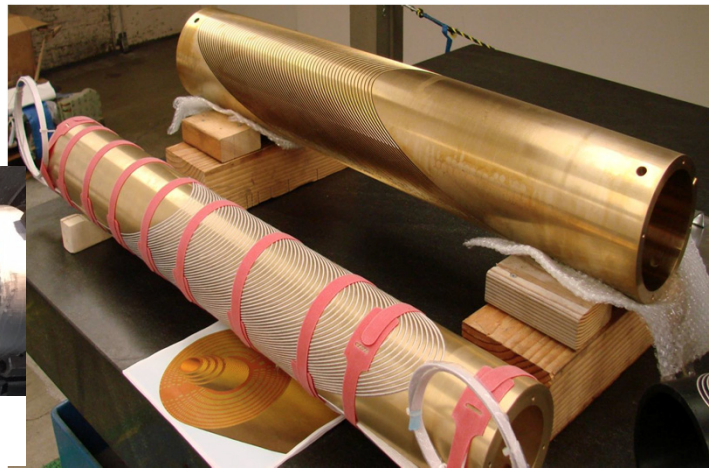

3 axis NC machining – field quality & pole assembly

Quench behavior and magnet protection

Magnet protection concerns the safe conversion of magnetic energy to thermal energy

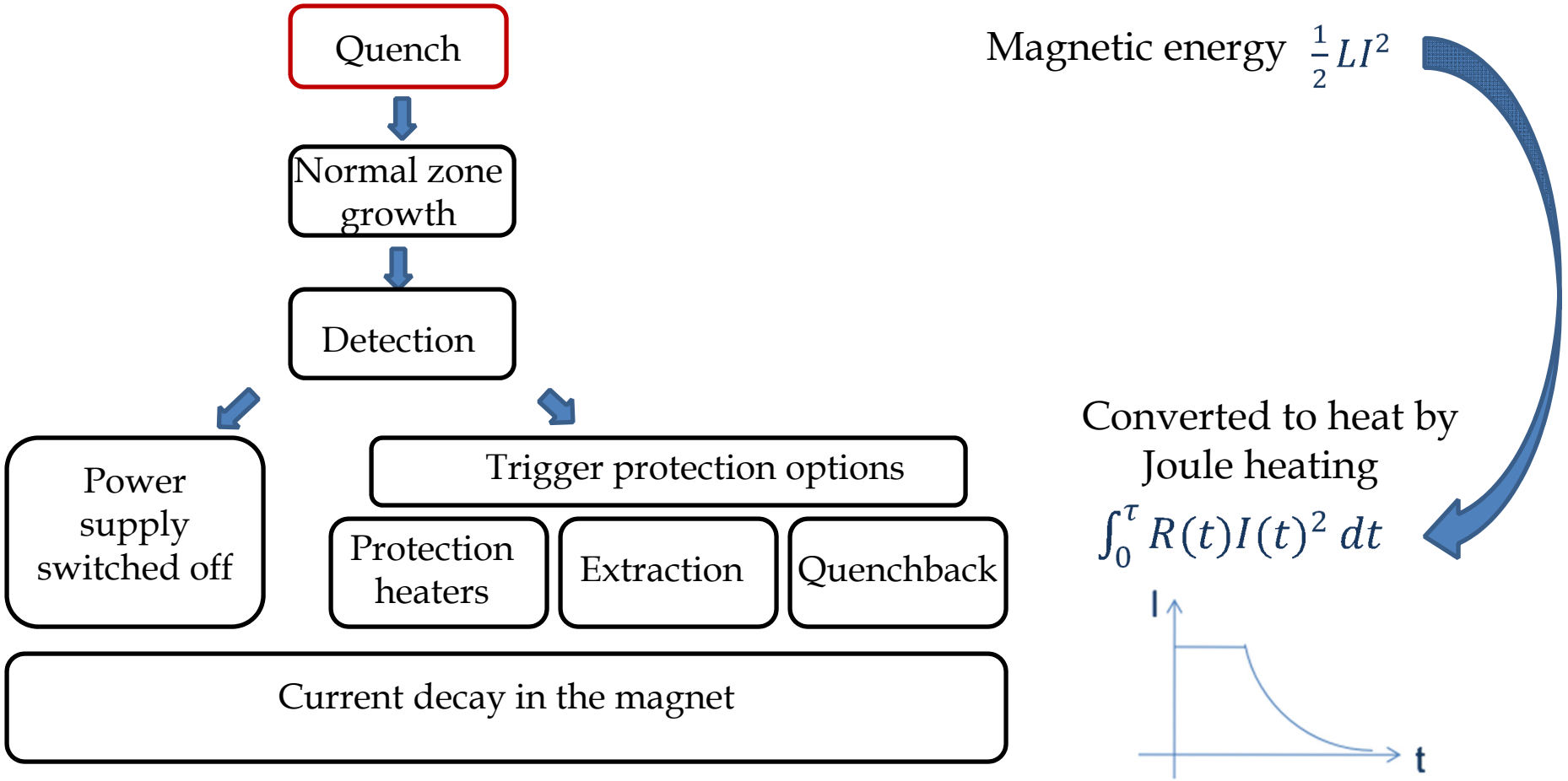

The faster this chain happens the safer is the magnet

Current decay/Hot spot correlation: the MIITs

- Basic energy conservation
  - Energy deposited by Joule heating inducing an increase in temperature based on the specific heat of the materials

$$\gamma C_p(T)dT = \rho J(t)^2 dt$$

  - With the assumptions that:
    - Joule heating only produced by stabilizer (Cu)
    - Heat capacity of conductor and insulation
    - Adiabatic condition: no longitudinal heat transfer

$$A_{tot} \sum_k \gamma_k v_k C_{p,k}(T)dT = \frac{\rho_{Cu}(T,B)}{A_{Cu}} I(t)^2 dt$$

$$10^6 MIITs = \int_0^\infty I(t)^2 dt = A_{tot} A_{Cu} \int_{T_0}^{T_{max}} \frac{\sum_k \gamma_k v_k C_{p,k}}{\rho_{Cu}(T,B)} dT$$

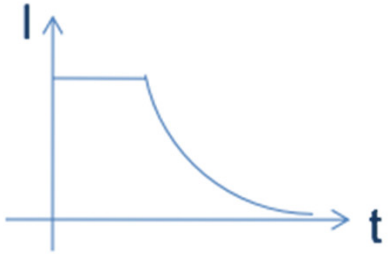

By evaluating the "MIITs" from the current decay, we obtain an estimate of the hot spot temperature T_{max}

A normal zone can also propagate turn-to-turn

- The heat is also propagating from turn-to-turn, resulting in transverse propagation
- But it is a much slower propagation, about 10 to 100 times slower
- Since the time scales are very different, including the transverse propagation does not affect the longitudinal propagation velocity estimate

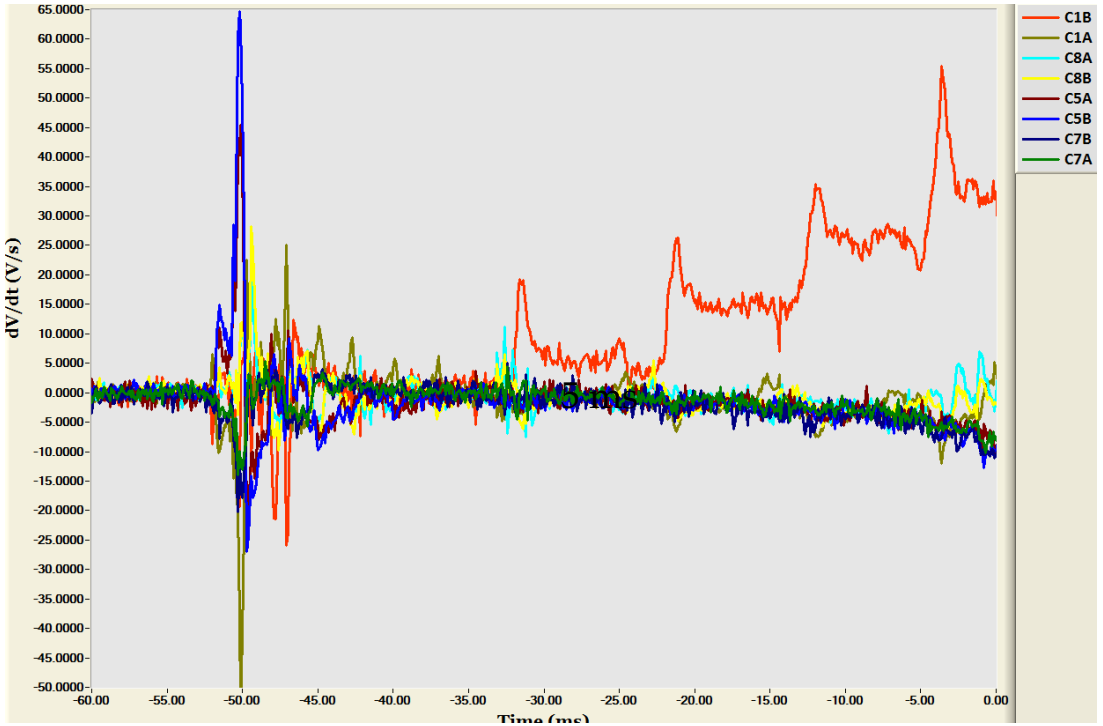

Quench propagation

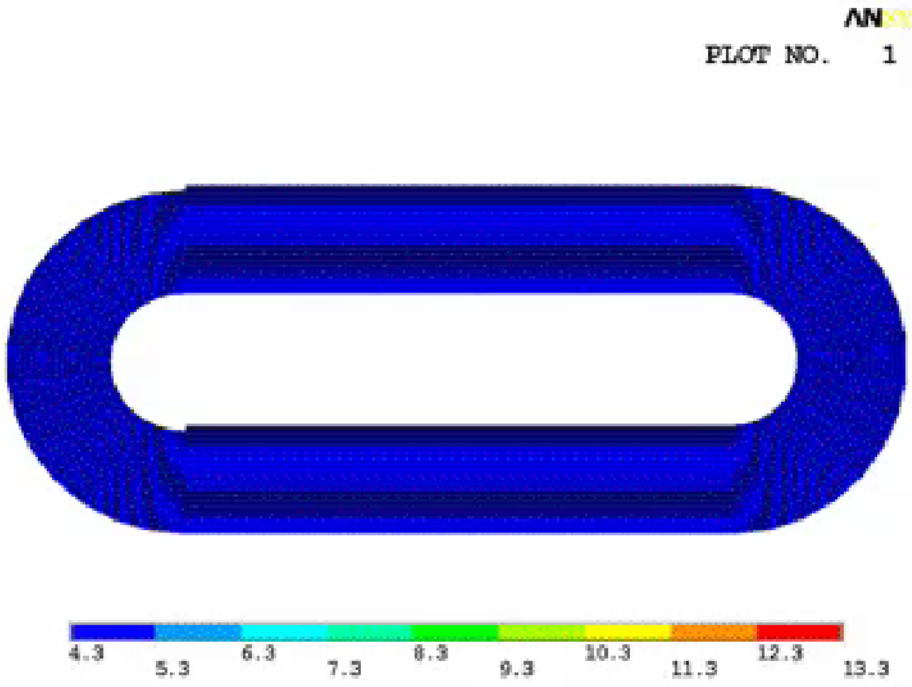

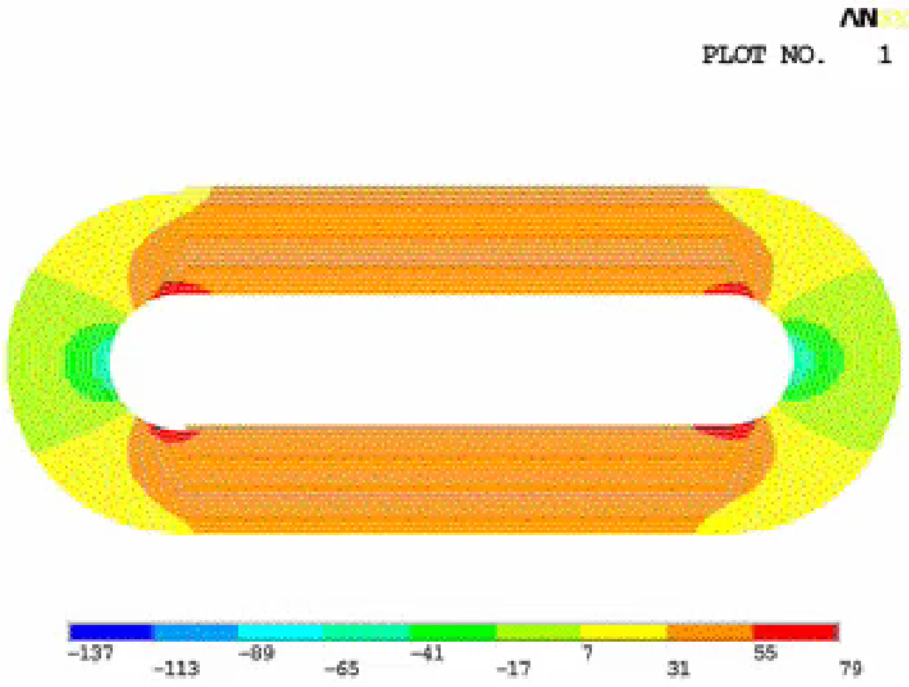

Tmax = 4.3

Time = 0 ms

σ_z = + 40 MPa

Caspi et al, TAS 2003

Ferracin et al, TAS 2004

Quench propagation

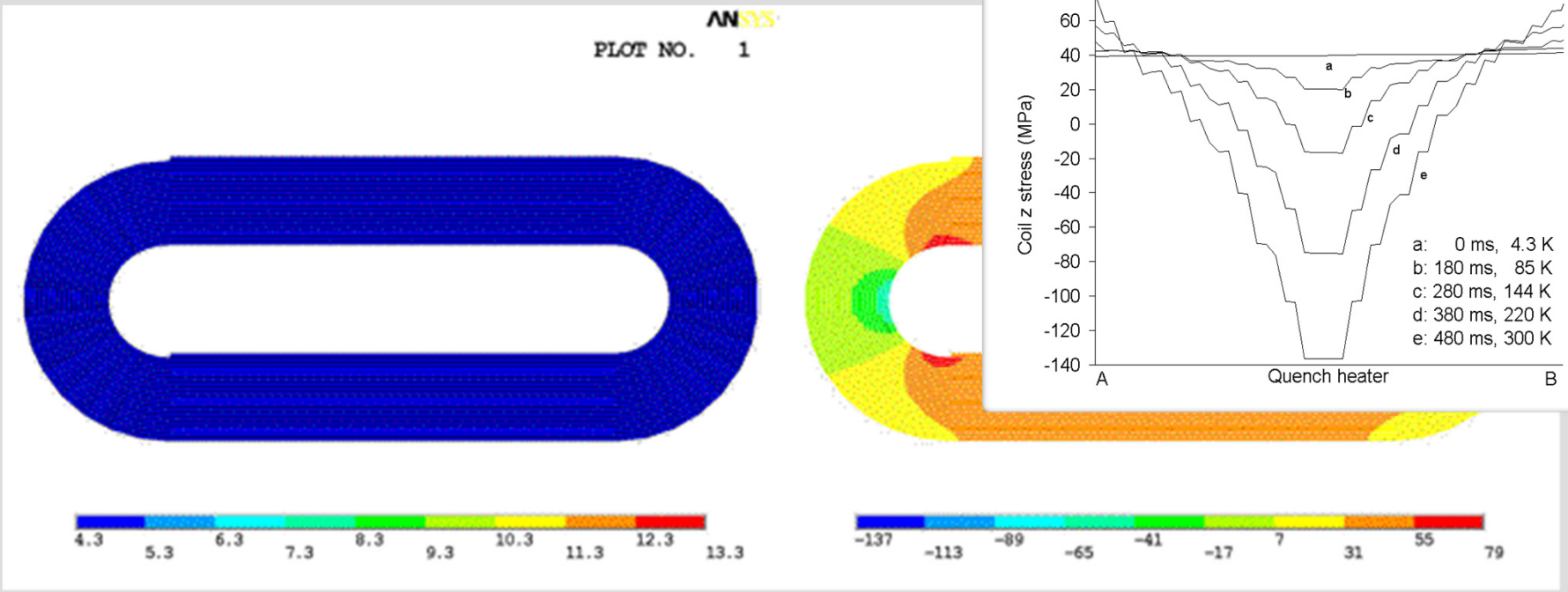

Tmax = 4.3

Time = 0 ms

σ_z = + 40 MPa

Caspi et al, TAS 2003

Ferracin et al, TAS 2004

Calculating Quench Propagation With ANSYS®

S. Caspi, L. Chiesa, P. Ferracin, S. A. Gourlay, R. Hafalia, R. Hinkins, A. F. Lietzke, and S. Prestemon

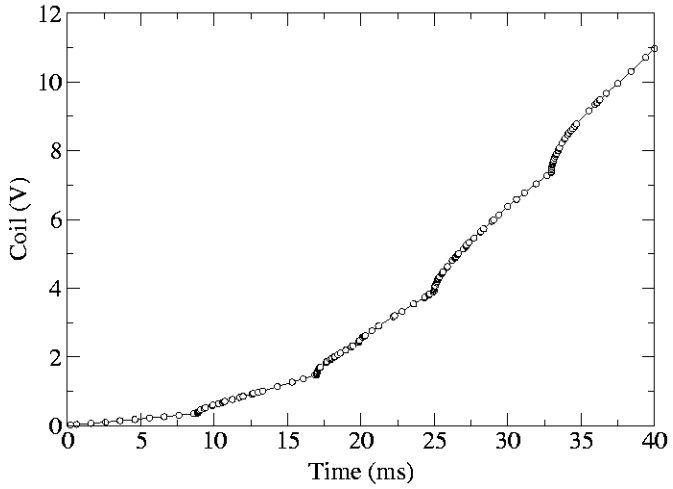

Fig. 7. Calculated voltage rise during a quench, 10 T, $I/I_c = 0.76$, $RRR = 90$

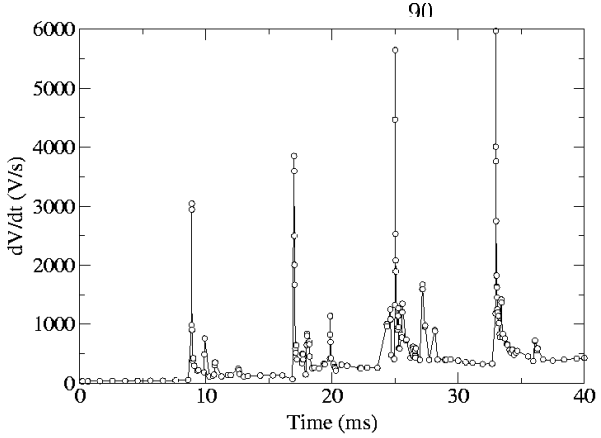

Fig. 8. Derivative of voltage with time shows local effects of turn-to-turn propagation and instantaneous changes of quench velocity due to pre-heating.

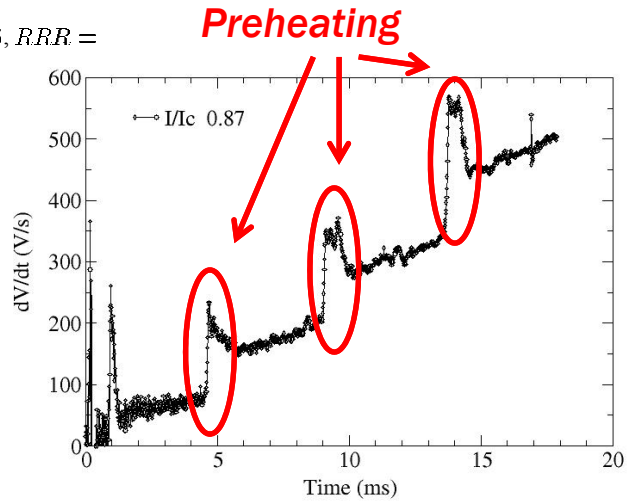

Fig. 9. Measured derivative of voltage verses time in magnet RD3-c.

How can we enhance the resistance? Protection Methods

- In most accelerator magnets, the "natural" resistance growth is insufficient to provide a good protection => **Need to enhance the resistance**
- ***Method 1:***
  - Add an external resistor
- ***Method 2:***
  - Apply additional heat to the coils to force them to become more resistive
    - Protection heaters mounted on the coils
    - Optimized to minimize thermal diffusion time
- ***Method 3:***
  - Use of couple secondary circuits
    - Can be external or internal to the coil
    - Energy dissipation in the secondary circuit through the voltage generated by the mutual inductance between the coil and the secondary
    - Can lead to quenchback in cases where secondary becomes a heat source
- ***Method 4***:
  - Coil subdivision

LQ protection heaters design

- Due to the length of the magnet: heating stations
- R_{PH} decreased to provide at least 50 W/cm^2 in heating stations
- Heater delay
  - Diffusion time + propagation between heating stations

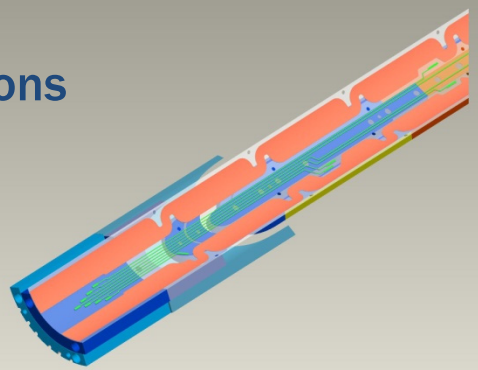

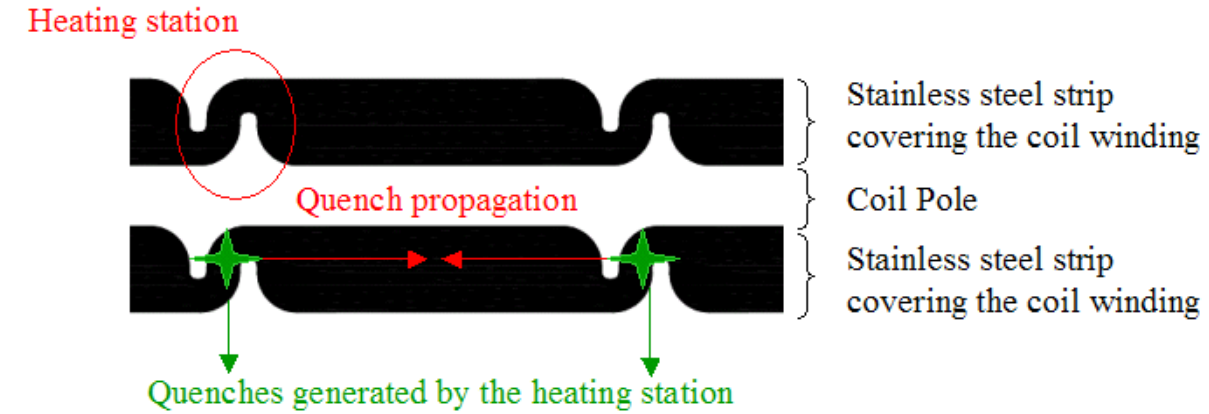

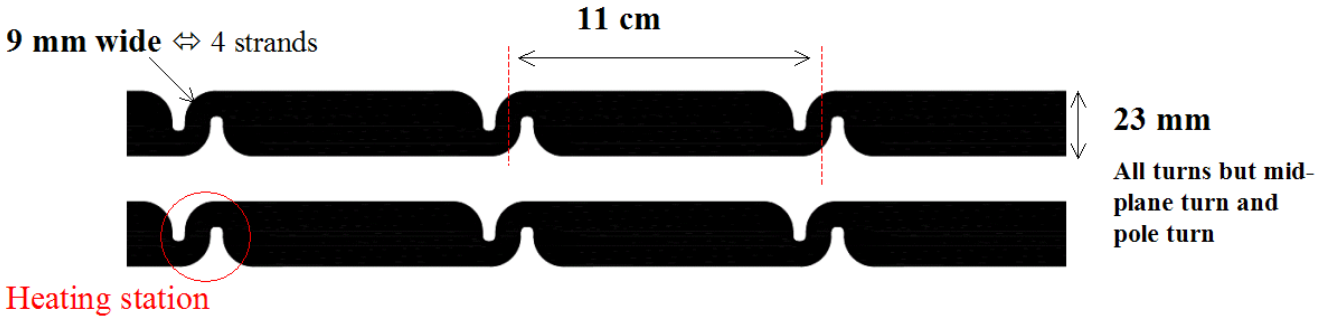

LQ test: 220 T/m 90% Iss
6 MIIts – no degradation

Impulse test failure/breakout

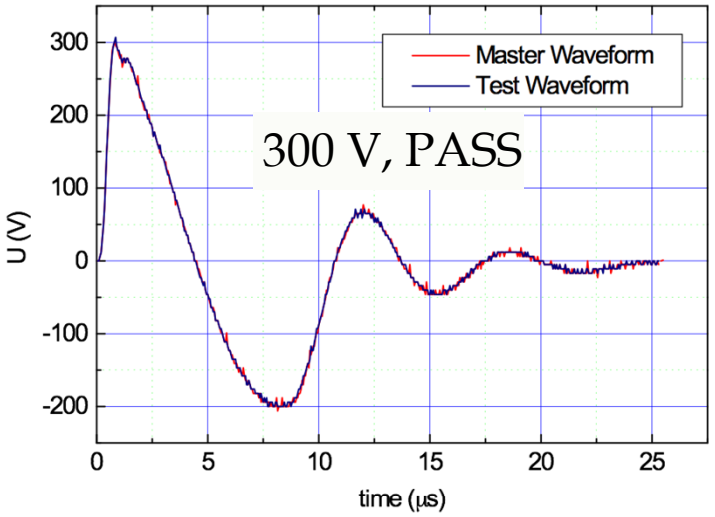

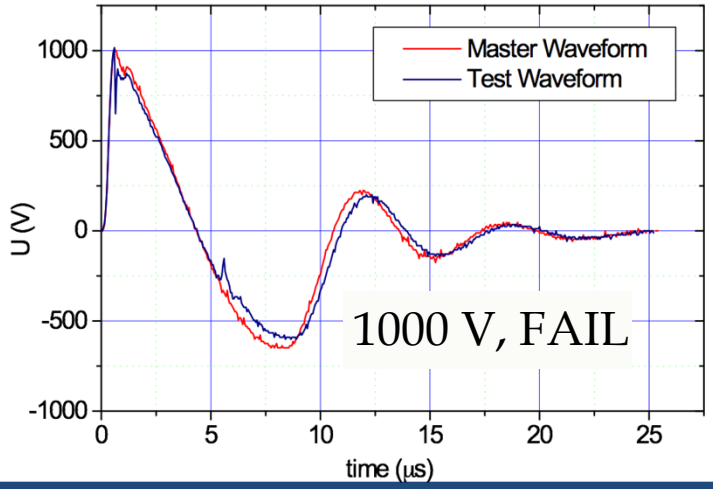

- A short through the **turn-to-turn** insulation will create a parallel path in the winding and reduce the effective inductance, thus **increasing** the oscillation frequency
- A short through the insulation between **winding and parts** (end parts, central pole, etc…) will increase the effective capacitance, thus **decreasing** the oscillation frequency.
- A discharge (arcing), either inside the winding (between the layers) or outside the winding (coil to parts), will cause a characteristic high frequency (> 1 MHz) noise to appear near the peaks of the oscillatory waveform.

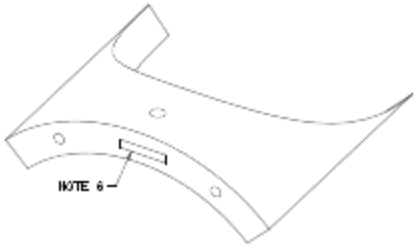

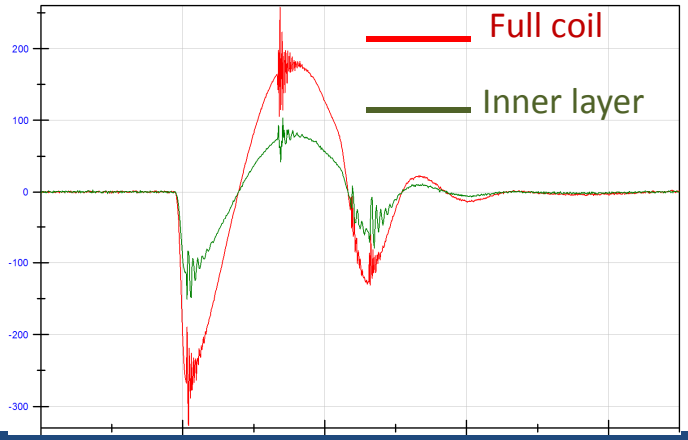

Courtesy of Maxim Marchevsky, LBNL

Quench Detection: a critical element of high-field superconducting magnet protection

- Need to detect the quench as soon as possible to **avoid MIITs build-up**
  - Choice of voltage thresholds to be compared with magnet signals
  - Optimization of these thresholds
- Principle: looking for **voltage imbalances** in the magnet
  - Difference between 2 voltages which are supposed to be the same
    - Cancelation of the inductive component
    - Allowing detection of resistive voltage growth
- The detection triggers the extraction and the firing of the protection heaters
  - In case of failure, all the protection scheme is impaired
  - **Redundancy** required to improve reliability

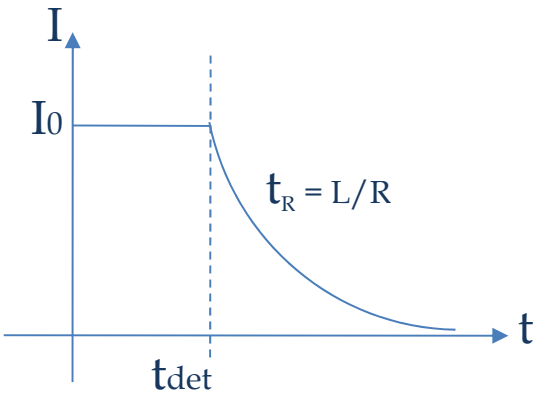

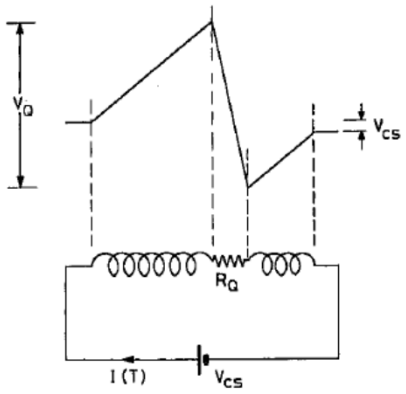

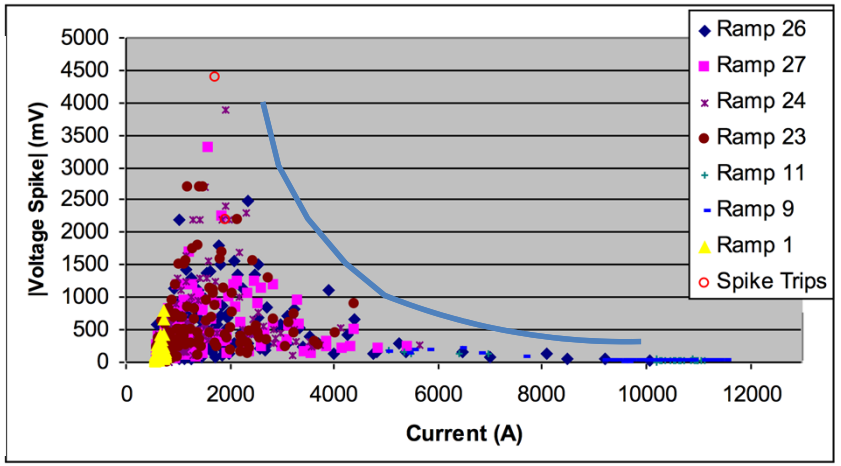

New instrumentation for quench diagnostics help understand magnet behavior

Amplified piezosensors (A1-A4, at the coil wedges). Sensing acoustic emissions

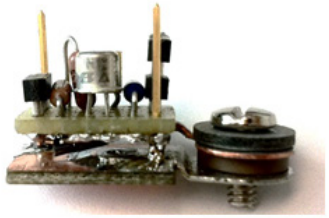

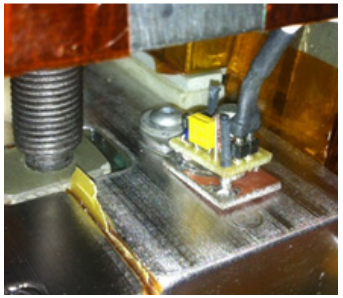

- Polarized across thickness
- $f_r = (154 \pm 4)$ kHz
- Cold amplifier, 0-100 kHz, 300 - 1.9 K operation

M. Marchevsky, X. Wang, G. Sabbi and S. Prestemon, "Detecting mechanical vibrations in superconducting magnets for quench diagnostics", Proceedings of the WAMSDO 2013 Workshop, CERN

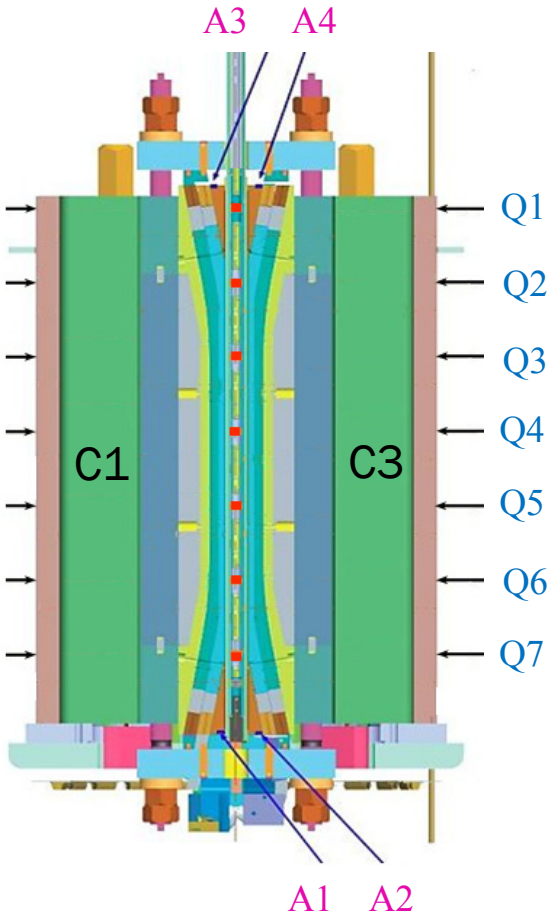

Inductive quench antenna (sensors Q1-Q7 in the bore anti-cryostat tube). Sensing **axial** field disturbances

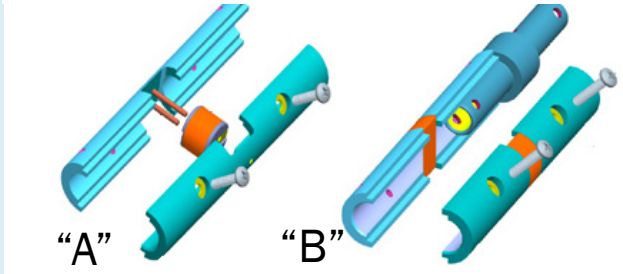

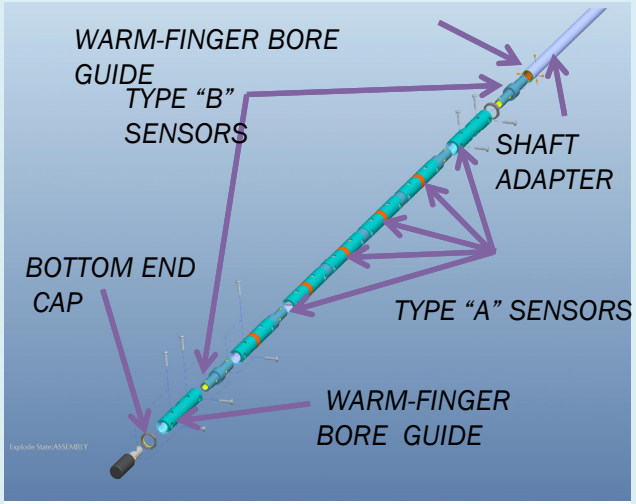

M. Marchevsky, J. DiMarco, H. Felice, A. Hafalia, J. Joseph, J. Lizarazo, X. Wang, G. Sabbi, "Magnetic Detection of Quenches in High-Field Accelerator Magnets", IEEE Trans. Appl. Supercond. 23, pp. 9001005, June 2013

HD3 - quench A76 (training, 16042 A)

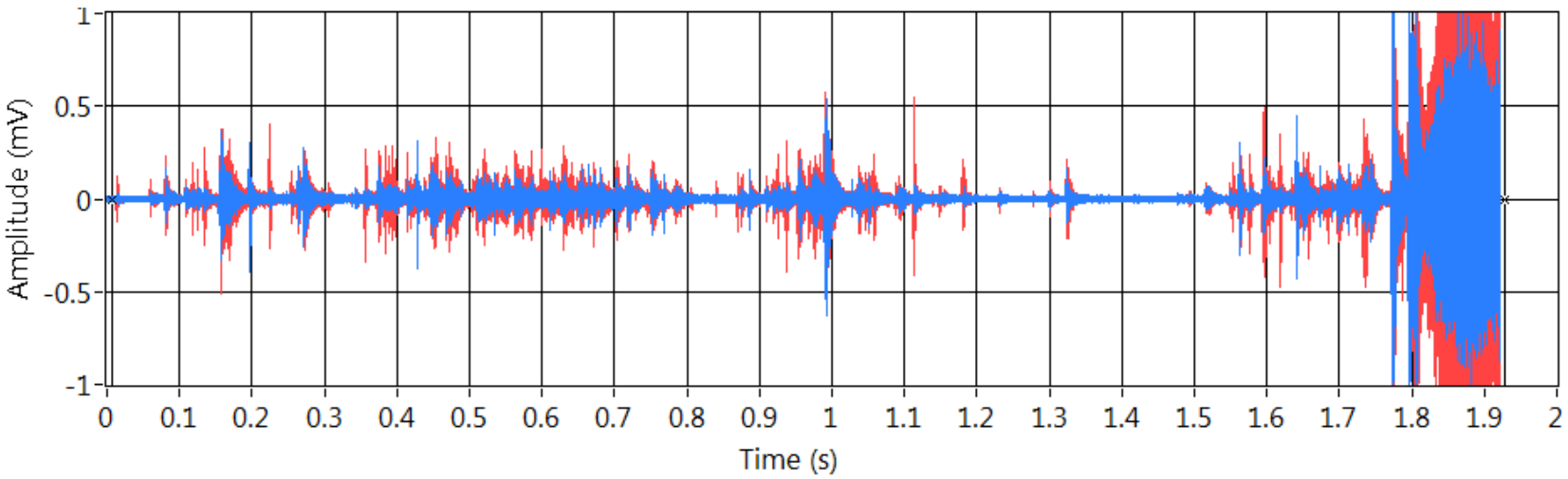

Sensor 1 (blue) – LE of Coil 3 -> Left sound channel
Sensor 4 (red) – RE of Coil 3 -> Right sound channel

Other applications within the broader accelerator community

Nb_3Sn Superconducting Undulator

- 1.5 m Nb_3Sn SCU prototype fabricated at LBNL and tested at ANL
  - Fast quench protection system developed
  - Good field quality was measured at ANL
  - Field correction method was successfully tested

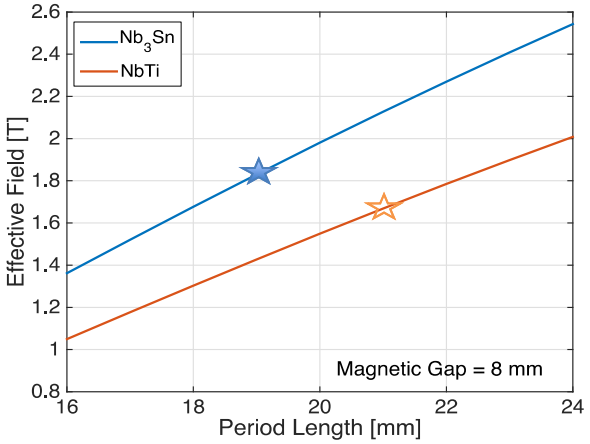

Magnetic Field

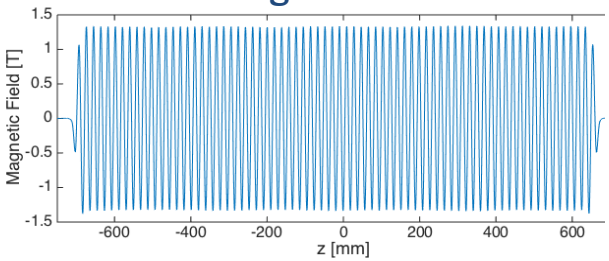

Second Field Integral

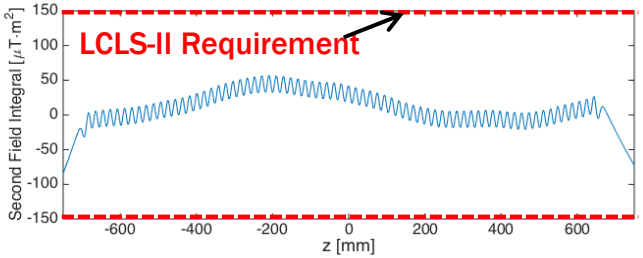

Field Correction Components

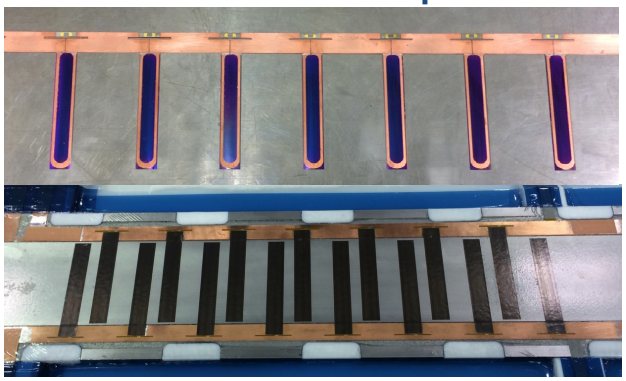

1.5 m Nb_3Sn Superconducting Undulator

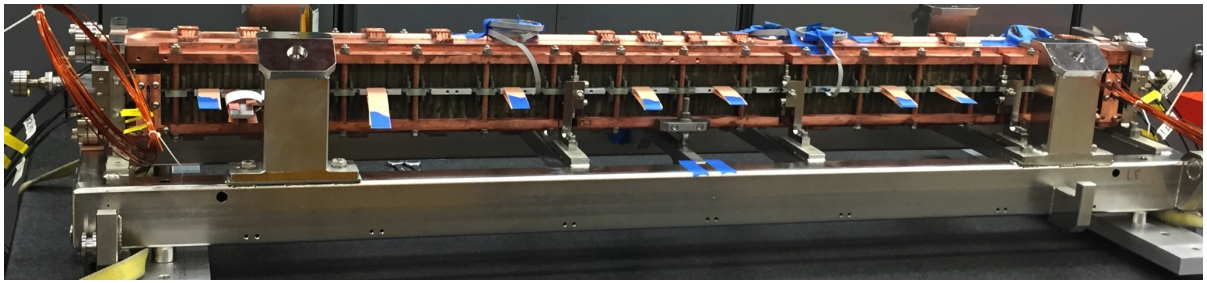

Superconducting Magnet for the FRIB ECR Source

- LBNL is responsible for the superconducting magnet for the 28GHz ECR source
  - Composed of 3 solenoids and a sextupole; similar in design to the VENUS ECR successfully operating at the 88" Cyclotron in NS Division
  - Utilizes the "Bladder-and-key" concept developed at LBNL; stepping-stone towards higher-frequency Nb_3Sn technology

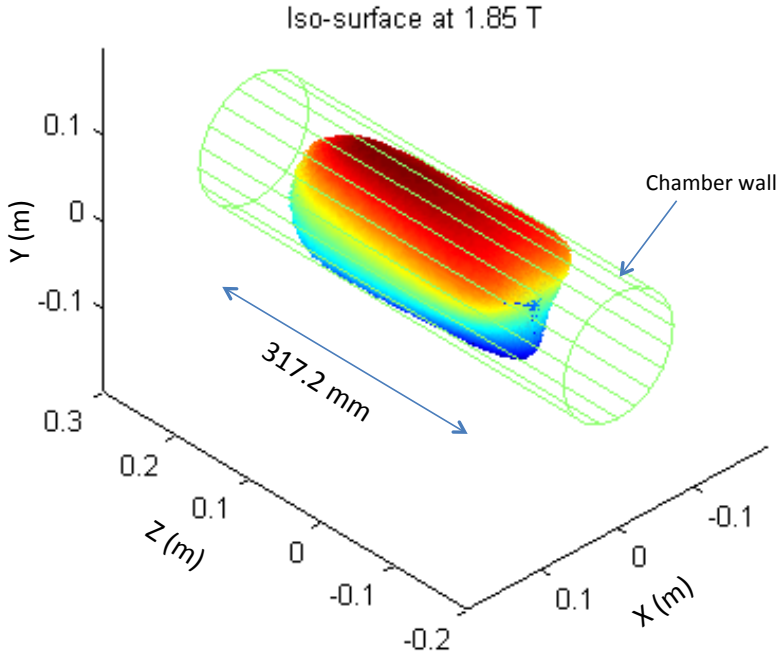

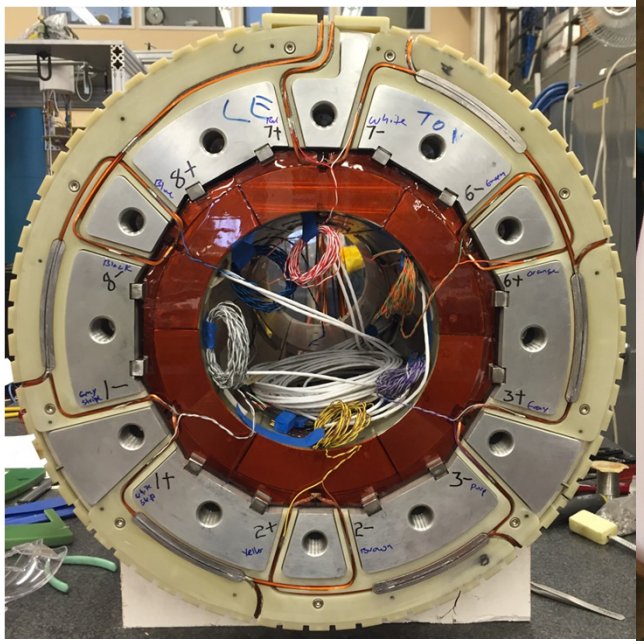

Design of 45 GHz Nb_3Sn ECR for IMP HIAF

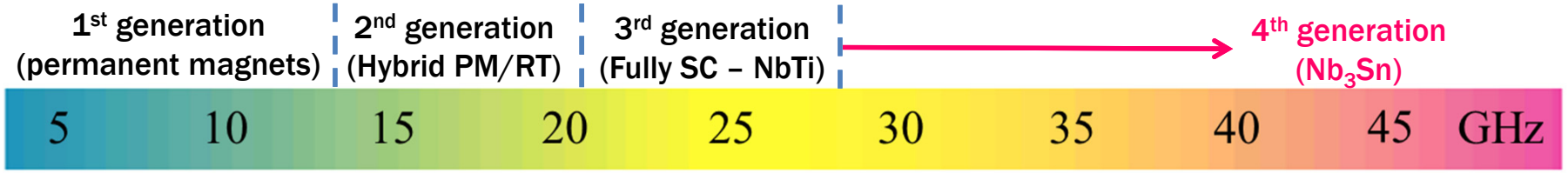

Design drivers:

- Ion current scales as square of microwave frequency
- Confinement field scales linearly with frequency
- Nb_3Sn required to move beyond state of the art (28 GHz)

Magnetic Layout

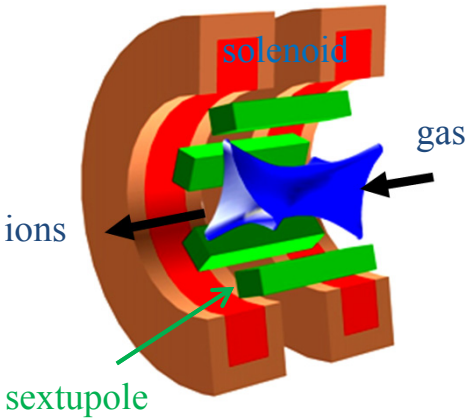

45 GHz Coil Peak Field: 12T

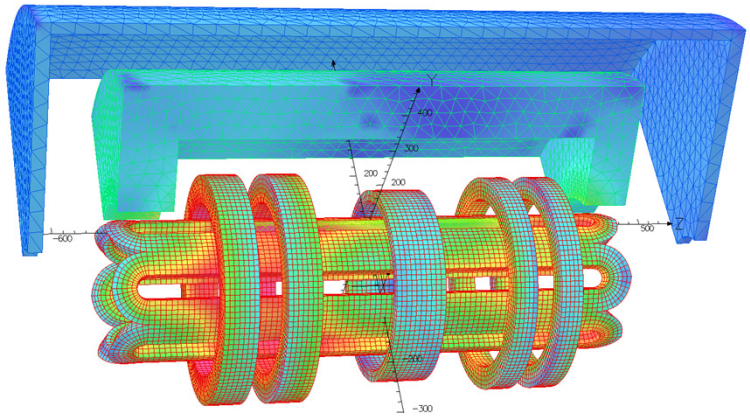

Coil Stress: 150 MPa

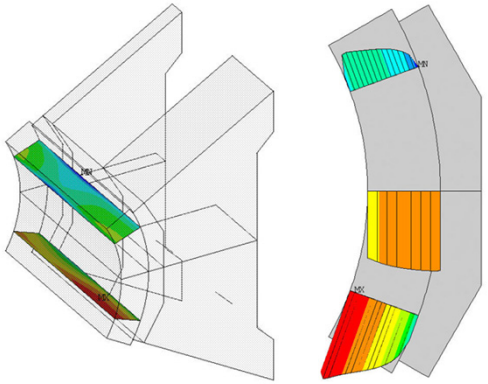

L. Sun, H. Zhao (IMP); W. Lu, D. Xie (NS); R. Hafalia, M. Juchno, I. Pong, E. Ravaioli, G. Sabbi, X. Wang (ATAP)

Superconducting gantry magnet for medical therapy

- HEP Stewardship grant to develop superconducti magnet technology for medical gantries
  - Collaboration between LBNL, Varian, and PSI
  - Motivation: reduce weight by ~x10, reduction in size
- Optics design results in dp/p~25% acceptance
  - Less/no ramping facilitates superconducting technology
  - May enable new treatment modalities

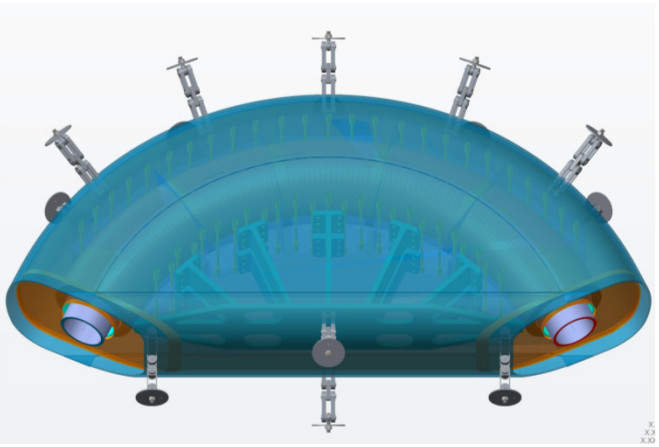

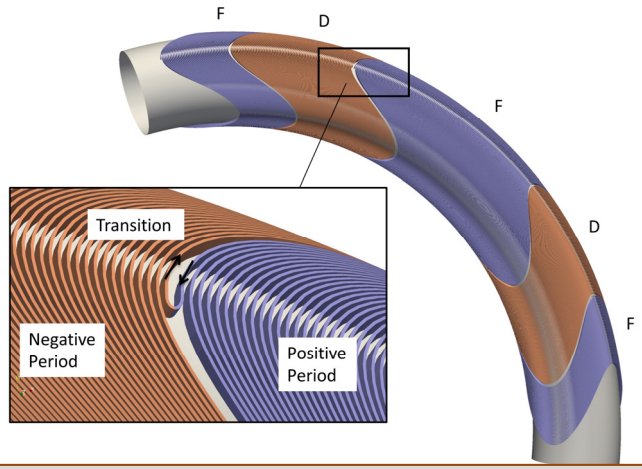

W. Wan et al., PRSTAB 18, 2015

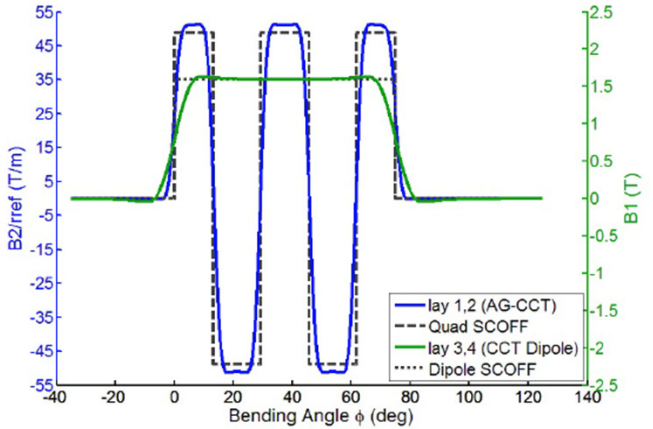

Conclusion

I hope this has served to give a flavor of what is involved in the design, fabrication and testing of superconducting accelerator magnets – it is an exciting technology area, touching on materials, magnetics, mechanics, and thermal sciences, and benefiting from novel diagnostics!

Thank You